REPORT

Under Oslo

WP1 - TEMPORARY STORAGE OF BLACK SHALES – A COMPILATION OF CASE STUDIES, EXPERIENCES AND OVERALL CONCLUSIONS

DOC.NO. 20200436-03-R
REV.NO. 0 / 2023-01-09

NORWEGIAN GEOTECHNICAL INSTITUTE
NGI.NO

Project

Project title:	Under Oslo
Document title:	WP1 - Temporary storage of black shales – a compilation of case studies, experiences and overall conclusions
Document no.:	20200436-03-R
Date:	2023-01-09
Revision no. /rev. date:	0 /

Client

Client:	NFR
Client contact person:	Guro Grøneng
Contract reference:	SP13

for NGI

Project manager:	Jenny Langford
Prepared by:	Frøydis Meen Wærsted, Gøril Aasen Slinde og Marion Børresen
Reviewed by:	Gunvor Baardvik

NORWEGIAN GEOTECHNICAL INSTITUTE
NGI.NO

Main office
PO Box 3930 Ullevaal St.
NO-0806 Oslo
Norway

Trondheim office
PO Box 5687 Torgarden
NO-7485 Trondheim
Norway

T 22 02 30 00
F 22 23 04 48
NGI@ngi.no

BIC NO. DNBANOKK
IBAN NO26 5096 05 01281
ORGANISATION NO.
958 254 318MVA

ISO 9001/14001
CERTIFIED BY BSI
FS 32989/EMS 612006

\\xfil1\prodata$\2020\04\20200436\05 leveransedokumenter\rapport\20200436-03-r temporary storage\20200436-03-r temporary storage of black shale_ny.docx

Summary

As a part of the internal R&D project "Under Oslo" at NGI, several aspects of temporary storage of black shale has been investigated. Information from different experiments and cases of black shale storage from the Cambro-Ordovician stratigraphy in the Oslo area have been gathered.

For the large scale, outdoor experiments with fresh black shale, minimum 14 months was necessary for acid rock drainage (ARD) to start. This is because the black shales have an inherent buffer capacity in the form of carbonates that buffers the acid and cannot be expected for already weathered shale where part of the buffer capacity may have been consumed. For small-scale column experiment at room temperature, the pH dropped after about 10 months.

Two cases of self-heating in alum shale are described. In both cases, the time until significant self-heating was more than a year. Factors affecting this probability will likely be reactivity of the rock masses (e.g. content of sulphides and neutralizing material), size distribution and porosity of the rock masses, storage conditions including height of pile, moisture and air circulation in the pile. Covering masses with tarpaulin can both increase and reduce the risk of self-heating.

One stage batch leaching tests are not appropriate for assessing the acid-producing properties of black shale, but may give information about the degree of weathering of the material. However, even by ongoing ARD, crushing the material can release carbonates resulting in neutral pH.

Downstream water quality of three sites with neutral leaching from black shale is presented and are mainly within environmental guideline values. Some elevated uranium values were however observed. Tests with different basic materials for neutralizing ARD gives varying results, showing the need for testing materials before use.

Based on the results of all these findings, a maximum of 6 months temporary storage before final disposal of acid producing black shales is recommended. This time period includes temporary storage at the disposal sites before the masses are properly covered.

Contents

Appendix

Review and reference page

1 Introduction

The Cambro-Ordovician black shales in the Oslo area are sedimentary black mudrocks formed under reducing conditions. They contain organic matter, sulphides and carbonates, and are often enriched in metals, including copper, nickel, uranium and vanadium (Owen et al. 1990, Pabst et al. 2017,).

As black shales are exposed to water and oxygen (for example after blasting or excavating) a weathering process starts. Sulphide minerals in the shale, like pyrite and pyrrhotite, can be oxidised and generate acid run-off, also known as acid rock drainage (ARD). In Norway, alum shales are of main concern, since they have been shown to be the most reactive of the black shales when weathered. The run-off from weathered alum shale is generally characterised by low pH (<4) and high concentrations of sulphate, uranium and other elements (Pabst et al. 2017). When the weathering process has started, it can quickly accelerate and self-reinforce (Appelo and Postma, 2010; Singer and Stumm, 1970).

The acidification process is also dependent on the content of carbonate in the rock, since carbonates can neutralise the acid. Therefore, the ratio of the neutralisation potential (NP) to the acidification potential (AP) is an important property when considering storage conditions for black shales. The neutralisation potential is calculated based on the total content of inorganic carbon (carbonates) in the rock, assuming these behave like calcite, while the acidification potential is calculated from the total sulphur content, assuming that all sulphur (S) in the rock comes from sulphides behaving like pyrite (Lawrence & Wang 1996).

According to the Norwegian regulations on limitation of pollution (forurensningsforskriften, § 2-3), excavated black shales can be considered contaminated ground because contact with water and/or air can generate acid drainage and leakage of environmental harmful substances (heavy metals and natural radioactivity) (Lovdata, 2010). When excavating black shales, the acidification potential of the shale should be quantified to decide an appropriate treatment of the shale to prevent possible contamination in the future. The environmental authorities have today two documents with guidelines for black shales, the first one (M-310) gives guidance on identification and classification of black shales occurring within a construction site (Norwegian Environment Agency, 2015a). The second (M-385) discusses methods for appropriate treatment and deposition of black shales to avoid environmental consequences (Norwegian Environment Agency, 2015b). An updated report (M-2105) based on these two documents and new knowledge was published in 2022 (Norwegian Environment Agency, 2022). The recommendation for temporary storage was updated based on the results presented in this report.

During the last few years, there has been a rising awareness and increased knowledge regarding the treatment of black shales. Hence, the need for clarification and delimitation related to the legislation around black shales is increasing. Recommendations given in the guide M-385 state that rock masses containing black shales should not be temporary stored before transport to a disposal site for longer than two months. It is assumed that the longer the temporary storage of black shales, the higher the risk for acid rock drainage is at a later point of storage.

In this study we have collected data from experiments and cases of inadequate and adequate storage of black shales from the Cambro-Ordovician stratigraphy in the Oslo area (Oslo Graben," Oslofeltet"). The cases have in common that they leaching data as well as total rock analyses. One case of black/grey shale from a higher horizon, that is not expected to be acid-producing, is also included. Container and column experiments were also set up at NGI to investigate the leaching of metals and acid with time during inadequate storage.

Topics investigated in this report are the following:

- The effect of storage of alum shale under varying conditions and time, to give recommendations for maximum duration and conditions for temporary storage.
- The potential of heat development and self-heating in alum shale masses.
- Results for mixing of black shale with basic materials are presented.
- The appropriateness of one stage batch leaching tests in assessing leaching potential is evaluated.
- Principal component analysis on rock data is performed to investigate trends in the gathered material (see appendix D).
- Some data for water quality downstream black shale sites are presented

The topics are investigated by discussing both historical data and newly gathered data from the ongoing column and container experiments at NGI.

While black shales in Norway are mainly found in the Oslo area, other acid-producing rocks can be found in other parts of the country, such as sulphide-containing gneiss in southern Norway. Other types of rock will be geologically and geochemically different from black shales and the results presented in this report are not necessarily relevant for other rocks than black shales.

We would like to direct our thanks to the Norwegian Public Road Authorities (Prosjekt Vestoppland) and NOAH AS for sharing data from their experiments, and Håkon Børresen and Lars Andre Erstad for allowing us to use results from their master theses. Thanks to Norwegian Public Road Authorities for letting us take over parts of their black shale leaching container experiments started in 2014/2015, and a special thanks to Halldis Fjermestad and Per Hagelia for helping out and answering all questions. Thanks to Skanska for providing alum shale masses for the new container and column experiments. The container experiments will continue until 2028, as a part of SP "Under Oslo" and earthresQue centre for research-based innovation (lead by Norwegian University of Life Sciences).

2 Background

2.1 The Cambro-Ordovician black shales

The black shales of the Oslo area were formed in the Cambro-Ordovician period, i.e. about 500 million years ago. The Ordovician successions in the Oslo area have been described by Owen et al. (1990). In this report a simplified lithological grouping is used (see table 1).

The different shale horizons have been deposited under different conditions, and consequently have different properties. The alum shale formation comprises horizons 1 to 3a, but of these the 1st horizon mainly consists of sandstone and is not acid-producing (Pabst et al., 2017). Horizons 2 and 3a are generally acid-producing and are the most likely to cause negative environmental consequences. Of the higher-lying horizons, the 3bβ Galgeberg horizon is also acid-producing, though with a smaller potential for acid production than the alum shales. The horizons 3bα, 3c and 4a can be net neutralizing and are less reactive.

Table 1 Shale and limestone units from Cambro-Ordovicium in the Oslo – Asker formation. The units are defined with numbers where 1 is the oldest and 4 the youngest. Geological events have caused a disorder in the stratigraphic succession at some places. Appearance and characteristics are given for the different horizons (modified after NGU bedrock maps and Owen et al., 1990).

Horizon	Name formation (Oslo-Asker)	Name Member (Oslo-Asker formation)	Appearance	Characteristics	Thickness
4d	Grimsøya	-	Nodular limestone	-	-
4cα	Venstøp	-	Shale	-	-
4bδ	Solvang	-	Shale with limestone	-	-
4bγ	Nakkholmen	-	Shale	Shale with concretions of pyrite in lower part	-
4bβ	Frognerkilen	-	Nodular limestone	-	-
4bα	Arnestad	-	Shale	-	> 50 m
4aβ	Vollen	-	Nodular limestone	Calcareous rich shale	-
4aα	Elnes	-	Grey-black to grey shale. Red-brown oxidation layer.	Calcareous rich shale containing some sulphides, but with very low acidification potential	> 80 m
3c	Huk	Svartodden (3cγ) Lysaker (3cβ) Hukodden (3cα)	Huk fm is divided in 3 with limestone at the top and bottom layers and calcareous rich shale in the middle.	Calcareous rich, considered not to have an acidification potential	Ca. 30 m
3bβ	Tøyen	Galgeberg	Black to grey-black shale. Rust-brown oxidation layer with yellow elements.	Moderately to low acidification potential, varying content of trace elements	10 – 20 m
3bα	Tøyen	Hagastrand	Green-black to grey-black shale. Red-brown oxidation layer.	Possible acidification potential, varying content of trace elements	5 – 10 m
3aγ	Bjørkåsholmen	-	Grey limestone with intercalations of shale	Calcareous rich, often massive limestone	1 – 4 m
3aα, 3aβ	Alum shale	Alum shale horizon 3	Black shale with yellow, red-brown and white oxidation layers.	High acidification potential, high to moderate content of trace elements, possible enrichment of radionuclides	5 – 20 m
2a-2e	Alum shale	Alum shale horizon 2	Black shale with yellow and white oxidation layers.	Highest acidification potential in the Alum shale fm., high content of trace elements, possible enrichment of radionuclides	60 – 80 m
1	Alum shale	Alum shale horizon 1	Sandstone, shale	No acidification potential	-

2.2 Mineralogy

Alum shale consists of silicate minerals, organic matter (kerogen), sulphides and carbonates (Falk et al., 2006; Owen et al., 1990; Pabst et al., 2017). The sulphide minerals, for example pyrite (FeS_2) and pyrrhotite (FeS), are formed due to the reducing conditions during sedimentation and formation of the rock and is the source of the acid-producing capacity of the rock. The carbonates in the alum shale is often calcite ($CaCO_3$), and can be present in the form of nodules, giving a very uneven distribution of the carbonates in the rock (Owen et al., 1990; Pabst et al., 2017). Kerogen is incompletely decomposed organic matter from sedimentation and is responsible for the characteristic black colour (Tourtelot, 1979).

2.3 Content of metals

The formation of black shales in shallow seawater with a reducing environment is partly responsible for the enrichment of a number of trace elements (Alloway, 2013). Black shale, and especially alum shale, is enriched in a range of trace elements including Cd, Co, Cu, As, Ni, Zn, V, Mo, Ba and U (Falk et al., 2006; Owen et al., 1990; Pabst et al., 2017). These can leach into the nearby aquatic environment or become enriched in soils developed on the alum shale.

2.4 Content of naturally occurring radionuclides

Black shales can potentially leak radioactive species, as the content of uranium often is elevated compared to other types of rock. Radioactivity in black shales is related to the content of uranium and thorium and to a lesser degree ^{40}K (potassium-40). The content of thorium is relatively low compared to the uranium content. Thorium also has a lower solubility than uranium. Uranium is therefore considered the most important component when it comes to radioactive run-off from black shales. Typical concentrations of uranium in shales from the Oslo area are given in Table 2. Alum shale has the highest content of uranium, followed by Galgeberg shale.

Table 2 Typical concentrations of uranium in different rocks (Norwegian Environment Agency 2015b).

Rock/shale type	**Horizon**	**Uranium (mg/kg)**
Alum shale	2	60 – 300
Alum shale	3a	30 – 150
Hagastrand shale	3bα	5 – 20
Galgeberg shale	3bβ	10 – 40
Huk shale	3c	1 – 7
Elnes shale	4a	<15
Granite	-	5 – 40
Limit of radioactive waste	-	*~80*

Excavated rock masses with ≥ 1000 Bq/kg natural uranium is in Norway defined as radioactive waste (Lovdata, 2010). Undisturbed rock is not considered radioactive waste and no measures are necessary unless the rock is to be relocated or removed. 1000 Bq/kg corresponds to a uranium content of 80 mg U/kg. When measuring the uranium content in mg/kg, the activity can be calculated and vice versa using the following equation (IAEA, 2003):

$$1\ mg\ U/kg \ = 12{,}35\ Bq/kg\ of\ {}^{238}U$$

There are no guidelines given for uranium in drinking water in Norway, but there are restrictions on emissions. For release greater than 100 Bq or 0.1 Bq/L, a permit is needed (Forskrift om radioaktiv forurensning og avfall, 2010). NGU (Geological Survey of Norway) has measured the uranium content of groundwater in Norway and found an overall range in the natural concentrations of uranium from <0.001 to 1000 µg/L (see Figure 1). For drinking water, WHO has set a limit of 30 µg U/L (WHO 2012).

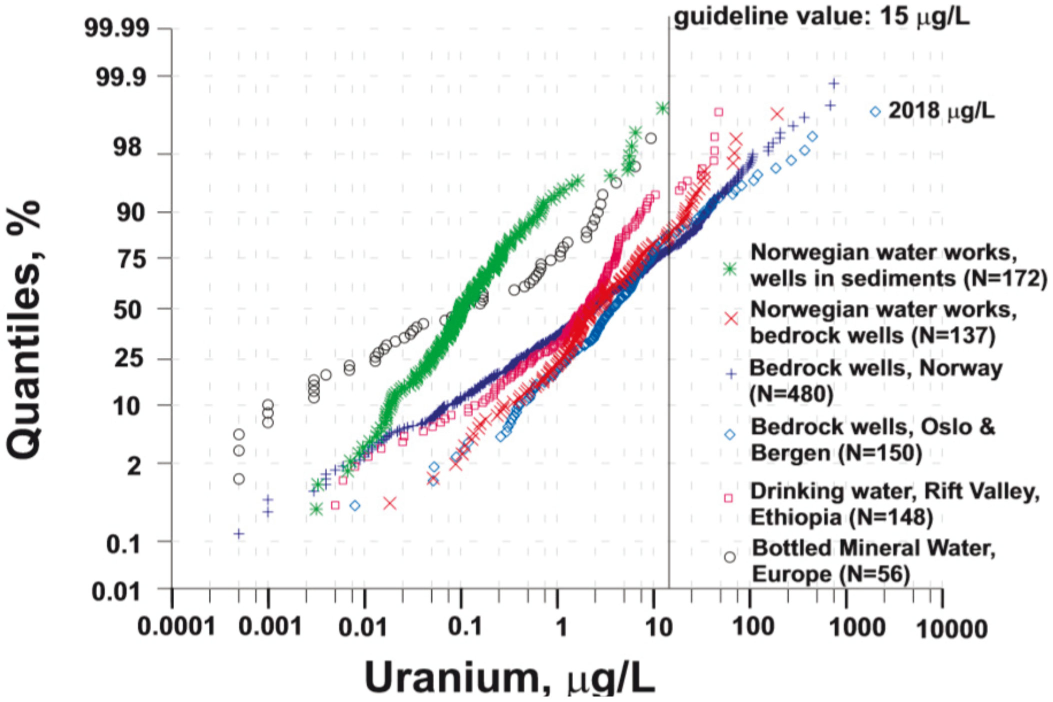

Figure 1 Uranium concentrations in groundwaters from surveys performed by NGU (NGU 2005).

2.5 Temporary storage of black shales

The duration of temporary storage of black shale masses is recommended to be as short as possible, not exceeding two months (Norwegian Environment Agency, 2015b). This value was set conservatively as there was little available information to back it up. In this report, results are gathered to create a foundation to evaluate this recommendation.

The weathering of sulphides in black shales is expected to start immediately after blasting, when the rock surface comes in contact with oxygen and water. The acidification process is however not instant, as black shales have a certain inherent neutralization potential due to the content of carbonates, and the weathering processes may be a bit slow. The time aspect is of great importance, as it on one hand is undesirable to get acid drainage from a temporary storage site, but on the other hand the quick delivery to an approved disposal site can in certain project be challenging. To avoid unnecessary costs and filling up disposal sites with clean masses, and at the same time protecting the environment, good knowledge about the time it takes before acid runoff forms is of crucial importance.

The tests and methods usually used to evaluate the potential of black shales to produce acid (see ch. 3) do not take the aspect of time (kinetics) into account, only the expected end result. Thus, they are relevant for assessing the need for special considerations for permanent storage, but not necessarily for assessing the short-term implications.

3 Collection of data and experimental set-up

The data collected, analysed and discussed in this report comes from different black shale projects around the Oslo area, as listed in Table 3. The cases have been chosen based on projects were both rock and water analyses were available. Maps of the sites are given in Figure 2 and Figure 3. The orange circles in the figure show sites where the shale samples are taken from the excavation site. The grey circles are deposit sites for shale originating in Oslo city centre. The black shales are mainly alum shales from horizon 2 and 3a, with some elements of horizon 3b and 4.

The data comes from geochemical analyses, XRF, mineral identification with XRD and ABA (Acid-base accounting) of the solid rock. In addition, it has been performed different leaching experiments, from standard leaching tests meant for waste handling purposes to experimental set-ups specifically designed for investigation of leaching properties from alum shale in rock piles, using columns and containers. In addition, there are some data from groundwater, excavation pits and nearby recipients.

Table 3 Case studies, collected data and experimental set-ups discussed in this report.

Case study	Geological horizon	Geochemical rock analyses	XRD	XRF	ABA*	Leaching experiment/ water analyses
E16 Kleggerud (NGI)	2 and 3a	X	X	X	-	Container + column tests. One stage batch leaching test for uranium. Recipient.
New road to Kistefos Museum	2 and 3a (4a)	X	X**	X	-	One stage batch leaching tests, recipient**
Rv. 4 Gran	2 and 3a, 3bβ	X	X	X	-	Container, recipient, temperature measurements
E6 Uthus - Kåterud	2 and 3a	X				One stage batch leaching test
NOAH Langøya	2 and 3a	X	-	X	-	Columns, one stage batch leaching tests
NOAH Langøya test cell	2 and 3a	-	-	X	-	Seepage water from rock piles, temperature measurements
Høvik	4	X	-	-	-	One stage batch leaching tests
Taraldrud	2 and 3a (3bα, 3bβ, 4a)	X	-	X	-	Seepage water from pits, recipient
Vilberg	2 and 3a, 3bα, 3bβ	X	-	-	X	Groundwater

* ABA – Acid-Base Accounting
** Results exists but were not included in this report

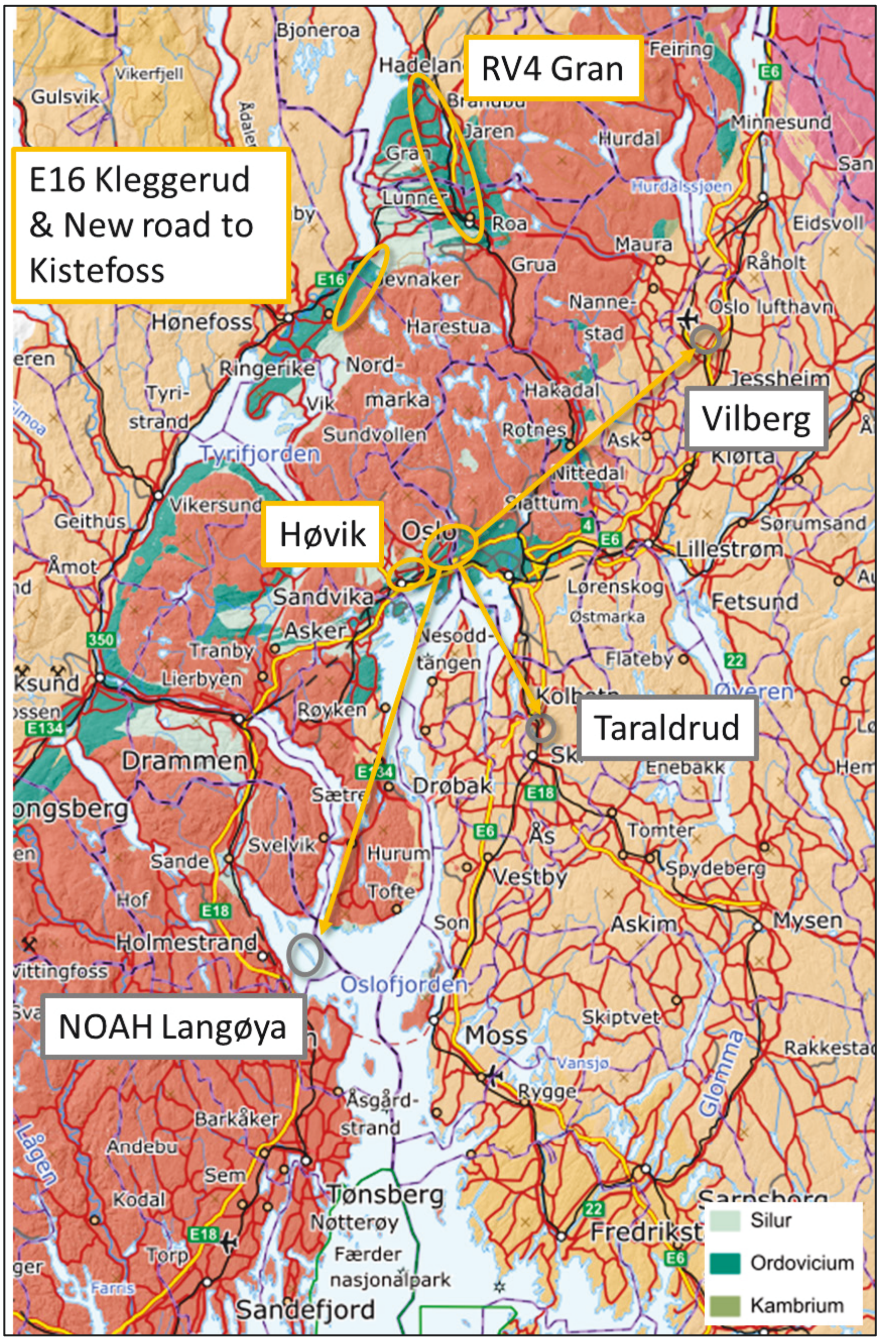

Figure 2 Map of the sites from where NGI has retrieved experimental data in this project (except E6 Uthus - Kåterud, shown in Figure 3). The orange circles show sites where the shales are directly from the excavation site. The grey circles are deposit sites for shales originating in Oslo city centre (area shown in orange colour with arrows). Colours in the background map shows geological formation age (http://geo.ngu.no/kart/berggrunn/)

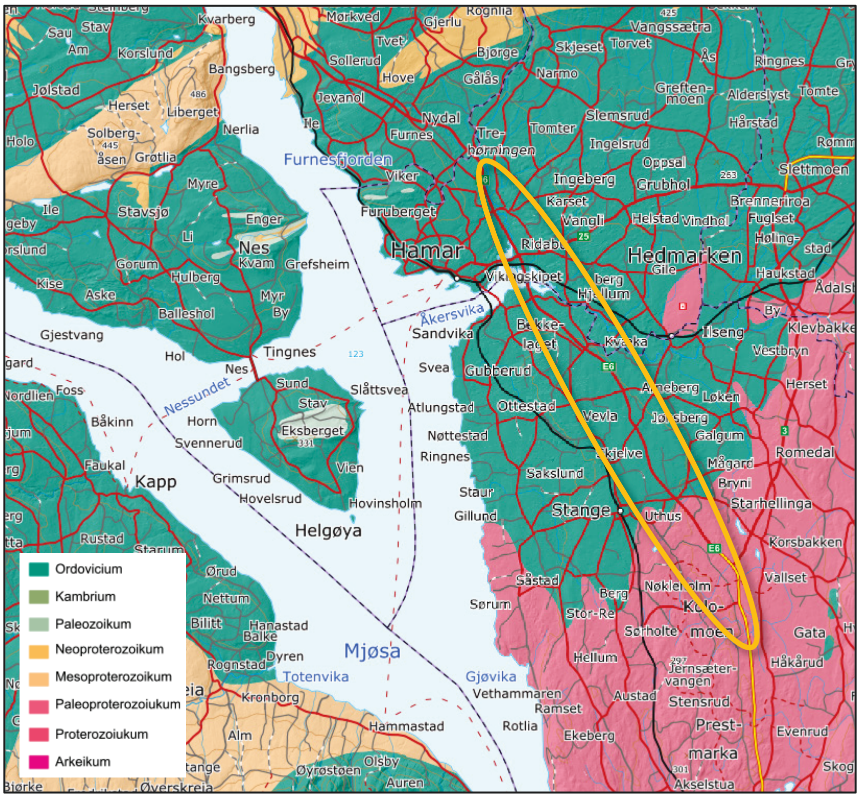

Figure 3 The area for the project E6 Uthus - Kåterud, where Nye Veier have built a new four-lane highway. Colours in the background map shows geological formation age (http://geo.ngu.no/kart/berggrunn/)

In the following, the methods for characterisation of the black shales and the standard leaching test (one stage batch leaching test) are described. For the set-ups for the non-standard experiments, such as column tests and container tests, the description is given in Appendix A.

3.1 Characterisation of the black shales

To characterize the black shales, different methods have been used. This includes chemical characterization and assessment of the horizon based on chemical data, XRF analysis, evaluation of neutralisation potential, acidification potential and the Fe:S relationship, XRD analysis, as well as the ABA method.

Rock samples were analysed for a wide range of elements and other parameters in a combination designed for black shales. The elements analysed were As, Ba, Be, Cd, Co, Cr, Cu, Hg, Mo, Nb, Ni, Pb, S, Sc, Sn, Sr, V, W, Y, Zn, Zr, Th and U. The quantity of SiO_2, Al_2O_3, CaO, Fe_2O_3, K_2O, MgO, MnO, Na_2O, P_2O_5, TiO_2 and LOI (loss on ignition) was also estimated. Analyses were performed at the accredited laboratory ALS Laboratory Group AS on ICP-SFMS after the standards ISO 17294-1 and EPA 200.8. Hg was analysed with AFS after ISO 17852. The content of total organic carbon (TOC) and total inorganic carbon (TIC) was determined by colometry, using the standards ISO 10694, EN 13137 and EN 15936. The combination of these parameters is called "the alum shale package".

Pabst et al. (2017) describes a method for determining which horizon a sample belongs to, based on comparison with reference materials of different Cambro-Ordovician formations (determined by geological methods including fossils). Different chemical parameters are plotted together in triangular diagrams, grouping the different reference materials together based on their chemical composition. The analysed samples can thereafter be placed together with the reference materials to sort the black shale samples into the: horizon 2 (Alum Formation), 3a (Alum Formation), 3bα (Hagastrand Formation), 3bβ (Galgeberg Formation), 3c (Huk Formation) or 4a (Elnes Formation). The triangular plots for the samples in this report are given in Appendix B and the determined horizons are given in Table 3 and Appendix C.

For some samples from the E16 Kleggerud and Taraldrud study sites, as well as all rock samples at NOAH Langøya, the elemental analysis was performed using an X-Ray Fluorescence (XRF) device. For the samples from E16 Kleggerud and Taraldrud, the sample analyses have been done at NGI. At NGI, the XRF instrument is mounted on a stand, and controlled by a separate control unit (PC). The XRF has been calibrated for samples of black shale, and only parameters with a satisfactory calibration curve have been reported. The reported elements are: Al, As, Ba, Ca, Cu, Cr, K, Mn, Mo, So, Si, Sr, Th, Ti, U, V and Y. Iron (Fe) is also reported, even though the calibration curve for Fe is not fully satisfactory. The uncertainties for iron are therefore somewhat higher than for the other elements. The analyses are done three times for each sample and the average of the three parallels is reported.

For the rock samples from NOAH, the analyses are done with an XRF as a part of the site's reception control. The analyses at NOAH were done for the following elements: Ag, Al, As, Ba, Ca, Cd, Ce, Cl, Co, Cr, Cs, Cu, Fe, Hg, K, La, Mg, Mn, Mo, Na, Ni, P, Pb, S, Sb, Si, Sn, Ti, Tl, U, V, Y and Zn.

According to the guidelines in M-310 (Norwegian Environmental Agency, 2015a), black shales can be identified as acid producing, non-acid producing or possibly acid producing based on a method for recognition of the chemical fingerprint of the rock. Interpretation of the chemical analyses involve the following steps:

- Triangular plots showing the relative content of different elements compared to reference samples of black shales, used to identify which horizon a sample belongs to.
- AP/NP diagram illustrating the ratio between the acidification potential (AP) and the neutralisation potential (NP) of the shale and thus indicating the potential for ARD. AP is calculated based on the total sulphur content and NP is calculated from the total content of inorganic carbon (TIC) in the rock:
    - NP:AP < 1:1 is acidification zone
    - 1:1 < NP:AP < 3:1 is uncertain zone
    - NP:AP > 3:1 is neutralizing zone

- Iron/sulphur diagram giving information about the iron-sulphur ratio. The ratio indicates if iron is combined as sulphides or other minerals and gives an indication how easily mobilized the other associated metals are:
    - Fe:S > 2:1 indicates that iron and metals are combined in silicates
    - Fe:S = 1:1 indicate that iron and sulphur are combined as pyrrhotite (FeS)
    - Fe:S = 1:2 indicates pyrite (FeS_2)
    - Fe:S = < 1:2 indicates that sulphur is bound in other minerals in addition to sulphides, or organic matter

Samples from one of the locations (Vilberg) were tested for modified Acid-Base Accounting (ABA). ABA is a series of compositional analyses and calculations, similar to the approach described in M-310:

- Analysis of pH.
- Analysis of sulphur species (total S and sulphate) and calculation of the acid potential (AP).
- Analysis of neutralization potential (NP) done with titration of HCl.
- Calculation of NP:AP (Neutralization Potential Ratio) and NP-AP (Net NP).

The tests were performed to quantify to what degree a rock sample is acid-producing or neutralising. Some clay samples were also tested for ABA to investigate if clay may have a neutralising effect on acid run-off. This kind of tests are usually done in the mining industry for detection of ARD. The samples were tested by SGS in Canada and the procedure is described by Lawrence and Wang (1996).

Neither of the methods described here say anything about how fast a potential acid forming process is but indicates if a sample is inclined to produce a lot, moderately or no acid. A well weathered alum shale, for example, can be classified with very low potential for acidification, since most of the potential has leached out from the rock already

3.2 One stage batch leaching test

Some of the black shale samples have been tested according to the European standard for characterization of waste, with a so-called one stage batch leaching test (EN-12457-2:2002). The test is a 24 hours long leaching test for granular waste materials and sludges at a liquid to solid ratio of 10 l/kg for materials with particle size below 4 mm (with or without size reduction). The standard has been developed to investigate mainly inorganic constituents from wastes. By crushing the material, new surfaces are exposed which may lead to a change in leaching properties..

3.3 Case studies

The different sites in Table 3 where materials and information were collected are described in appendix A, together with results from each case. The results are thematically discussed together in chapter 4.

Results from both planned experiments and infrastructure projects are used. Planned experiments include container experiments and a large-scale test cell with black shale exposed for natural weathering conditions. Samples taken in the field around construction work and stored black shale are used to investigate spreading in a natural environment. Results from column experiments and one stage batch tests are also presented.

4 Results across projects

In the following chapters results from all the case studies presented in Appendix A are compared.

4.1 Characterization of the black shales, geochemical analyses

The black shales described in this report have all been characterised, either by geochemical analyses, by XRF or by both, see Table 3 and description in chapter 3.1 for details, and appendix C for analysis results. The results from the characterisation have been used in triangular plots (appendix B) for identification of the appropriate horizon and to make the NP:AP and Fe:S ratios for identification of the rock sample's ARD (acid rock drainage) potential, presented under each case study.

4.1.1 Risk of acid rock drainage

One important factor for determining risk of acid rock drainage (ARD) from black shales is the ratio of the neutralisation potential (NP) to the acidification potential (AP).

In Figure 4 and Figure 5, the samples are presented in plots for AP versus NP, and in Figure 6 and Figure 7 as total content of sulphur versus total content of iron. The samples are categorized according to either site or horizon. The analysed samples cover all aspects in both diagrams. From the acidifying, to the uncertain or neutralizing zones in the AP:NP and from silicate minerals to sulphides in the Fe:S diagram. The samples from horizon 2 and 3a mainly classify as acid producing, but there are some exceptions. Samples from horizon 3b are spread all over, while samples from horizon 4 are all in the neutralizing zone.

The alum shale used in the container and column experiments at NGI (from E16 Kleggerud, called NGI) and the shale from NOAH are from horizon 2 and/or 3a and falls under the line 1:1 in Figure 4, in the acidification zone. The Fe:S ratio (Figure 6) for the NGI sample falls between the lines of 1:1 and 1:2, indicating that the iron and sulphur can combined both as pyrrhotite and pyrite. The NOAH samples are gathered around the 1:1 line, indicating that iron and sulphur mainly are combined as pyrrhotite, or that part of the Fe is bound as pyrite and part as silicates. The shales are classified as potentially acid producing.

The Taraldrud samples come from several horizons and distribute accordingly in the NP_AP diagram: samples from horizon 2 and 3a are acid-producing and have the lowest NP (<39), 3bα and 3bβ are in the neutralizing and uncertain/acid-producing zones and 4a is in the neutralizing zone.

The Vilberg samples are classified as horizon 2, 3a, 3b and they gather around (over and under) the 1:1 line in the AP:NP diagram, indicating an acid producing potential in half of the samples and an uncertain potential for the other half. In the S:Fe diagram they also gather around the 1:1 line, indicating that iron and sulphur mainly are combined as pyrrhotite, or that Fe exists part in pyrite and part in silicates.

The samples from Høvik (horizon 4) are all plotted in the neutralizing zone, with iron and metals combined as silicates. These shale samples are classified as not acid producing. Høvik is the only sampling site were all the samples are classified as not acid producing.

The results show that alum shale from horizon 2 and 3a in general, but not always, are classified as acid producing. The guidelines (M-2105) nevertheless recommend that masses from these horizons are treated as acid-producing, as one might have sampled a chalk-rich part of the horizon and this might not be representative of the total masses to be disposed of. This demonstrate the importance of representative sampling, collecting several samples from each layer/horizon and proper classification of the samples.

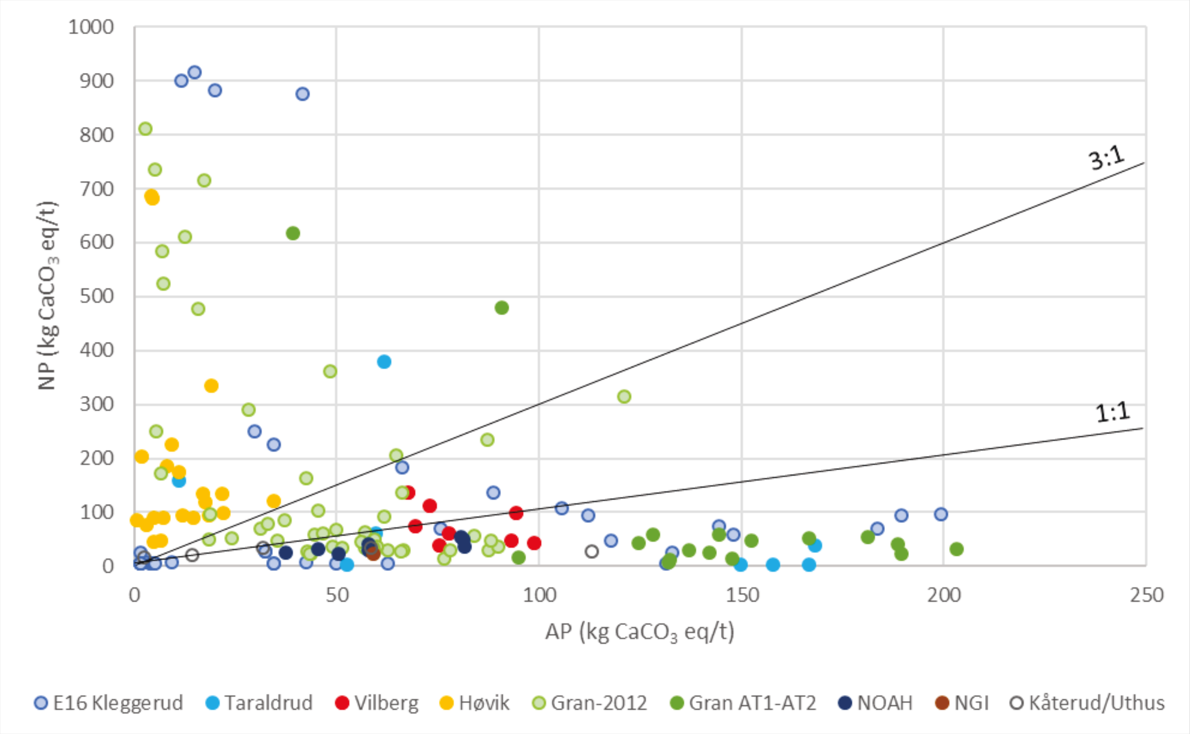

Figure 4 The relationship between acidification potential (AP) and neutralisation potential (NP) for the different rock samples, categorized according to site.

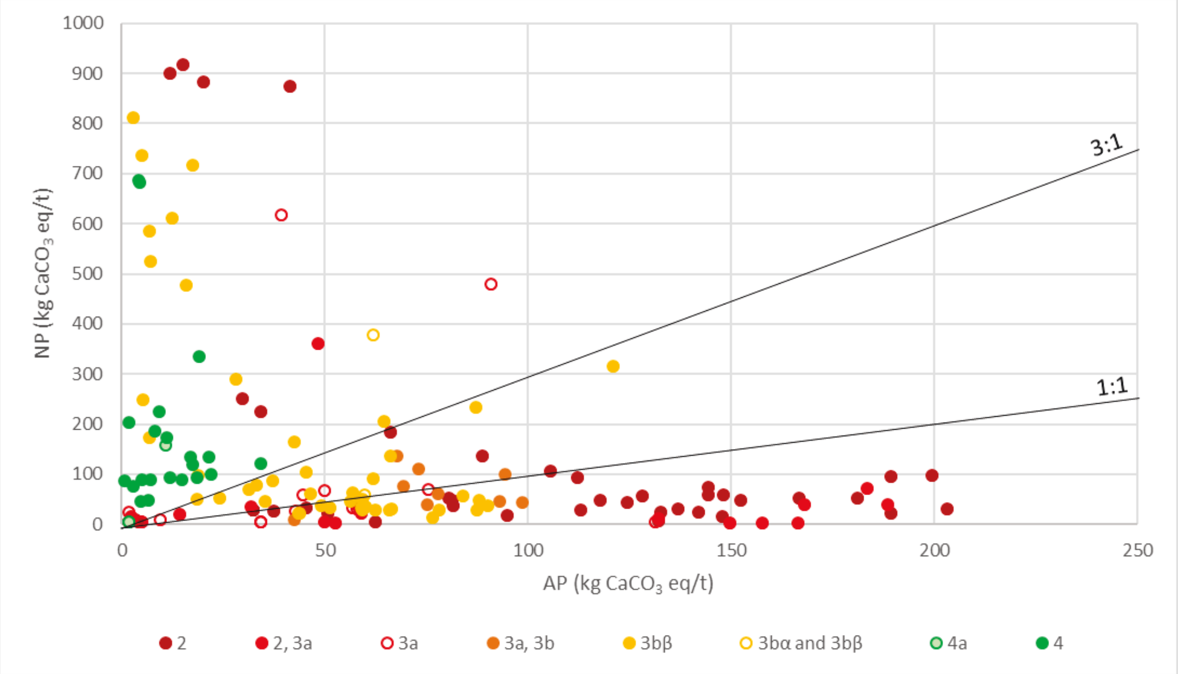

Figure 5 The relationship between acidification potential (AP) and neutralisation potential (NP) for the different rock samples, categorized according to horizon.

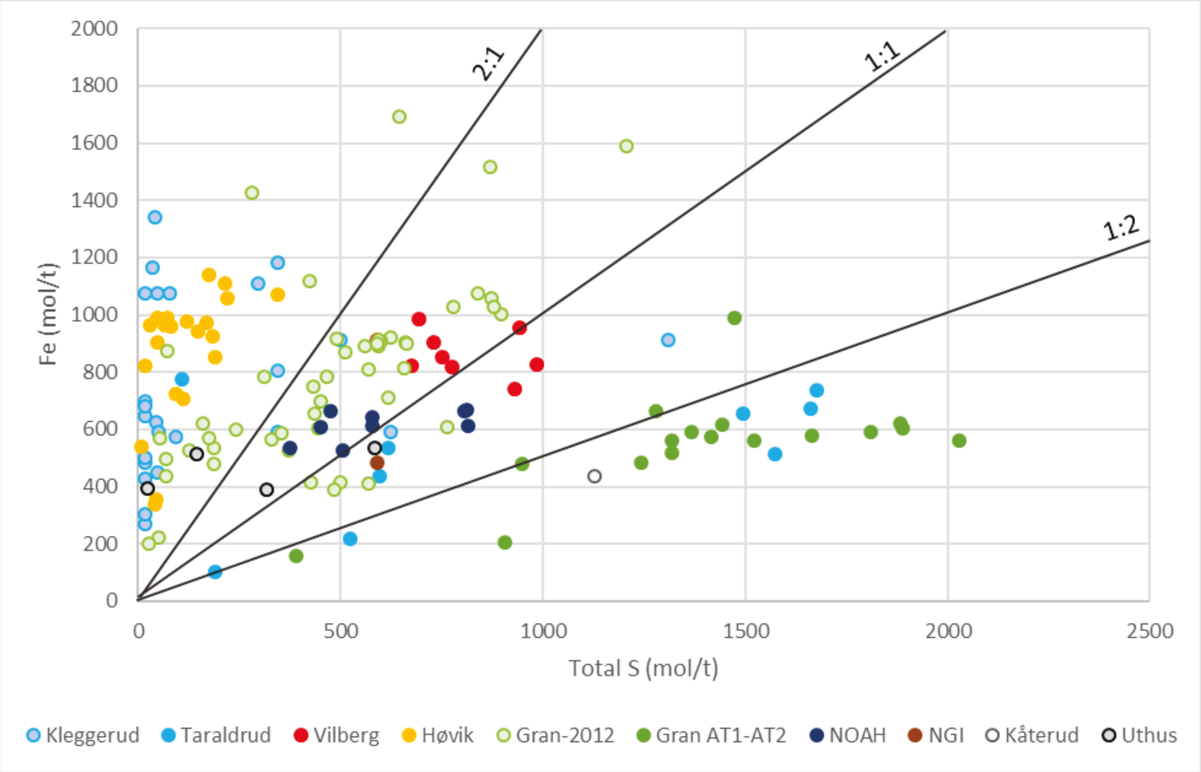

Figure 6 Total sulphur and iron contents in the different rock samples, expressed in mol/t. Samples are categorized according to site.

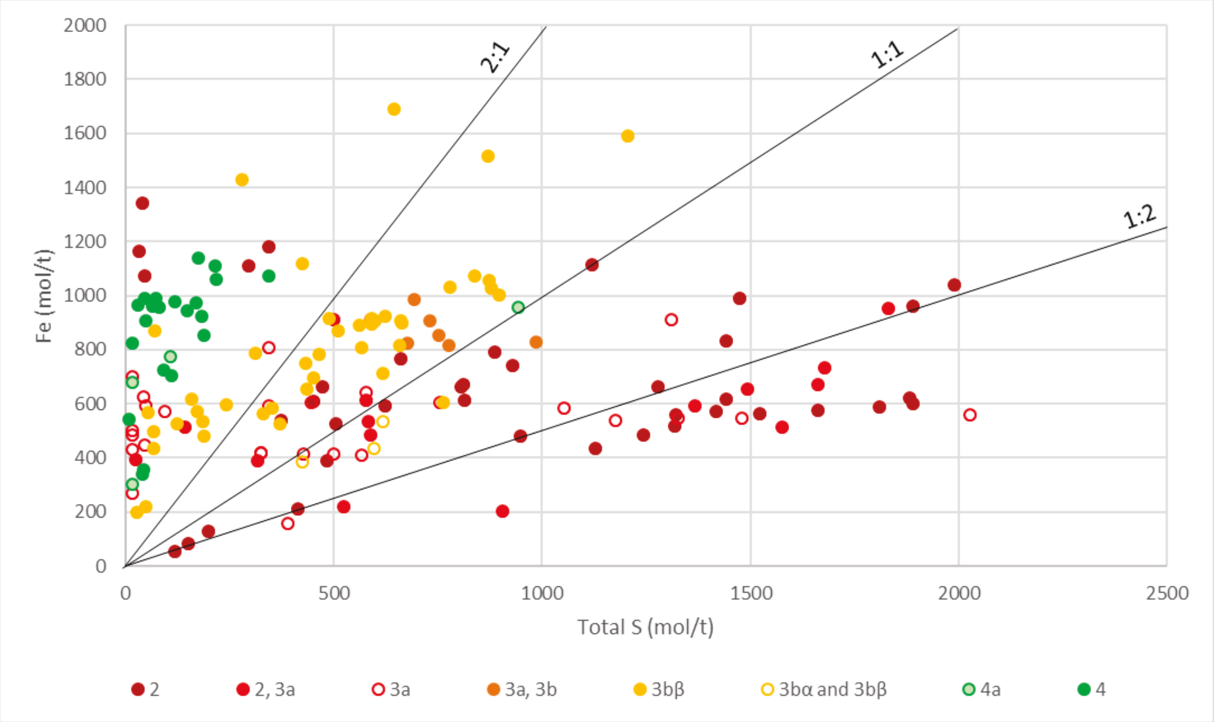

Figure 7 Total sulphur and versus total iron contents in the different rock samples, expressed in mol/t. Samples are categorized according to horizon.

Uranium is plotted as a function of the NP to AP ratio in Figure 8 and Figure 9. Higher uranium concentrations tend to be found in the samples with lower NP:AP, but the spread in the data is large (notice the logarithmic x-axis).

Samples from E16 Kleggerud, Taraldrud, Gran 2012, Gran AT1-AT2, NOAH and Kåterud all have contents of uranium exceeding the limit of radioactive waste (80 mg U/kg). All samples from Vilberg, Høvik, Uthus and NGI are beneath the limit.

High contents of uranium are related to the shales from horizon 2 and 3a, but shales from these horizons might also show low contents, ranging from 7 to 244 mg U/kg.

The uranium content of shales from horizon 3b, 4a and 4 is 52 mg U/kg or lower, except for one sample (3bα and 3bβ at 92 mg U/kg),

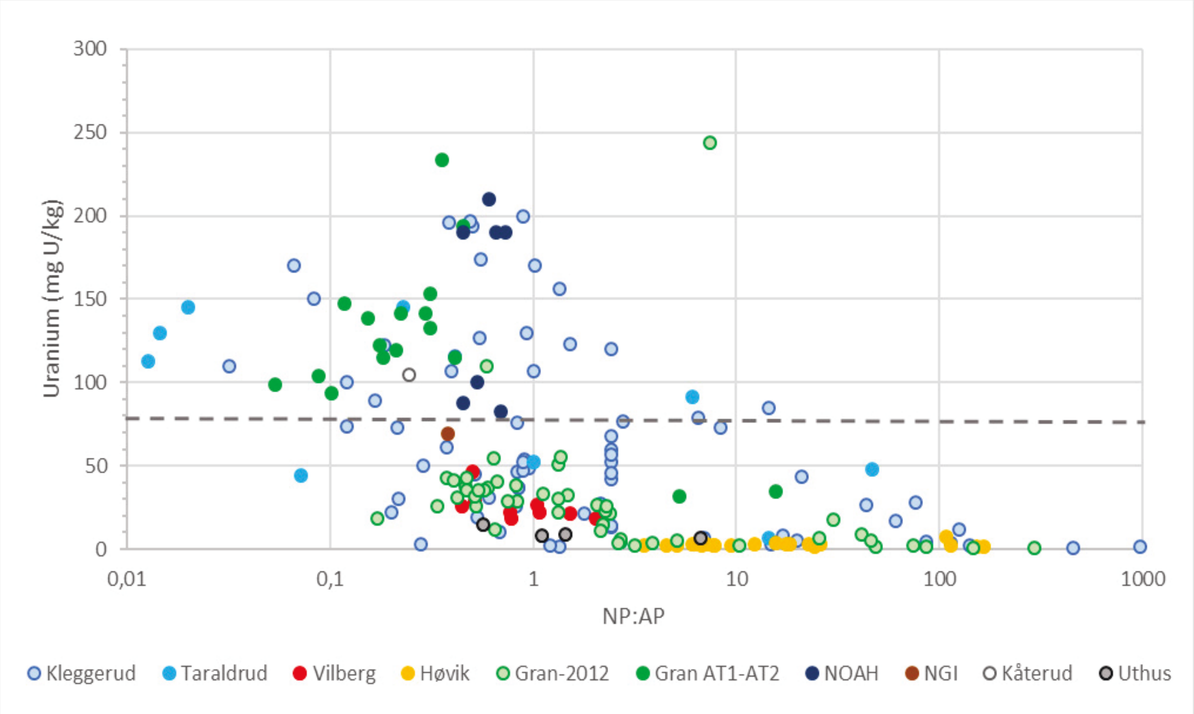

Figure 8 Uranium as a function of NP:AP in the rock samples. Samples are categorized according to site. Dotted line indicates the limit for radioactive waste (80 mg U/kg).

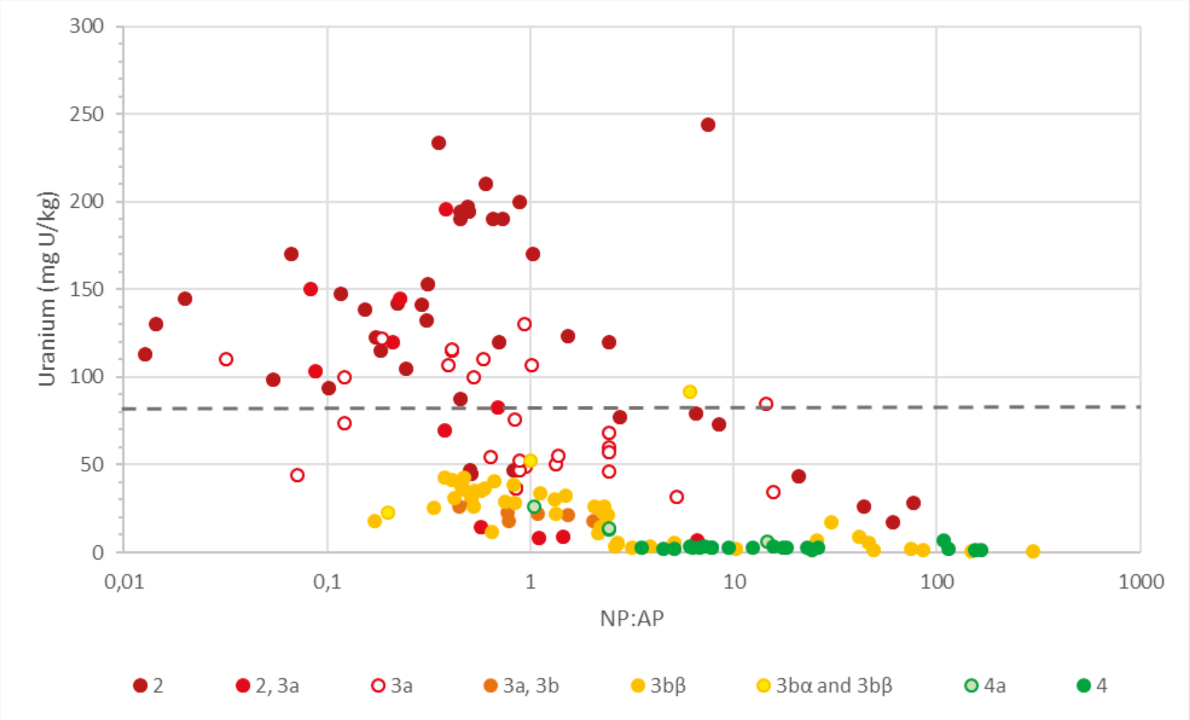

Figure 9 Uranium as a function of NP:AP in the rock samples. Samples are categorized according to horizon. Dotted line indicates the limit for radioactive waste (80 mg U/kg).

4.2 One stage batch leaching tests

One stage batch leaching tests were performed on shale samples from different locations, E16 Kleggerud (horizon 2 and 3a), NOAH (horizon 2), E6 Uthus/Kåterud (horizon 3a) and Høvik (horizon 4). One stage batch leaching test is a standard test used to predict the leaching behaviour of inorganic waste. In our case it was used to investigate the short-term leaching behaviour of black shales.

The acidification potential (AP) is, together with the neutralising potential, of importance to decide if a rock is potentially ARD producing or not. The AP is calculated using the sulphur content in the rock and NP by using the content of inorganic carbon (calcium for the NOAH samples). As the acidification process leads to lower pH values in the run-off, it was investigated if this was reflected in the results from the leaching tests.

The total sulphur content in the rock was plotted against pH in the leachate as seen in Figure 10 (top). There is no clear correlation between the sulphur content in the rock and pH in the leachate. The pH was then plotted with the NP:AP ratio as seen in Figure 10 (bottom). The NP:AP ratio seems to correlate with the pH, where pH is decreasing with decreasing NP:AP ratio ($\mathrm{pH} = 0.39 \times \ln(\mathrm{NP{:}AP}) + 7.5$, $R^2 = 0.30$). This is in accordance with the interpretations in M-310 (Norwegian Environmental Agency, 2015a), where rocks with $\mathrm{NP{:}AP} < 1$ are classified as expected to produce acid run-off, $1 < \mathrm{NP{:}AP} < 3$ are uncertain and $\mathrm{NP{:}AP} > 3$ are not expected to constitute a risk of ARD. However, even samples with NP:AP below one, mainly gives a circumneutral pH in the test, reflecting that the acidification processes take time. Low pH and high concentrations of metals in the leachate in a one stage batch leaching test indicate that the shale sample is weathered.

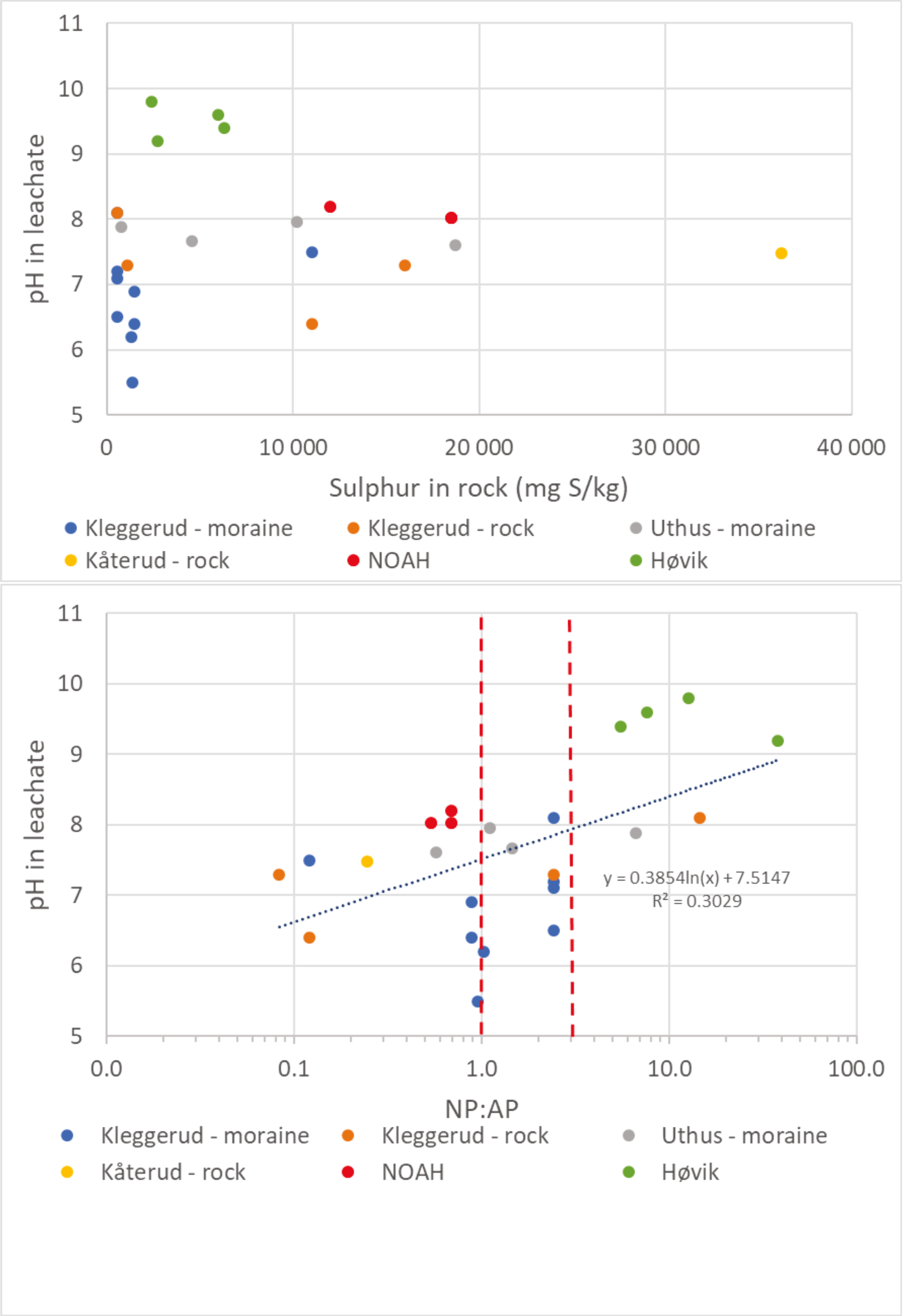

Figure 10 pH in the leachate (L/S=10) plotted as a function of total sulphur content (top) and NP:AP ratio (bottom) in the rock and moraine samples. Red dotted lines are NP:AP = 1 and 3

There is a good correlation between the content of total sulphur in the rock and sulphate detected in the leachate ($y = 0.0042\ x + 8.47$, $R^2 = 0.49$; Figure 11-A), with some outliers. Also, when NP:AP is plotted against sulphate in the leachate there is a correlation. The highest concentrations are found when AP:NP is < 1. Lowest concentrations are found at NP:AP > 3, see Figure 11.

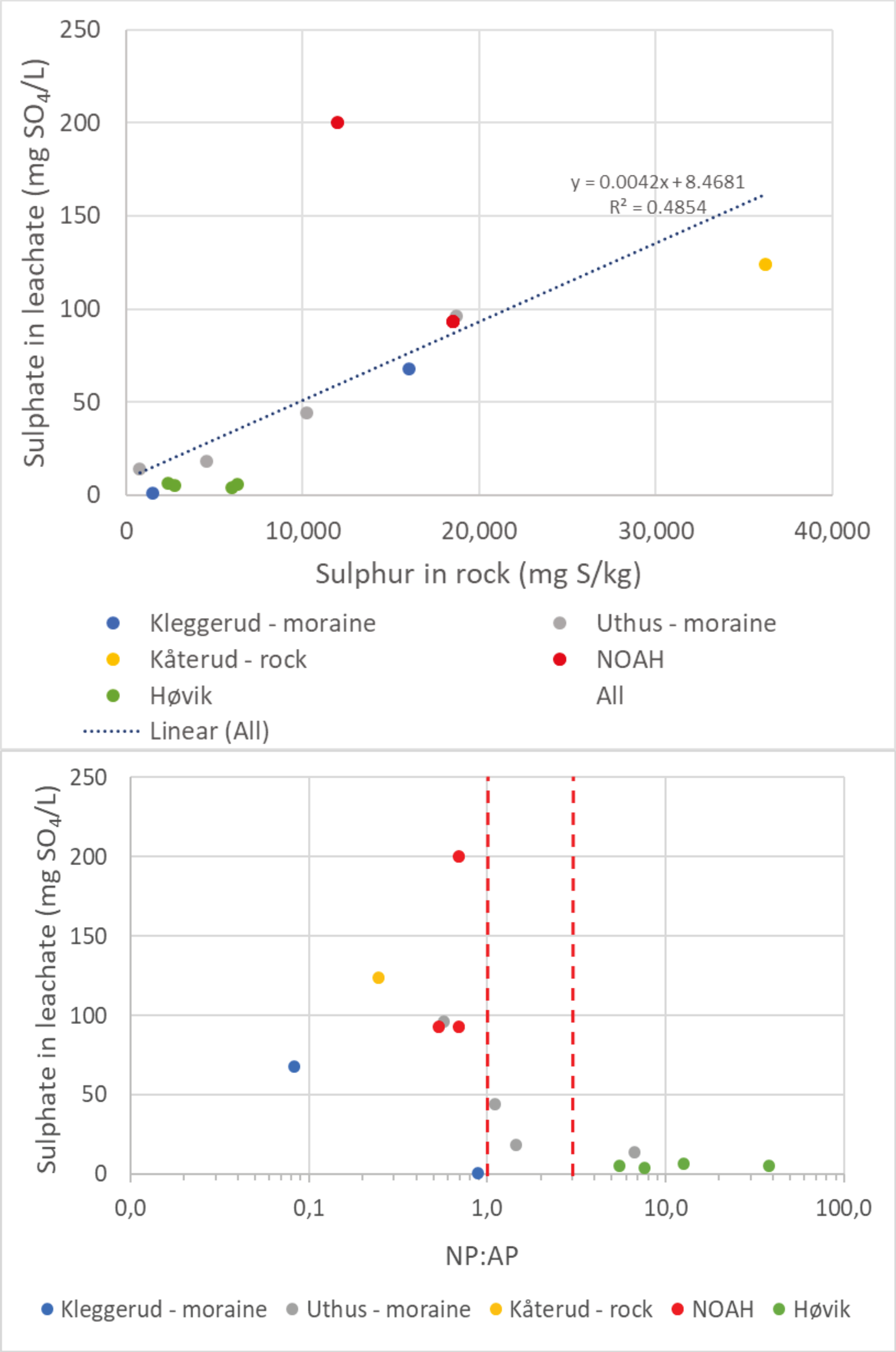

Figure 11 Sulphate concentrations in the leachate (L/S=10) plotted as a function of total sulphur content (top) and NP:AP ratio (bottom) in the rock and moraine samples. Red dotted lines are NP:AP = 1 and 3

The concentrations of uranium in the leachate compared to the total uranium content in the rock samples are given in Figure 12. There appears to be no correlation between the uranium contents in the solid rocks and their corresponding leachate. The figure shows that all the rock samples and three of the moraine samples exceed the limit of 80 mg U/kg (for radioactive waste), while the uranium concentrations in the leachates varied from 0.09-146 µg/L, which is within normal variations for Norwegian groundwater (NGU 2005). Three of the leachates exceed WHO guideline for U in drinking water (30 µg U/L).

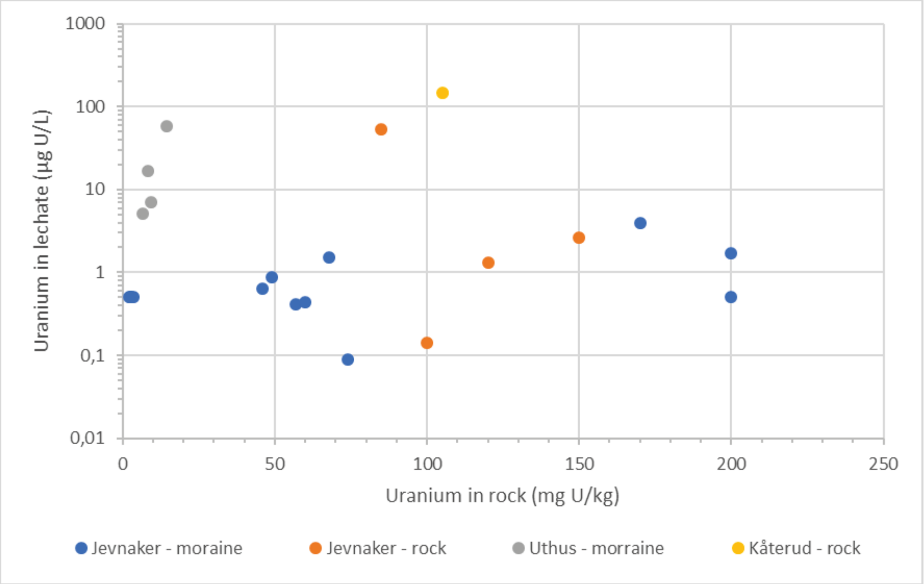

Figure 12 Uranium content in leachate (L/S=10) plotted as a function of the uranium concentration in rock and moraine samples and . The uranium content in Høvik leachates were under the detection limit (0,5 µg/L) and NOAH leachates were not analysed for uranium.

4.3 Effect of time on temporary storage

Some of the case studies are experiments that have been running for an extended period, giving valuable input on the time effects on temporary storage. It should be noted that the container tests at NGI will be continued until at least 2028, and there will be more data in the years to come.

The three projects where time effect best can be studied, are the test cell at NOAH Langøya, the containers containing pure black shales from the Rv.4-project at Gran and the containers with pure black shale set up at NGI. In these three projects, alum shales (horizon 2 and 3a) are tested, but the geographical origin of the shale is different. In the test cell at Langøya, the shale originates from a project in Oslo city centre, and in the containers set up at NGI alum shale from Kleggerud was used. In the containers set up at Gran, the alum shale is from local tunnels and cuttings, and there is also a container with Galgeberg shale. The results shown here from Gran, are from the selected containers that were transferred to NGI for further research.

As can be seen in Figure 13 and Figure 14, pH drop and metal concentration increase (here shown for U, Fe and Al) happened faster for the alum shale test cell at NOAH, than in the container experiments from Gran and NGI. Uranium concentrations are also an order of magnitude higher in the leachate from the test cell. This could be related to the different origins of the black shales. If that is the case, it seems like the alum shale from the Oslo area pose a greater environmental risk than the Gran shale. The differences in metal concentrations could also be a result of much larger quantity of shale being stored in the NOAH Langøya test cell than what is stored in the containers, giving a different ratio of solid to liquid (precipitation). It should also be noted that the sampling has been much more scattered for the containers from Gran, and longer periods have been without sampling. Thus, the highest concentrations that have leached from these containers might not have been measured.

In the Gran containers, there is a distinct difference between the shale that originates from the tunnel (AT1 and G2) and the shale from the cuttings (A3). The pH drop happened faster in the shales from the tunnel, and there seem to be a seasonal variation in leachate pH of the A3 container. This is likely due to a greater neutralizing potential in the shale from the road cutting (A3), estimated from Ca content measured by XRF (Statens Vegvesen, 2017)

There is also a difference between the two shales taken from the tunnels, where one container contains Alum shale (AT1) and the other Galgeberg shale (G2). The Galgeberg shale is expected to have a lower potential for acid production compared to the alum shale (Pabst et al., 2017), but some of the highest measurements of metals is in leachate from the G2 container. Concentrations in the G2 leachate gets especially high in the 1.5 year of sampling, when pH falls below 3. The AT1 alum shale container has a pH below 3 for almost all sampling points measured after year 5.

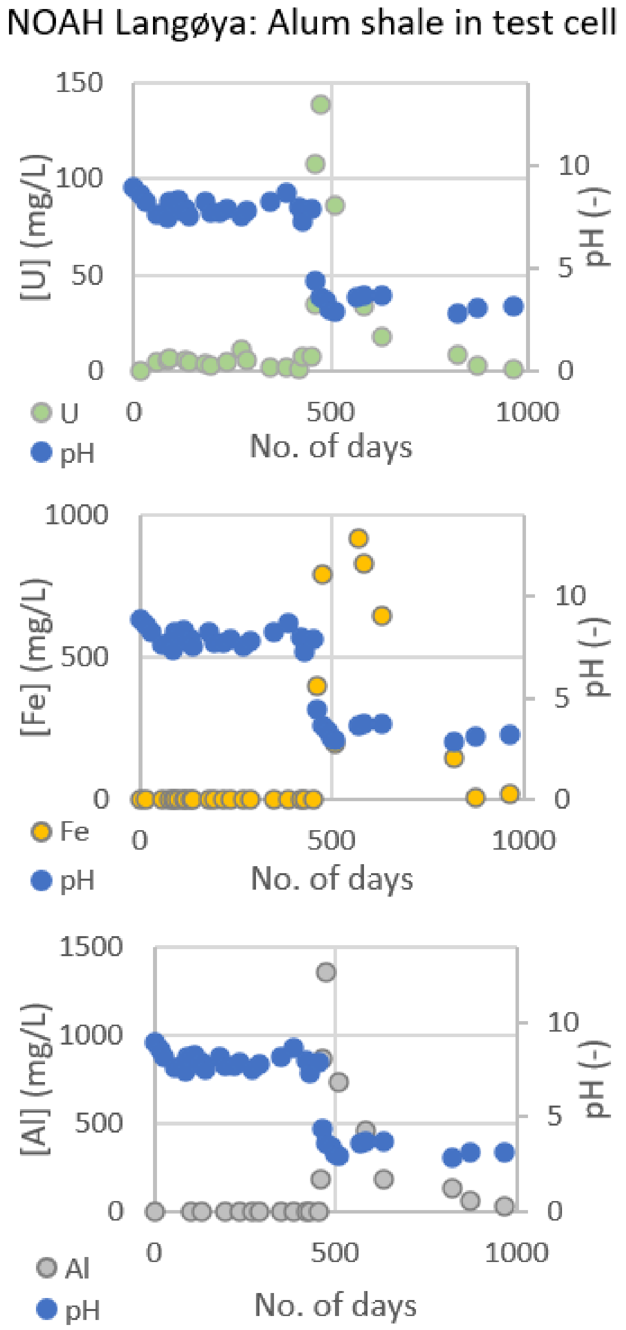

Figure 13 Concentrations of uranium, iron and aluminium in leachate from test cell with alum shale set up by NOAH.

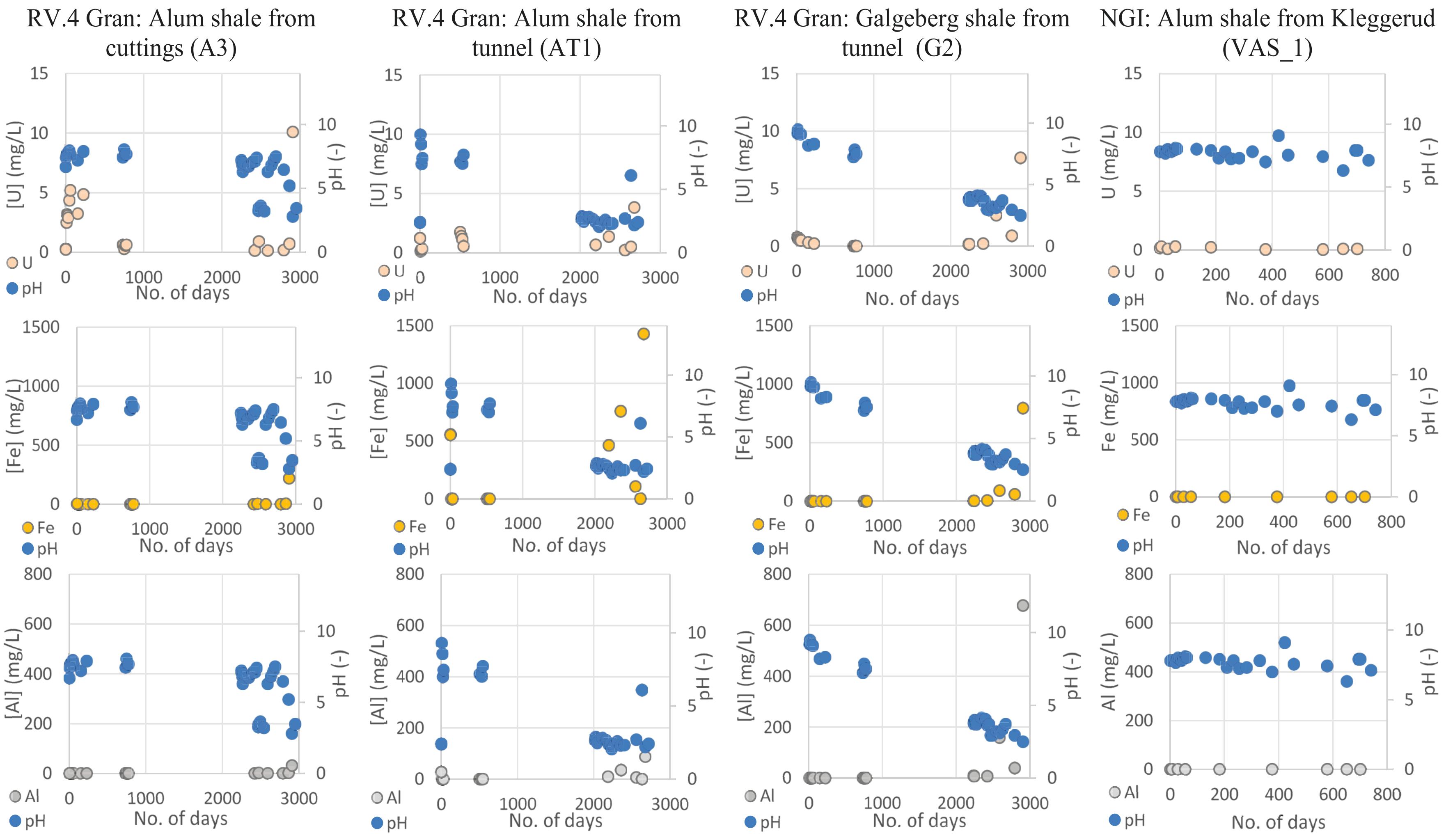

Figure 14 A comparison between container experiments with long time series for pH, uranium, iron and aluminium.

In addition to the cases of NOAH Langøya and Gran, there are the even longer-term cases like Taraldrud. Here, we don't have time series with results, but we know that the shale has been lying there for 25- 45 years. Through sampling of the shale it is evident that only parts of the shale have been oxidized and are producing leachate with low pH, even though most of the deposited rock masses have low NP:AP and are expected to be acid producing. Thus, this shows the importance of storage conditions, and when arranging proper storage conditions, acid-production can be postponed or avoided.

4.3.1 Column experiments: NOAH Langøya and NGI (Kleggerud)

Both NOAH Langøya and NGI (Kleggerud shale) set up large scale, outdoor experiments and small-scale, indoor column experiments with the same rock masses. When comparing the two treatments, we see that pH drops faster in the column experiments in both cases. For the NGI (Kleggerud) shale (Figure 15), pH in the columns started dropping after almost 10 months, while in the container experiments the pH is still neutral after 2 years of sampling. For the NOAH columns, pH dropped after a bit more than 10 months, and in the test cell with the same shale it took about 15 months (Figure 16). The faster pH drop in the lab experiments is likely caused by larger surface area (smaller grain size), higher temperature or different watering frequency. It can also be caused by preferential flow in the column that can occur if the water always flows in the same path and the carbonates are spent in this specific area.

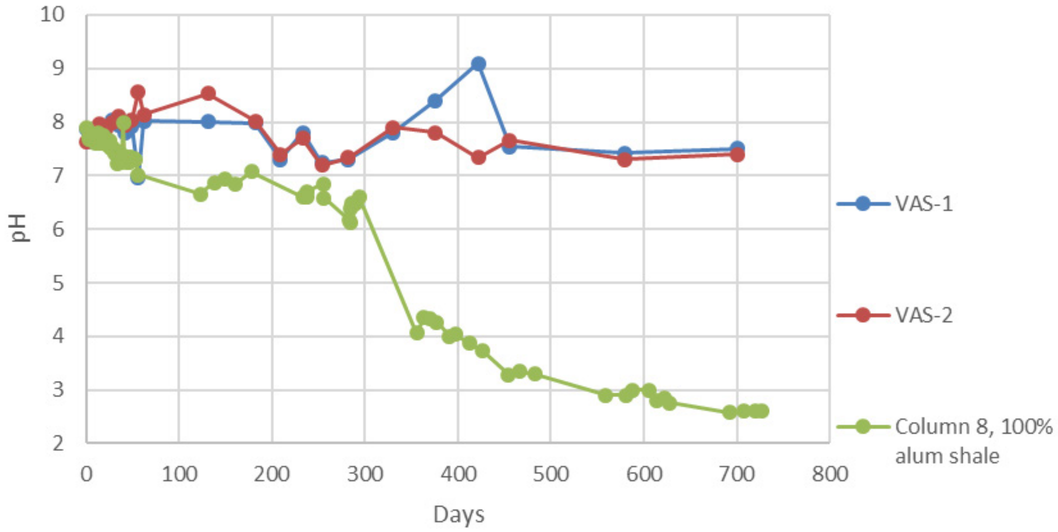

Figure 15 Comparison of pH measured with time in leachate from column and containers (VAS-1 and VAS-2) with alum shale, set up by NGI with Kleggerud shale. Columns have grain size 0-22 mm and containers have all sizes of blasted rock (0-250 mm).

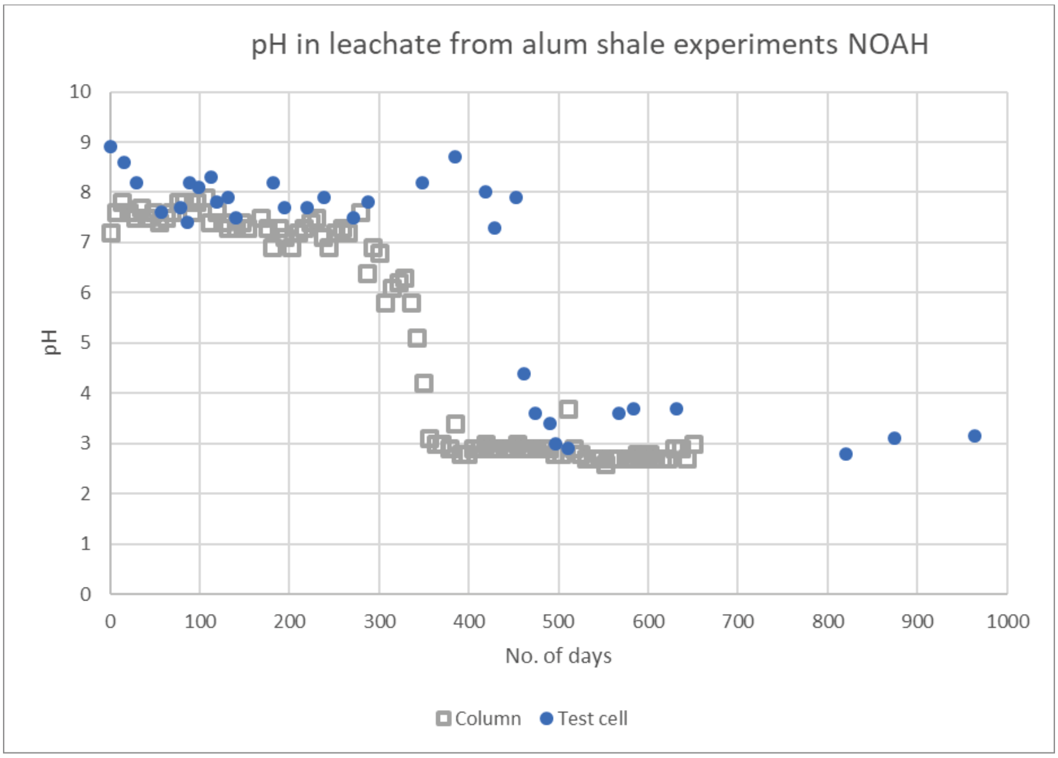

Figure 16 pH measured with time in leachates from column and test cell set up with the same alum shale (NOAH, Oslo centre).

4.4 Effect of mixing with basic materials

Both in the column tests at NOAH and in some of the container experiments at Gran (not the ones presented in Appendix A), alum shale was tested together with basic materials (Statens vegvesen, 2017). At Gran, shale was mixed with limestone ($CaCO_3$) or dolomite ($CaMg(CO_3)_2$), to prevent acid formation. In some of the columns at NOAH, the alum shale was covered with basic waste material, partly to test for the same pH effect as at Gran. In the Gran samples, adding limestone increased the leaching of Pb from the Galgeberg shale, while adding dolomite increased leaching of U, Ni and Cu from both the alum shale and the Galgeberg shale, compared to other parallels without limestone or dolomite mixed in. This does not mean that adding neutralizing materials is negative, as these relatively higher concentrations of selected elements represent better water quality than will prevail during acid runoff. The most important in the long term is to avoid acid runoff, but it is worth noting that the addition of basic materials can increase the leaching of certain elements on the short term.

Figure 17 shows pH and aluminium in the leachate from alum shale from NOAH Langøya and Gran, with and without addition of limestone. From the comparison, it can be noticed that the pH drop in the tests without limestone facilitates a release of metals, here aluminium. There is no such pH drop observed in the tests with added limestone, and hence no drastic increase in detected aluminium concentrations in the leachate. However, for the alum shale added limestone for NOAH Langøya, the pH-values show a decreasing trend from almost eight to about six, and the second-to-last sample that was measured had a pH of 2.5. This might indicate that a drop in pH was close to happening. This was supported by results for U, Ni and Cu that were elevated in the same sample, thus supporting that this was not simply an erroneous pH measurement.

From the tests, it seems like addition of basic materials helps buffering the pH drop. Keeping the pH above neutral will prevent the release of some of the metals that are tied up in the alum shale.

In the column tests performed at NOAH, the effect seen might also be a result of prevention of weathering due to little oxygen present in the system. The watering of columns was done to mimic natural conditions, and therefore the water was applied periodically, also allowing oxygen to intrude between watering. The air flow can still be restricted, potentially making oxygen the limiting reagent to the reactions.

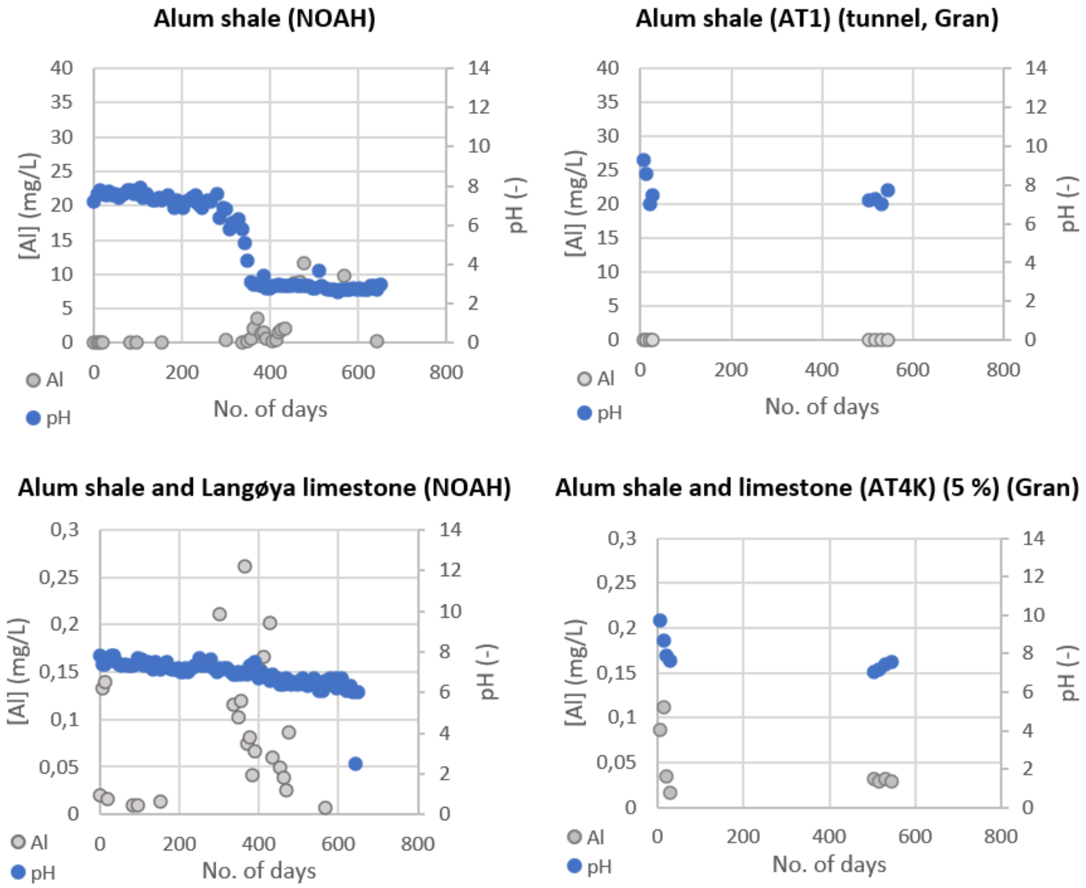

Figure 17 Results from column leaching tests with alum shale and alum shale added limestone at NOAH and Gran. Note that the y-axis varies from graph to graph. For the AT1 containers, results from later time points are presented in Figure 14.

A comparison of leachate concentrations for tests at NOAH Langøya and Gran is shown in Figure 18 (alum shale with bottom ash and limestone (5%)) and Figure 19 (limestone and limestone (5%)). As the plots show, the development of pH is quite similar at both locations. For all additives there is a slow decrease of pH in the leachate, probably due to shale weathering. No drastic pH drop is seen within the time frame of the experiments with these additives. The metal concentrations in the leachate though varies a bit, but the Gran experiment has too few datapoints to conclude if there is a real difference or that the variations are not detected.

High iron values for the column with bottom ash and column with limestone was unexpected as the pH was neutral and iron is not expected to be soluble.

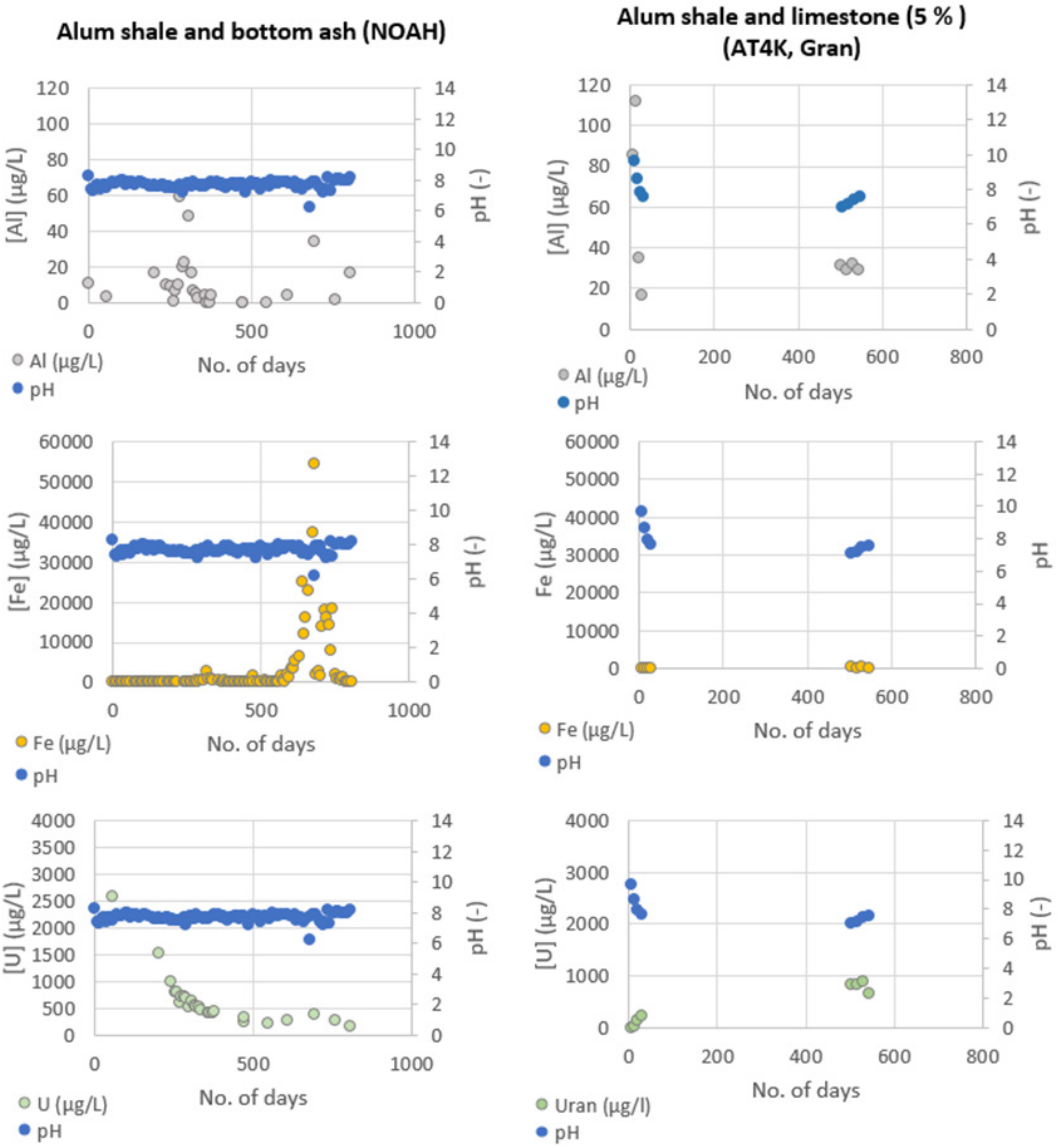

Figure 18 Results from leaching tests with alum shale added bottom ash (NOAH) and 5 % limestone (Gran)

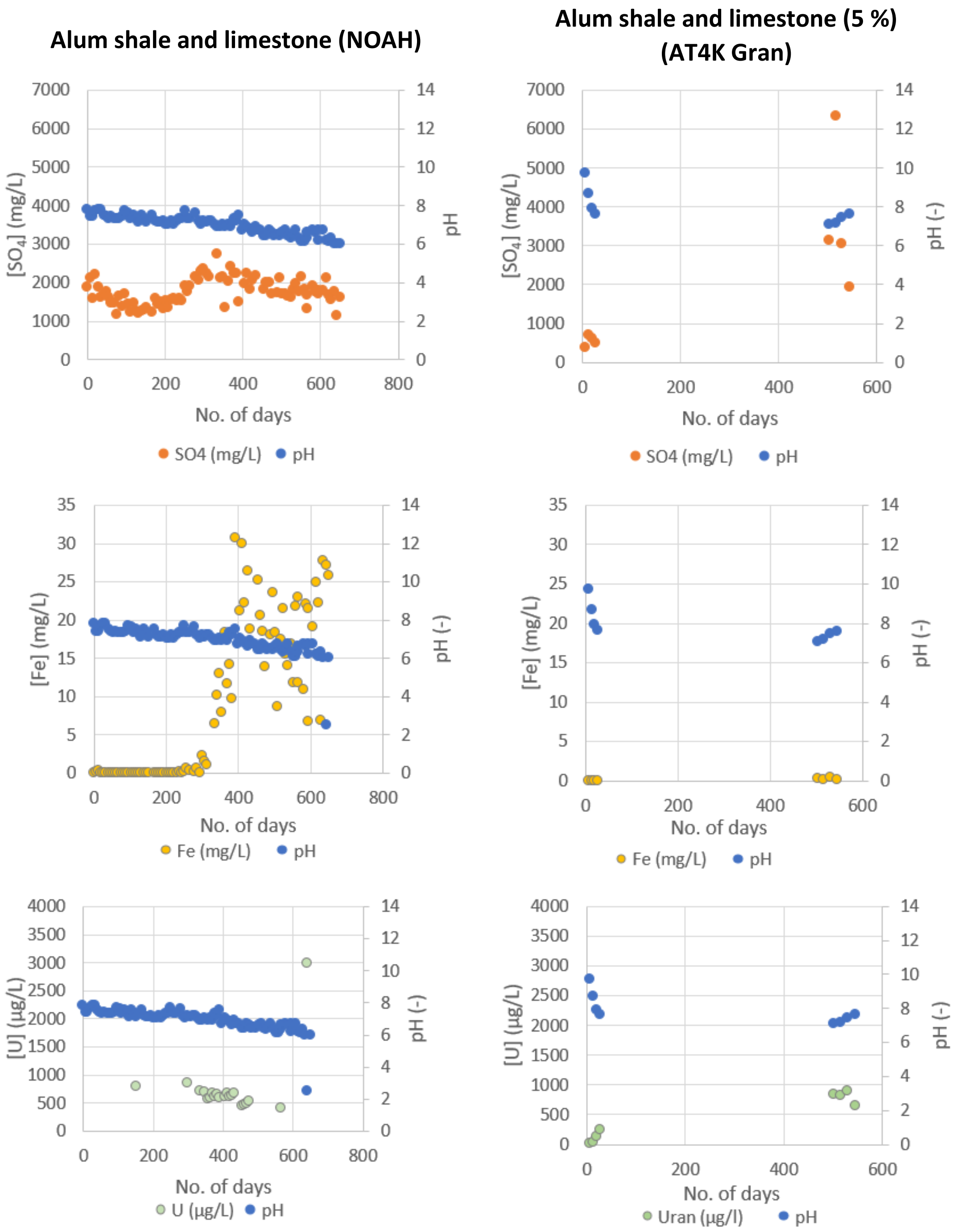

Figure 19 Results from leaching tests with alum shale added limestone (NOAH) and 5 % limestone (AT4K Gran)

4.5 Self-heating

An important reason to prevent long-time temporary storage of ARD producing black shales is the risk of self-heating. Self-heating can occur in crushed sedimentary rocks containing significant amount of organic matter, such as shales, oil sand and coal. These materials are permeable for water and air and have a large surface area allowing chemical or bacterial oxidation of certain minerals to take place if oxygen is supplied. Oxidation of sulphide minerals is an exothermic reaction which raises the temperature in waste rock piles. As temperature increases, the rate of oxidation is accelerated, which again will rise the temperature even further. Fine particles are more reactive than coarse particles. The reaction alone is not enough for the shale to self-ignite. The temperature rise is determined by the balance between the rate of heat generation and the rate of heat losses (Restuccia et al., 2017). The temperature can rise to the point of self-ignition, but to ignite, the air pressure and the access of oxygen have to be favourable (NOMIKO, 2019).

Two of the projects in this report have documented self-heating; NOAH Langøya and New access road to Kistefos Museum.

In the test cell at NOAH Langøya, the temperature was measured continually. Temperatures the first year were below 30, but generally higher than surrounding outdoor temperature. The results showed that after about a year, the temperature rose to approximately 40 °C. NOAH chose to intervene in the experiment at this point, flushing the cell with basic water and covering the cell to slow down the chemical reactions causing the temperature to increase. The measurements of temperature and leachate quality continued. The temperature in the test cell was about 25 °C throughout the winter, after flushing of the cell. Temperatures in other alum shale disposals at Langøya are also elevated with temperatures up to 40-50 °C even in winter (personal communication, Toril Roberg, 2018).

At Jevnaker (New road to Kistefos Museum), the mixed piles consisting of monzonite, syenite and black shale (about 20 % in pile 1 and > 30 % in pile 2) were left in open air for about two years before pile 2 was covered by a tarpaulin (excavated in April 2017, covered in January 2019). The tarpaulin was first not well maintained, and the pile was only partly covered from April to June 2019. In the summer months, the tarpaulin was better secured, and there was a better protection of the pile. In August 2019, self-heating was reported in pile 2. The probable cause of the self-heating was that the sulphuric minerals in the shale had started oxidizing due to the two years long period with access of water and oxygen, generating heat. When the pile was covered, the tarpaulin probably contributed to trapping the heat building up in the pile, consequently accelerating the oxidizing reactions in the pile to a point of self-heating.

Based on the limited project experiences summarized in this report, a few advices can be given to prevent self-heating. Preventing self-heating goes hand in hand with preventing acid rock drainage and leakage of metals from the black shales. The test cell at NOAH shows that the rise in temperature is seen simultaneously to the lowering of pH and release of heavy metals detected in the leachate. This is logical, as it is the same chemical reactions causing all effects. Pyrrhotite can be an important factor in this context, as it has been shown to catalyse the oxidation of pyrite (NGI, 1957).

The chemical reactions were resulting in self-heating about a year after start of storage at NOAH. For the Kistefos samples the start of self-heating is unknown as temperature was not monitored in the beginning, but high temperatures were measured after two years. Factors that likely affect heat production are amount of alum shale (at Kistefos there was mixed masses), amount of fine-sized material, and the access to moisture and oxygen. Factors affecting the heat loss will include the size of a pile of materials and covering of the pile. The NOAH test cell was not covered when self-heating started, while the Kistefos samples were covered when high temperatures were measured. At Kistefos, Pile 2 had lower porosity than pile 1, which contained coarser material and did self-heat.

These examples show that by inappropriate storage of black shale masses, there is a risk of self-heating if storage time exceeds about a year (for previously unweathered masses).

4.6 Permanent storage solutions

Vilberg and Taraldrud are deposits of black shale from similar geographic origin (Oslo city centre, mainly alum shale from horizons 2 and 3a). Both were established as permanent storage solutions. At Taraldrud, the material has been stored for 25-45 years (see Appendix A). In 2008 it was discovered acid drainage from parts of the area (NGI, 2017). The masses at Vilberg were previously stored at Enebakk for several years, and started to produce acid drainage. When moved to Vilberg the masses were encapsulated in clay to prevent water flow and air intrusion.

Even though the geographic origin of the shale is quite similar, the different storage conditions makes the end result different. At Vilberg, groundwater wells have been established in, downstream and upstream the deposited masses and have been sampled regularly. No negative effects on the groundwater have been detected, 13 years after deposition. At Taraldrud, parts of the deposit have acid runoff with high concentrations of metals. A purification facility has been established, but there are still elevated concentrations of metals detected downstream. The main difference between these two storage areas is that the storage solution at Vilberg is better than at Taraldrud.

At Taraldrud, there was a large rebuilding of the area around 2000-2004, when two lanes were added to the road E6 and the access ramp was changed. During this work, the access ramp was established on top of parts of the alum shale deposit, with a very short distance for runoff to percolate down to and through the shale. A continuous cycle of watering and drying of the masses have been happening, accelerating the weathering processes in the shale, leading to large flushes of water with low pH and high concentrations of heavy metals.

4.7 Downstream water concentrations

For some of the projects, downstream water concentrations are available. For these projects, it is possible to evaluate the risk that the storage solution poses to the natural environment:

- Vilberg: Concentrations in filtered water from downstream groundwater well B3 (average of 16 samples, 2017-2020), from NGI (2020a).
- Taraldrud: Concentrations in unfiltered water from downstream creek (point V6 in Snipetjernsbekken, from NGI (2016a)). A purification dam (fellingsdam) for water from the deposit area is established between the landfill area and the creek so the concentrations would presumably be higher without purification.
- E16 Kleggerud: Concentrations in filtered water from downstream creek (point V3, reported in NGI (2020), see table 6 in Appendix A). The concentrations in the creeks are mainly a result of natural runoff from alum shale bedrocks in the area but are also influenced by the waste rock fills from the new road to Kistefos stored along E16.

The measured concentrations of Al, Ni, U and Mo are compared in Figure 20. As the figure shows, the concentrations of aluminium and nickel are much higher downstream Taraldrud than at the other locations. This is probably because the purification dam is not efficient enough to remove all the elements from the deposit water, possibly due to lack of maintenance. The water sample from Taraldrud is unfiltered. As the pH at all sites is circumneutral (Figure 21), aluminium is expected to be present as colloids or precipitated, thus not available for uptake in organisms (Rosseland et al. 1992).

For uranium and molybdenum, the concentrations at Taraldrud are low and similar to the concentrations found at Kleggerud, where the concentrations are mostly due to natural leaching from the bedrock. The concentrations of molybdenum and uranium are higher at Vilberg than at the other locations, but still lower than PNEC (= predicted no-effect concentration) for the element (12 700 µg Mo/L (Heijerick and Carey, 2012) and 5 µg U/L (Sheppard et al. 2005)), and therefore poses no risk to the environment.

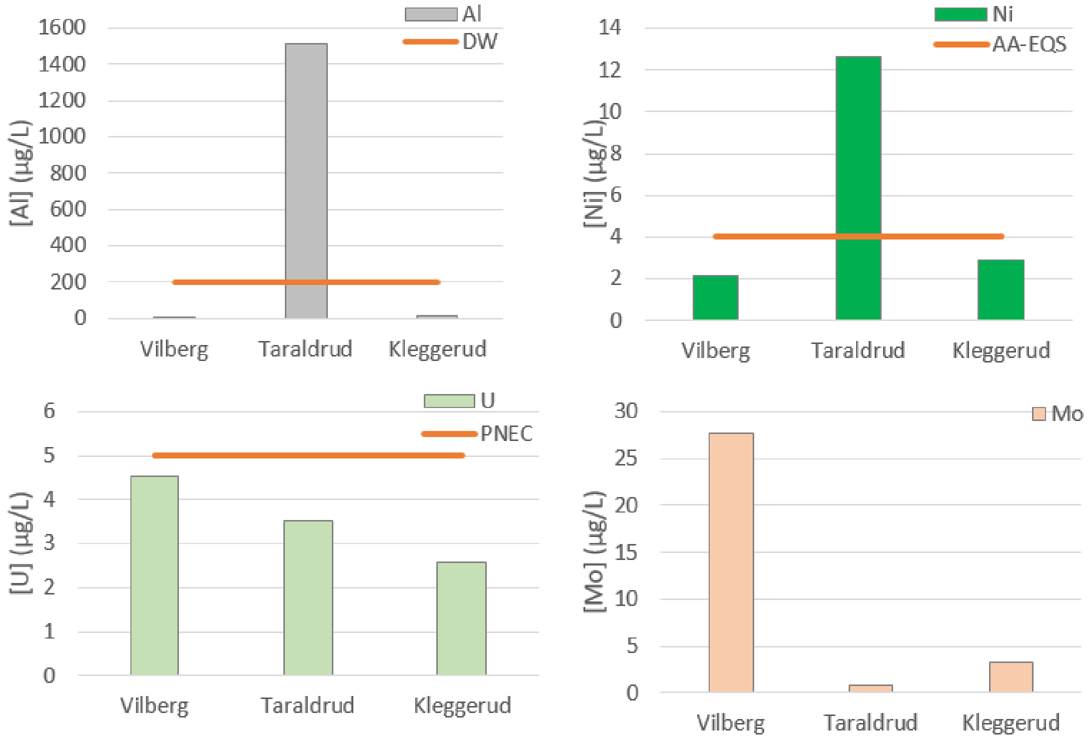

Figure 20 Concentrations of Al, Ni, U and Mo detected downstream sites Vilberg, Taraldrud (after treatment) and E16 Kleggerud. Note that the Taraldrud sample is unfiltered while the other samples are filtered. Relevant threshold values are also shown (DW = threshold value for Norwegian drinking water; AA-EQS = annual average environmental quality standard, defined by the water framework directive; PNEC = predicted no-effect concentration). Note that for Mo, the PNEC (12 700 µg/L) is much higher than the measured concentrations and therefore not shown in the graph.

Measured pH is shown in Figure 21, and is circumneutral for all sites.

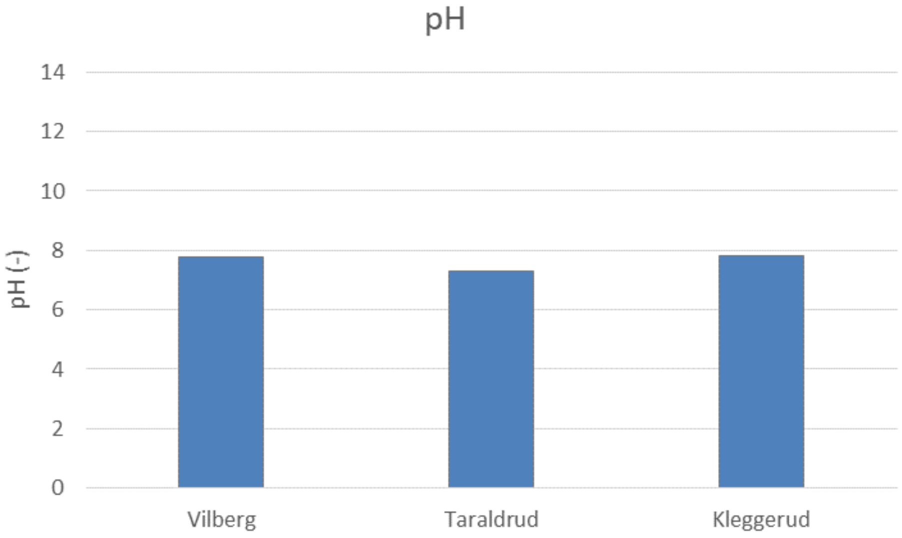

Figure 21 pH-values measured downstream the sites.

5 Conclusions

5.1 Change in pH with time

The various case studies discussed in this report indicate that black shale can be stored temporarily for a longer period than the current recommendation of 8 weeks. This is seen through the case studies with container experiments at Gran and at NGI (with rock from Kleggerud), and the test cell at NOAH Langøya. In these three cases, alum shale has been stored in open air for minimum a year without a drop in pH. The drop in the test cell at NOAH Langøya happened shortly after a year, while the pH-drop in the Gran containers happened after 1.5 years but before 5.5 years of experiment. The container experiments with alum shale from Kleggerud set up at NGI have not had a pH drop yet (after 2 years), but s will run for 6 more years giving a long time series providing results for future evaluations of alum shale properties.

The laboratory column experiments that were associated with two of the big scale experiments (the test cell at NOAH and the container experiments at NGI) got faster pH drops. This is likely due to smaller grain size and higher average temperature in the lab experiments but can also be affected by a different frequency of drying and wetting. The results for temporary storage are pertaining to blasted rock masses, that have varying size fractions including quite large pieces.

These suggestions for temporary storage are meant for freshly excavated black shales. For already weathered shales, there can be a much quicker development of acid, metal rich leachate and these results are thus not applicable.

Even if the results from different projects show that the acidification process is not instant, it is always recommended to minimize the time of temporary storage. Avoiding water flowing through the masses will reduce the environmental impact, and also reduce the deposit costs as wet masses will weigh more on delivery to a disposal site. While it can be challenging to avoid precipitation on piles or stored masses, one should always avoid contact with flowing surface water.

5.2 Metal leaching during temporary storage (neutral rock drainage)

While temporary storage of black shales should be too short for acid runoff to form, stored masses can still release metals and radionuclides (neutral rock drainage). The metal concentrations measured downstream Vilberg, Taraldrud and Kleggerud (E16) are mainly below the environmental limits (Norwegian Environmental Agency, 2016), except Ni that exceeds the AES-EQS and Al that is likely present as colloids, not toxic, monomeric Al. These sites represents active NRD sites (as the acid runoff at Taraldrud is neutralized), and there is not a great concern regarding these data.

The pH and metal concentrations in the presented results demonstrate that if the acid-producing masses are already weathered or are stored long enough for acid runoff to form, there can be detrimental effects on the downstream water environments.

Note that the levels of uranium in the leachates often makes it necessary to apply for a release permit from the Norwegian Radiation and Nuclear Safety Authority during construction work. The same can also apply to leaching of metals and a release permit from the relevant authorities may be necessary.

It may be necessary to do a site-specific risk assessment for places for temporary storage to identify if there are any vulnerable recipients and to predict whether metal leaching from temporary stored black shale masses will be a problem.

5.3 Addition of neutralizing materials

The addition of basic or neutralizing materials to acid-producing shale can delay or prevent a pH drop. Different basic materials were tested at NOAH Langøya, yielding varying results regarding the efficiency in neutralizing acid. Thus, materials should be tested for their efficiency before use. Results from container experiments from Gran indicates higher release of metals on the short term with addition of limestone or dolomite. For short-term temporary storage, such treatment is anyway normally not necessary, but the possible increase in release of metals should be taken into account if this is considered.

5.4 One stage batch leaching test (Ristetest)

One stage batch leaching test do not predict the resulting pH of acid-producing rock masses as the weathering reactions are too slow to be observed in such a test. For acid-producing black shales, the greatest leaching of heavy metals happens after weathering has triggered a reduction in pH, and a short-term leaching test will give little information about the long-term leaching potential.

We did see a relation between S content of the tested masses and sulphate in the leachates, and there was a positive correlation between the pH and the NP:AP ratio.

One stage batch leaching test may give useful information for leaching of metals during a period of temporary storage, as well as the weathering degree of tested masses. Already weathered material can give low pH and high concentrations of sulphate when tested with one stage batch leaching test. If larger pieces of weathered material are crushed to do the test, low pH and ongoing ARD may be masked by carbonates released from the inner parts of the rock pieces.

5.5 Self heating

The results from the test cell at NOAH and the piles of mixed rock from Kistefos demonstrates that there is a risk for self-heating in masses of black shales that are not properly stored. Factors affecting this probability will likely be reactivity of the rock masses (e.g. content of sulphides and neutralizing material), size distribution and porosity of the rock masses, storage conditions including height of pile, moisture and air circulation in the pile. The example from Jevnaker (New road to Kistefos Museum) shows that even masses mixed with other types of rock can heat up to 400 °C locally if the conditions are right.

Generally, the results show that to reduce the risk of self-heating, temporary storage should be limited to as short as possible. Secondly, while covering the masses with e.g. a tarpaulin can be advantageous to reduce the oxidation reactions, this can likely function as a heat trap if the weathering reactions are already going strong and are not sufficiently slowed down by the covering. Thus, such covering measures should be done from the start of the temporary storage period. According to Hudak (2002) spreading the material in thin layers and compacting it will inhibit air circulation and segregation of fines that might otherwise lead to self-heating. Note that compacting may increase the content of fines (surface area).

5.6 Further work

Results from the case studies also show that the reactivity of alum shale can differ substantially even though it is characterized to origin within the same alum shale horizon, and more information is needed to predict reactivity of black shales with regard to foresee acid-producing properties as well as the risk of self-heating.

The container experiments are planned to continue until 2028 as a part of centre for research-based innovation earthresQue (NMBU). Follow up of such long-term experiments should be regular to avoid missing information causing uncertainties.

6 References

Alloway, B. J. (2013). *Heavy Metals in Soils: Trace Metals and Metalloids in Soils and their Bioavailability* (B. J. Alloway & J. T. Trevors Eds., 3rd ed.): Springer.

Appelo, C. A. J., & Postma, D. 2010. Geochemistry, groundwater and pollution (2nd ed.): CRC press.

Falk, H., Lavergren, U., & Bergbäck, B. (2006). Metal mobility in alum shale from Öland, Sweden. *Journal of Geochemical Exploration, 90*(3), 157-165. doi:http://dx.doi.org/10.1016/j.gexplo.2005.10.001

Forskrift om radioaktiv forurensning og avfall (2010). Forskrift om forurensningslovens anvendelse på radioaktiv forurensning og radioaktivt avfall. Klima- og miljødepartementet, https://lovdata.no/dokument/SF/forskrift/2010-11-01-1394.

Heijerick and Carey 2012. The toxicity of molybdate to freshwater and marine organisms. II. Effects assessment of molybdate in the aquatic environment under REACH. Sci Total Environ. 2012 Oct 1;435-436:179-87. doi: 10.1016/ j.scitotenv.2012.05.075.

Hudak P.F. 2002. Spontaneous combustion of shale spoils at a sanitary landfill. Waste management 22:687-688.

IAEA 2003. Guidelines for Radioelement Mapping Using Gamma Ray Spectrometry Data. IAEA-TECDOC-1363. IAEA, Vienna.

Lawrence, R. W., & Wang, Y. 1996. Determination of Neutralization Potential for Acid Rock Drainage Prediction. MEND Project 1.16.3. A report of laboratory investigations prepared for Environment Canada and Hudson Bay mining and smelting.

Lovdata 2010. Forskrift om forurensningslovens anvendelse på radioaktiv forurensning og radioaktivt avfall. FOR-2010-11-01-1394.

NGI 2017c. Taraldrud – Grunnforurensning svartskifer. Geokjemisk kartlegging og volumestimat av svartskifer. NGI report 20160766-01-R.

NGI 1957. Bidrag til belysning av visse bygningstekniske problemer ved Oslo-områdets alunskifere. Publikasjon nr. 22.

Norwegian Environmental Agency (Miljødirektoratet) 2022. Håndtering av potensielt syredannende svartskifer. Fagrapport M-2105.

Norwegian Environmental Agency (Miljøfirektoratet) 2016. Grenseverdier for klassifisering av vann, sediment og biota – revidert 30.10.2020. Veileder M-608.

Norwegian Environment Agency (Miljødirektoratet) 2015a. Identifisering og karakterisering av syredannende bergarter. Veileder M-310.

Norwegian Environment Agency (Miljødirektoratet) 2015b. Deponering av syredannende bergarter. Fagrapport M-385.

NGU 2005. Uranium in drinking-water? NGU-fokus No. 6-2005.

NOMIKO 2019. Branner i avfallsbransjen – årsaker og tiltak. Rapport datert: 2019-03-20.

Owen A.W., Bruton D.L., Bockelie J.F. and Bockelie T.G. 1990. The Ordovician successions of the Oslo region, Norway. NGU special publication 4.

Pabst T., Sørmo E. and Endre E. 2017. Geochemical characterisation of Norwegian Cambro-Ordovician black mudrocks for building and construction use. Bull Eng Geol Environ (2017) 76:1577–1592. DOI 10.1007/s10064-016-0941-z.

Restuccia F., Ptak N. and Rein Guillermo 2017. Self-heating behaviour and ignition of shale rock. Combustion and flame 176:213-219.

Rosseland, B. O., Blakar, I. A., Bulger, A., Kroglund, F., Kvellstad, A., Lydersen, E., Oughton, D. H., Salbu, B., Staurnes, M., & Vogt, R. (1992). The mixing zone between limed and acidic river waters: complex aluminium chemistry and extreme toxicity for salmonids. Environmental Pollution, 78(1–3), 3-8. doi:http://dx.doi.org/10.1016/0269-7491(92)90003-S

Sheppard S.C., Sheppard M.I., Gallerand M.-O. and Sanipelli B. 2005. Derivation of ecotoxicity thresholds for uranium. J Environ Radioact. 2005;79(1):55-83. doi: 10.1016/j.jenvrad.2004.05.015.

Singer, P. C., & Stumm, W. 1970. Acidic Mine Drainage: The Rate-Determining Step. Science, 167(3921), 1121-1123. doi:10.2307/1728684.

Statens vegvesen (Norwegian Public Roads Administration) 2017. Utlekkingsforsøk med svartskifer fra Rv. 4, Hadeland. SVV report no. 665.

Swanson, V. E. (1961). *Geology and Geochemistry of Uranium in Marine Black Shales, A Review. Uranium in Carbonaceous Rocks*. https://pubs.usgs.gov/pp/0356c/report.pdf

Tourtelot, H. A. (1979). Black shale - its deposition and diagenesis. *Clays and Clay Minerals, 27*(5), 313-321.

WHO 2012. Uranium in drinking water. Background document for development of WHO guidelines for drinking water. World Health Organization.

Appendix A

CASE STUDIES

Contents

Introduction

The data collected, analysed and discussed in this report comes from different black shale projects around the Oslo area. The cases have been chosen based on projects were both rock and water analyses were available.

A1 E16 Kleggerud (NGI container and column experiments)

A1.1 Characterisation of the rock masses

During construction of new E16 between Eggemoen and Olum, about 7-9 tons of alum shale (horizon 2 and 3a) was taken from an alum shale blast performed 17.09.2020 in Kleggerudkrysset (see Figure 1 and Figure 2) and transported to NGI 21-09-2020. These masses were used to set up container and column experiments, and in the main report these masses are referred to as "NGI" in figures.

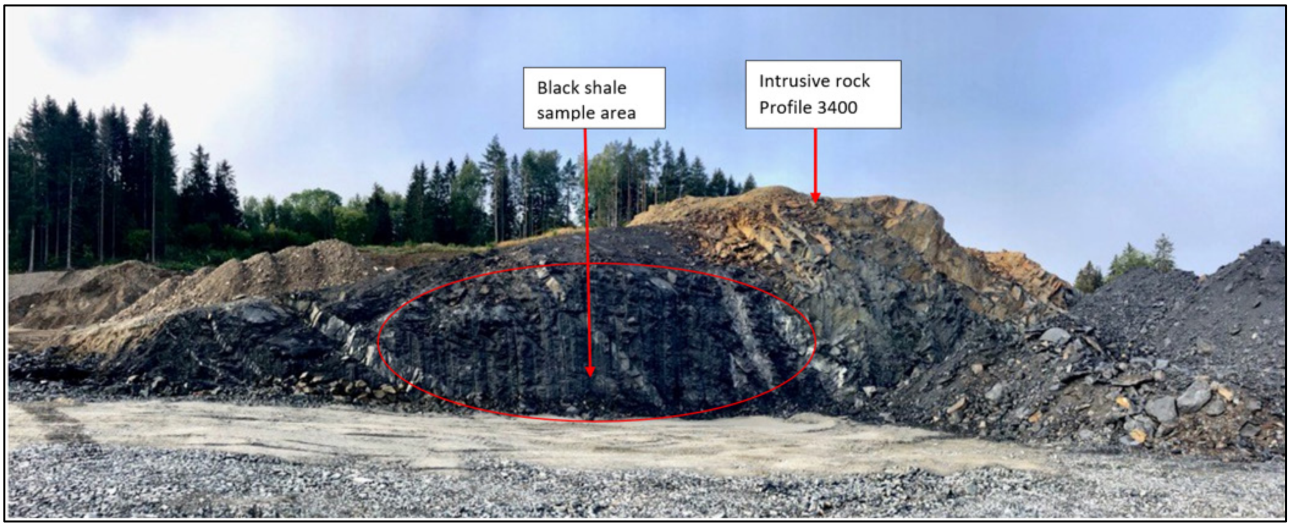

Figure 1 Black shale sampling area at Kleggerud for alum shale used in the container experiments set up at NGI. Photo: Andreas Harstad, Skanska AS.

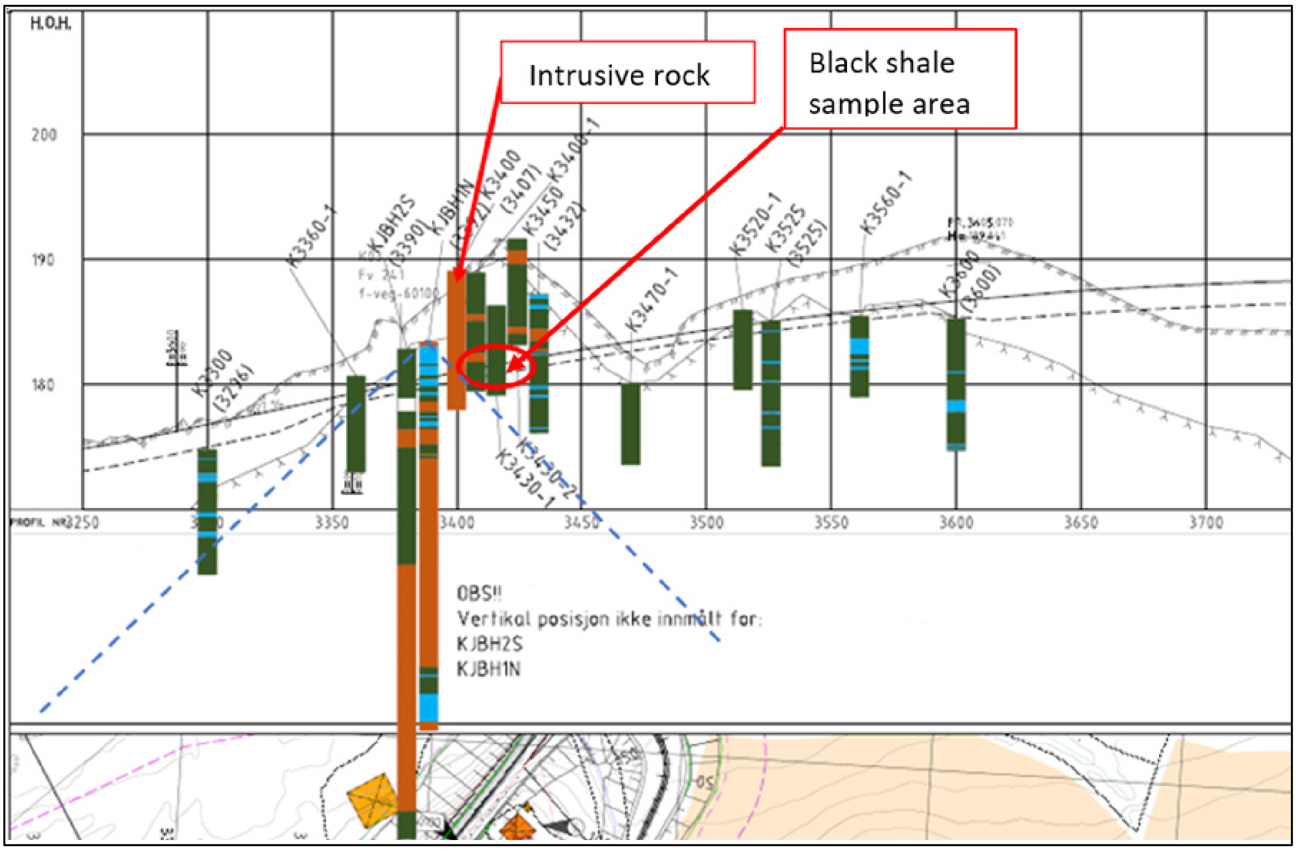

Figure 2 Cross section of road cutting at E16 Kleggerud. Placement and name of boreholes are indicated (Statens vegvesen Region Øst, 2019)

The chemical composition of the samples from Kleggerud were measured both with total chemical analyses of the rock samples at an accredited laboratory, and with pXRF calibrated specifically for use with black shales at NGI's laboratory. The results are given in Table 1. The analyses from the accredited laboratory show that the shale contains 18 900 mg/kg sulphur, 5.9 % organic carbon and 1.2 % CaO.

Table 1 Chemical composition (mg/kg) of black shale samples from E16 Kleggerud, measured with ICP-MS and pXRF.

Parameter		Black shale, accredited lab	Black shale, pXRF
As	mg/kg	46.4	45
Ba	mg/kg	733	523
Be	mg/kg	3.6	-
Cd	mg/kg	7.0	12
Co	mg/kg	19	-
Cr	mg/kg	89	83
Cu	mg/kg	94	83
Hg	mg/kg	0.0767	-
Mo	mg/kg	102	105
Nb	mg/kg	18	16
Ni	mg/kg	238	223
Pb	mg/kg	31	34
S	mg/kg	18 900	13 398
Sc	mg/kg	17	-
Sn	mg/kg	3.7	-
Sr	mg/kg	93	118
V	mg/kg	1860	1931
W	mg/kg	2.5	56
Y	mg/kg	39	45
Zn	mg/kg	379	476
Zr	mg/kg	158	162
Th	mg/kg	17	19
U	mg/kg	69	78
TOC	%	5.92	-
TIC	%	0.269	-
SiO_2	%	53.3	31.8
Al_2O_3	%	16	7.4
CaO	%	1.15	1.74
Fe_2O_3	%	5.23	4.17
K_2O	%	5.14	4.83
MgO	%	1.57	0.65
MnO	%	0.0268	0.018
Na_2O	%	0.476	-
P_2O_5	%	0.185	0.834
TiO_2	%	0.936	-
Loss on ignition (LOI)	%	9.1	-

The XRD results show that the black shale consists of 4.5 % pyrite and 1.2 % calcite (Table 2). In comparison, according to the ICP-MS analysis there is 18 900 mg/kg of sulphur, which would be equivalent of 7% pyrite assuming all sulphur in the form of FeS_2.

Table 2 Results from XRD of black shale from E16 Kleggerud as % of total weight.

Mineral	Content (%)
Illite+Mica	44.8
Kaolinite	0.1
Chlorite	TR
Quartz	29.9
K Feldspar	6.2
Plagioclase	4.3
Calcite	1.2
Dolomite	TR
Pyrite	4.5
Amorphous	9.1*

TR – trace (< 0.5 %)
* Amorphous matter for black shale was estimated from LOI.

To identify the black shale horizon of origin, the samples are plotted together with reference samples from the Oslo area, as described in chapter 3.1 in the main report. The results from the triangular plots are shown in Appendix B. The alum shale is from horizon 2 or 3a. There is an overlap between the reference material in these horizons and it is difficult to decide with certainty which horizon the alum shale belongs to.

To evaluate the potential acid rock drainage (ARD) from the two rock samples, AP and NP were plotted as seen in Figure 3. The alum shale ends up in the acidification zone and is expected to produce ARD.

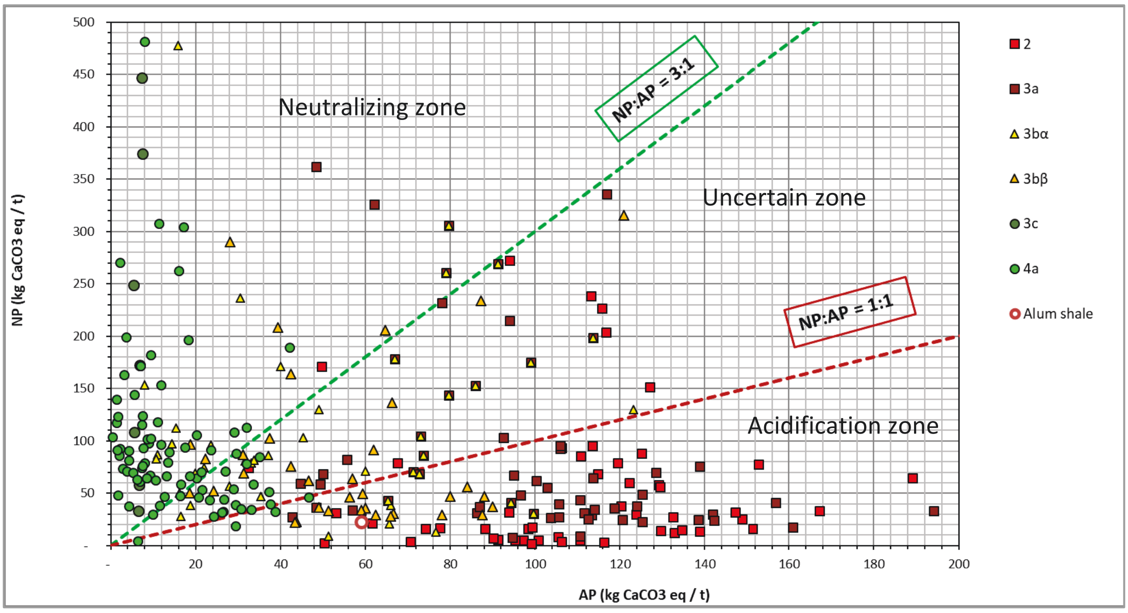

Figure 3 Acidification potential plotted against neutralizing potential for the alum shale from Kleggerud and reference samples (2, 3a, 3bα, 3bβ, 3c and 4a).

The ratio between iron and sulphur can be used as an indicator if the metals are tied up as sulphides or silicates. If the iron is in surplus compared to sulphur, it indicates that a greater part of the metals in the sample is combined in silicates or oxides. Heavy metals tied in silicates or oxides are less exposed to leaching since these minerals will not be oxidised and therefore are less soluble.

Samples at the line Fe=S 1:1 line in Figure 4 indicate that the metals mainly are combined as sulphide minerals. Samples over the Fe:S = 2:1 line indicate that the metals mainly are combined in silicates and oxides. The metals in the alum shale, are likely mainly combined as sulphides with an elevated potential for leaching.

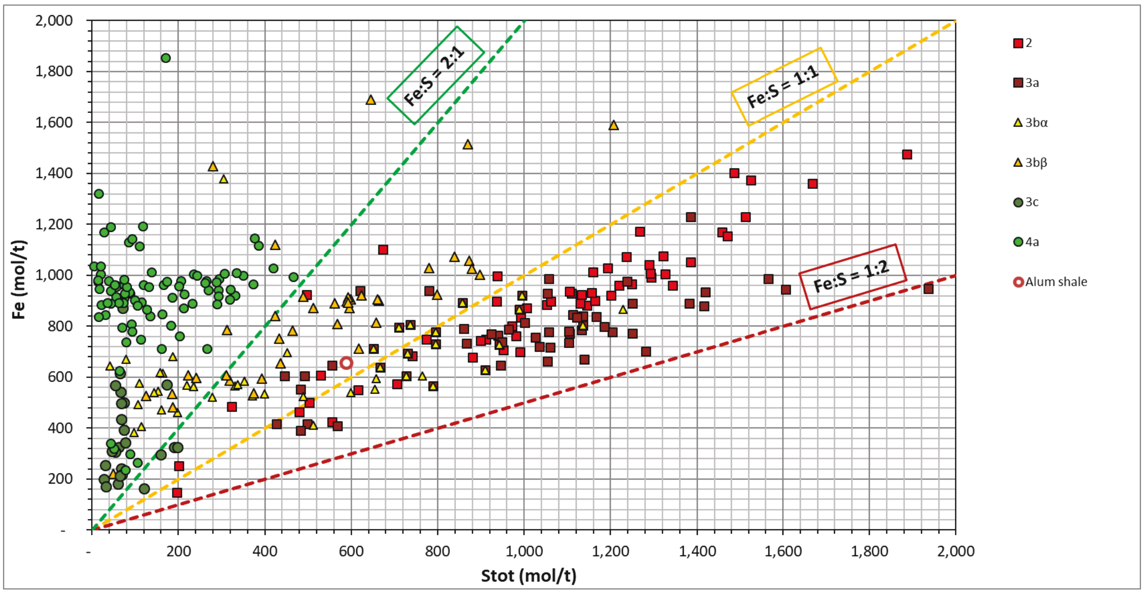

Figure 4 Total content of sulphur plotted against iron for the alum shale from Kleggerud, and reference samples (2, 3a, 3bα, 3bβ, 3c and 4a).

A1.2 Column experiments

The alum shale was also used for column experiments investigating the effect of grain size and mixing ratio (mixing with rhomb porphyry) on the leaching of metals and pH development. In this report the column with 100% alum shale is reported only. For details about the set-up of the column experiments and results for the mixed columns, see NGI (2022b, report 20200436-02-R).

Four kg alum shale with grain size distribution 0-20 mm was built into a column. The inner diameter of the column was 10 cm and the height of the alum shale masses was 35 cm. See Figure 5 for picture of the experimental set-up.

The column was watered manually with 500 mL distilled water five days a week for eight weeks (55 days) and sporadically thereafter for a total of 365 days. At every day with watering, pH, conductivity and redox potential were measured in the eluates.

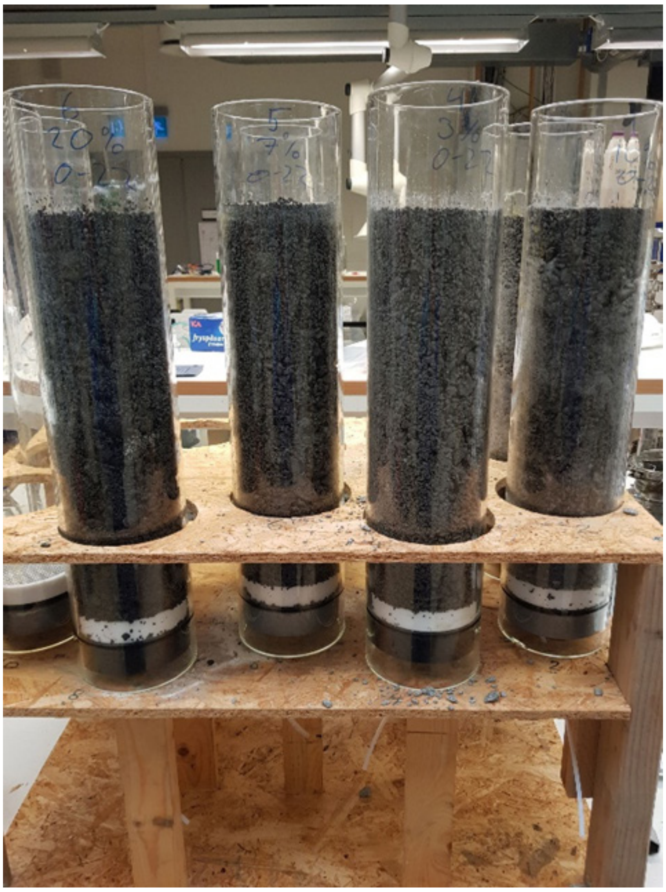

Figure 5 Experimental set-up of the column experiments in NGI's laboratory. Column diameter is 10 cm.

The eluates from the column with 100% alum shale showed a gradual decrease in pH from around 8 in the beginning to around 7 after 55 days and down to 4 after a year. After about 1.5 years, the pH is below 3. The conductivity is increasing from around 300 µS/cm from the start to 847 µS/cm after 40 days and 3-4000 µS/cm after 1.5 year (Figure 6).

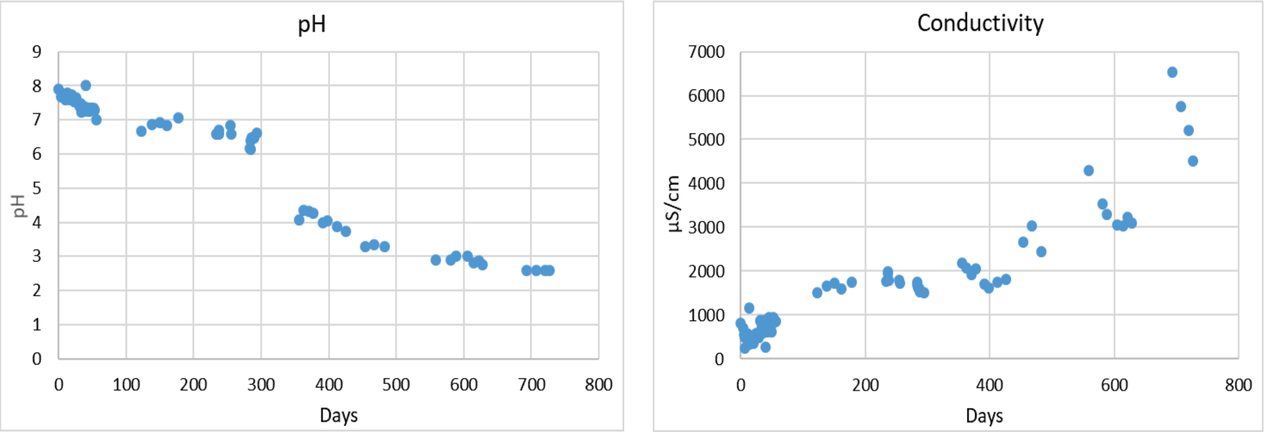

Figure 6 Development of pH and conductivity with time for eluates from columns with 100 % alum shale from E16 Kleggerud (grain size distribution of 0-22 mm).

At day 40, 365 and 730 of the column experiment eluates were sent to chemical analyses and results are presented in Table 3.

There is a significant increase with time for most of the metals and compounds in the eluates. The content of uranium for example, is more than five times higher in the 365 days eluate than in the 40 days eluate. Due to a misunderstanding uranium was not measured in the 730 days sample. For sulphate and magnesium, there is about a threefold increase in the concentration for each measurement, while calcium was stable from 1 to 2 years, see Figure 7 and Table 3. The metals nickel, zinc, cadmium and cobalt (Figure 8) increased 2-3 orders of magnitude in this period. Aluminium was 5000 times higher in the 365-days sample and further 150 times higher in the 730-days sample. This is explained by the lower pH affecting solubility of aluminium and weathering of the rock. A decrease in concentrations was measured for barium and molybdenum.

Table 3 Results chemical analyses of filtered eluates from columns with 100 % alum shale from E16 Kleggerud at day 40, 365 and 730. Note that not all the same analyses were done at day 730 compared to the two other measurements.

Element/compound	Unit	Day 40	Day 365	Day 730
Ca	mg/l	159	395	385
Fe	mg/l	<0.0004	0.0555	241
K	mg/l	9.44	13.2	8.18
Mg	mg/l	22.5	63	176
Na	mg/l	0.862	1.55	8.72
Al	µg/l	0.206	1 070	162 000
As	µg/l	0.197	<0.2	16.5
Ba	µg/l	20.5	12.2	6.06
Cd	µg/l	3.97	505	5 170
Co	µg/l	5.29	461	6 340
Cr	µg/l	<0.01	<0.05	114
Cu	µg/l	<0.1	280	19 800
Hg	µg/l	<0.002	<0.002	<0.002
Mn	µg/l	388	5 170	61 200
Mo	µg/l	319	0.64	<2
Ni	µg/l	960	10 500	118 000
Pb	µg/l	<0.01	14.8	81.8
Zn	µg/l	300	20 600	203 000
V	µg/l	0.0131	0.0334	72.5
U	µg/l	75	410	
Th	µg/l	0.074	<0.02	
S	mg/l	141	465	
Si	mg/L			48.3
Sr	µg/L			4 590
P	µg/L			869
pH		7.3	4.4	
Conductivity	µS/m	847	2 070	
Alkalinity at pH 4.5	mmol/L	1.5	-	
TOC	mg/l	0.57	1.8	
F-	mg/l	0.064	0.17	4.7
Cl-	mg/l	0.9	<1	<0.600
SO_4	mg/l	320	1 300	3 330
NO_3	mg/l	0.089	<0.10	<0.400
NO_2	mg/l	0.1	0.001	<0.300
NH_4^+	mg/l	0.062	0.0072	0.81

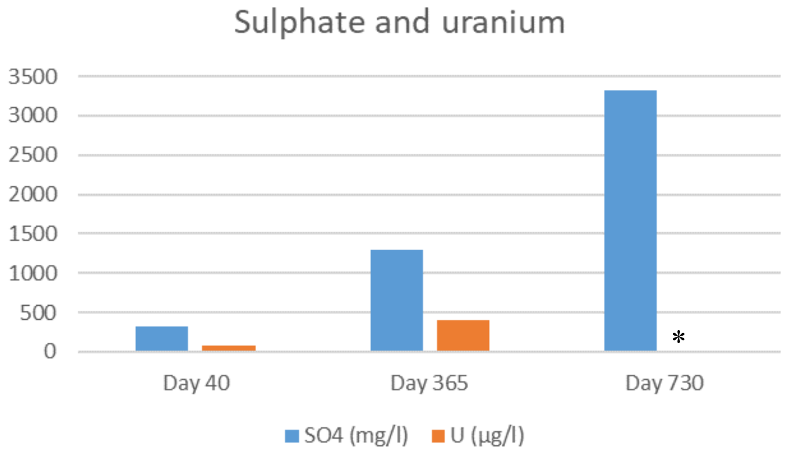

*Figure 7 Concentration of uranium and sulphur in the eluates from columns with alum shale from E16 Kleggerud after 40, 365 and 730 days. Note that uranium was not measured at 730 days. * Uranium was not measured in the 730 days leachate.*

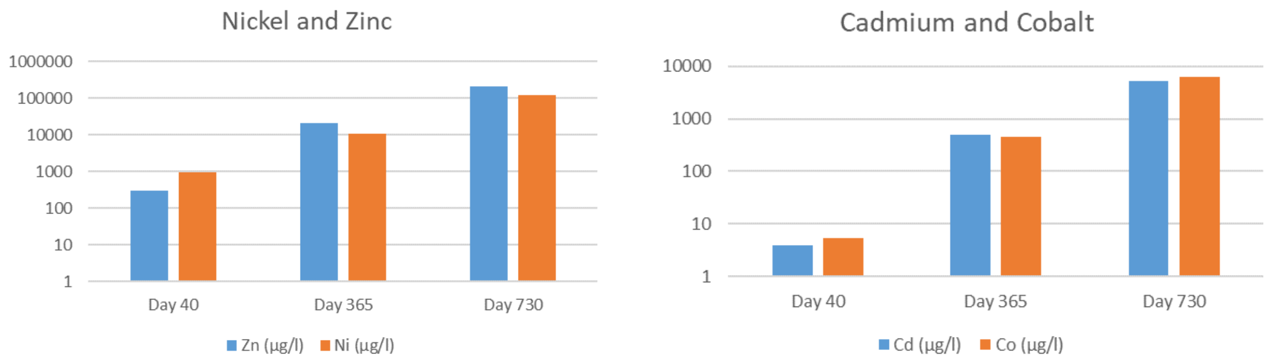

Figure 8 Concentration of Ni, Zn, Cd and Co in the eluates from columns with alum shale from E16 Kleggerud after 40, 365 and 730 days.

In the 100 % alum shale column, the development of eluates with high concentration of metals and other elements, low pH reduction and high conductivity was faster than what was seen in the container experiment with the same type of rock masses (see chapter A1.3). This is likely explained by smaller grain size, increased availability of oxygen and water and higher temperature for the column experiments. For the laboratory experiments the indoor temperature has been minimum 20 degrees, while the average temperature for the Oslo area is 5.7 °C (Mamen, 2022).

A1.3 Container experiments

Container experiments were set up outside NGI with the intention of simulating rainwater percolating through alum shale masses. The alum shale was taken from E16 Kleggerudkrysset. The alum shale is used for different treatments and mixes, and the experimental setup is described in detail in NGI (2022a, report 20200436-09-R). A summary of setup and results for temporary storage of pure alum shale is given here. A photo of the set-up of the container experiments is given in Figure 9, and in Figure 10 the content of a container with alum shale is shown. The containers with 100% alum shale are named VAS_1 and VAS_2.

Two containers with 200 L of alum shale were left open for rain to pass through, and the resulting leachate was analysed at the sampling times shown in Table 4 to investigate the leaching of acid, metals and radionuclides. The experiment is planned to continue until 2028 (8 years). Results from the first year are presented here.

Table 4 Experimental set-up at NGI with E16 Kleggerud alum shale, containers are named VAS.

Name	**Content**	**Replicates**	**Water addition**	**Start date**	**Sampling times full water analysis***	**Sampling times pH, temperature, conductivity, redox**
VAS	200 L Alum shale	2	Rain	21.10.2020	1 day, 2, 4, 8 weeks, 6 months, 1, 2, 3, 4, 5, 6, 7, 8 years	The first 8 weeks: weekly Later: Monthly

*Sampling times in grey are planned but have not yet happened.

Figure 9 Set-up of container experiment at NGI.

Figure 10 Content of container VAS (100 % alum shale) from E16 Kleggerud.

The containers were sampled according to the time points presented in Table 4. The time points marked with grey are planned but have not yet been performed. At three weeks (week 46, 2020) 20 L tap water was sprinkled over the containers to get a sample in a week of dry weather.

Field measurements of pH and conductivity in the eluates from the first two years are presented in Figure 11. The pH was fairly stable around 7.5 during the first two years of measurements, with one sampling point at about 6.5 at 650 days. The conductivity was stable in the beginning and has then been increasing, except in the winter period were there were some lower measurements.

Concentrations of sulphate, alkalinity, calcium and uranium are also presented in Figure 11, and zinc, nickel, cadmium and cobalt are presented in Figure 12.

The highest measurement for uranium (704 µg/L) was the 1-day sample from the VAS_2 container, and in the rest of the year the concentrations varied between 38 and 303 µg/L. For the first sample of VAS there was high concentrations of several elements, and one could suspect contamination of the sample with e.g. particles, but similar concentrations in the filtered and unfiltered sample supports that the values are correct.
Alkalinity peaked two months after start-up of the experiment and has been declining thereafter.

After one year, concentrations of sulphate, calcium, zinc, nickel, cadmium and cobalt started increasing and the high concentrations were also reflected in the high conductivity measurements. The increase in concentrations suggest that the reaction rates were increasing, but the pH was so far not affected meaning the buffer capacity of carbonates in the rock was still sufficient.

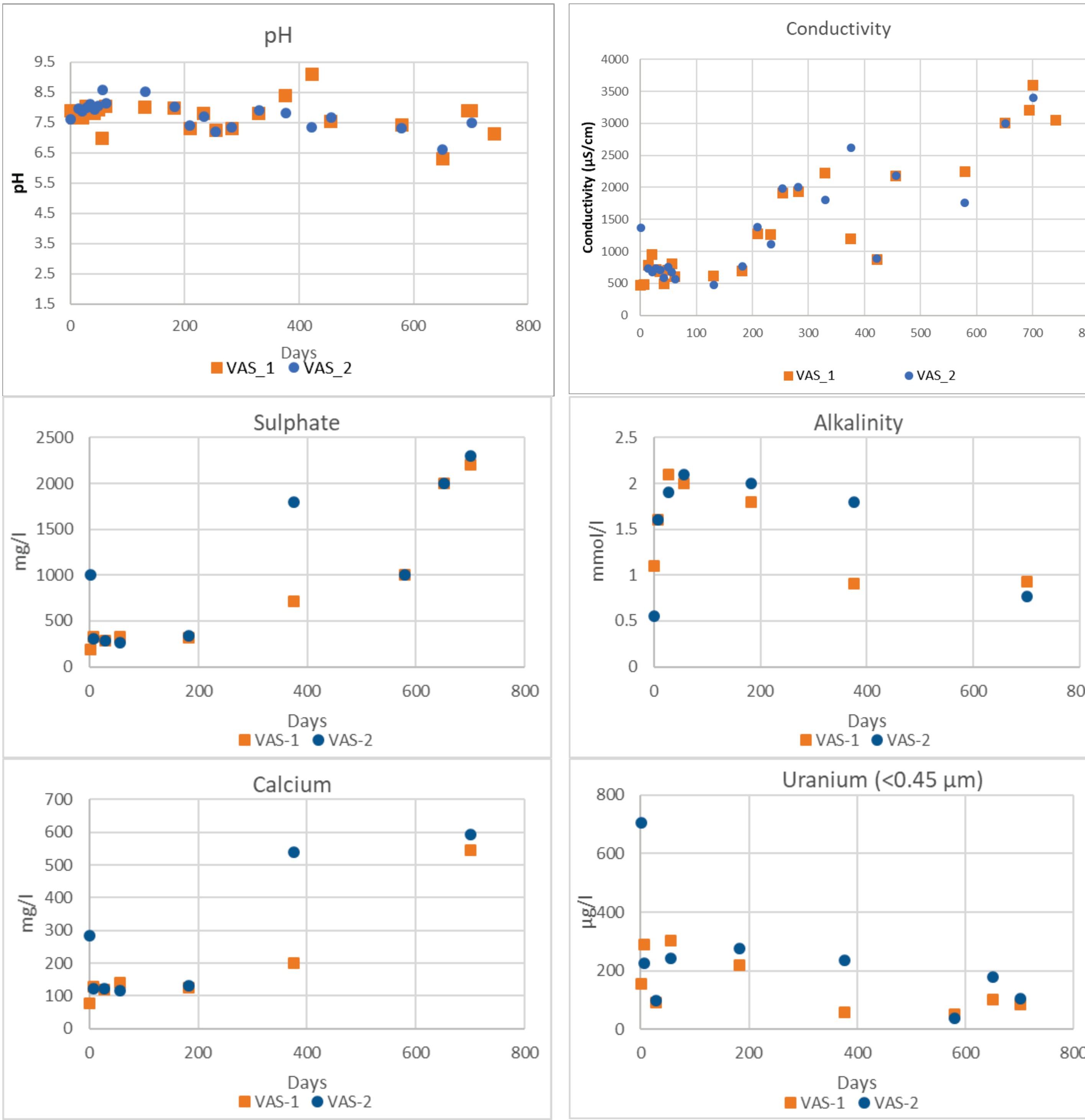

Figure 11 pH, conductivity, sulphate, alkalinity, calcium and uranium in leachate from the containers with alum shale from Kleggerud (field measurements).

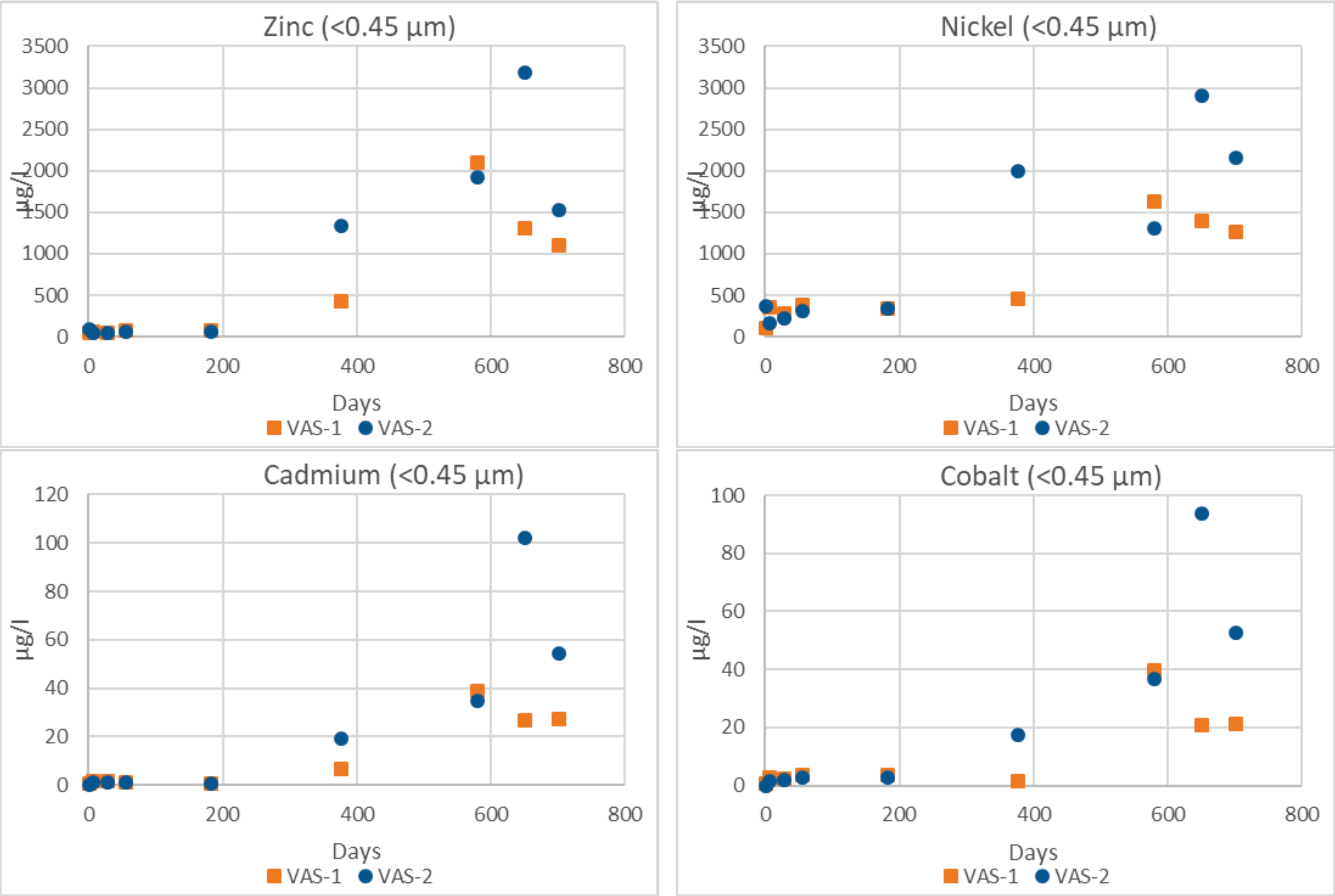

Figure 12 Content of zinc, nickel, cadmium and cobalt in leachate from the containers with alum shale from Kleggerud.

A1.4 One stage batch leaching tests and natural run off

It has been done one stage batch leaching tests on some samples of weathered and unweathered shale (0-4 mm) originating from the construction site at E16 Kleggerud/Jevnaker. Results from the tests are given in Table 5.

Table 5 Uranium concentrations in rocks and leachates. Placement of the boreholes are shown in Figure 2 (NGI 2020a, 20190261-01-R).

Sample name	Type of masses (visually determined)	Uranium in solid rock (mg/kg)	Uranium in leachate (µg/L)	Sulphur in solid rock (mg/kg)	Sulpur in leachate (µg/L)	pH
3380-a	Sand			<1100	68	7,8
3380-b	Weathered shale	68	1,5	< 1100	29	7,1
3380-c	Weathered shale	60	0,44	< 1100	31	7,2
3435-a	Weathered shale	170	3,9	1300	86	6,2
3435-b	Weathered shale	200	1,7*	1500	19	6,4
3435-b	Weathered shale	200	0,504**			6,9
3520-a	Weathered shale	49	0,87	1400	39	5,5
3520-b	Weathered shale	57	0,41	< 1100	33	8,1
3520-c	Weathered shale	46	0,64	< 1100	24	6,5
3520-d	Weathered shale	74	0,09	11000	250	7,5
3360-b	Rock (unweathered shale)	150	2,66**			7,3
3380-d	Rock (unweathered shale)	85	53			8,1
3435-c	Rock (unweathered shale)	120	1,3			7,3
3520-e	Rock (unweathered shale)	100	0,14	11000	300	6,4
Average all samples			5,2			
Average rock samples			14,3		300	

*sample 3435-b is tested at two different laboratories, but the material is tested as parallels not duplicates

** Tested at another laboratory than the other samples

The recipients that can be affected by the construction work at Kleggerud has been sampled up- and downstream the enterprise to document the present pH value and level of metals in the water. It was not found to be elevated concentrations of pollutants in the water samples before the construction work started. The recipient was classified as in good chemical state (class II according to Direktoratsgruppen (2018)). The most important results are given in Table 6 For map over the sampling points, see Figure 13.

Table 6 Concentration of metals in filtrated water samples from the creek up- and downstream the prospective enterprise at Kleggerud (in µg/L), classified after guideline M-608, (up) = upstream and (down) = downstream the enterprise (NGI 2020a, 20190261-01-R).

Point	V1 (up)						V2 (down)				V3						V3a		V3b		V4 (up)
Sampled by (time)	NIBIO (Apr 2018)	NIBIO (Sept 2018)	Skanska (Sept 2019)	Skanska (Jan 2020)	Skanska (May 2020*)	Skanska (Aug 2020*)	Skanska (Sept 2019)	Skanska (Jan 2020)	Skanska (May 2020*)	Skanska (Aug 2020*)	NIBIO (Apr 2018)	NIBIO (Jun 2018)	NIBIO (Sept 2018)	Skanska (Sept 2019)	Skanska (Aug 2020*)	Skanska (Sept 2020*)	Skanska (Jan 2020)	Skanska (Sept 2020*)	Skanska (Jan 2020)	Skanska (Sept 2020*)	Skanska (Jan 2020)
As	0.13	0.45	0.17	0.1	-	-	0.23	0.13	-	-	0.16	0.17	0.61	0.2	-	-	0.13	-	0.12	-	0.13
Cd	0.02	0.02	0.013	0.005	0.064	<0.028	0.023	0.025	0.033	0.3	0.008	0.022	0.007	0.089	0.11	0.055	0.022	0.044	0.016	0.032	<0.004
Cr	<0.050	<0.050	<0.050	<0.050	-	-	<0.050	0.06	-	-	0.07	0.07	0.07	0.11	-	-	0.07	-	0.068	-	0.18
Cu	0.65	0.35	0.97	0.56	<0.01	<LOD	0.58	0.56	<LOD	<0.01	0.97	0.95	0.89	1.6	<LOD	<0.01	0.69	<LOD	0.88	<LOD	0.28
Ni	0.75	1.9	1.2	0.62	2.7	1.5	1.5	1.3	1.1	13	0.84	0.8	1.3	8.7	13	9.4	1.2	6.2	0.75	1	0.44
Pb	<0.010	<0.010	<0.010	<0.010	<0.4	<0.4	<0.010	<0.010	<0.4	0.57	<0.010	<0.010	0.054	<0.010	<0.4	<0.4	<0.010	<0.4	0.16	<LOD	0.041
Zn	5.3	0.66	0.86	0.92	0,02	<LOD	1.3	2.5	<0.02	<LOD	0.63	1	0.69	3.6	<LOD	<0.02	2.3	0.03	3.1	<0.02	0.63
U	0.4	3.2	0.23	0.24	2.5	0.8	1.1	1.1	0.6	170	0.5	2.4	4.1	3.3	5.6	5.3	2.6	33	0.81	2	0.079
Al	9.5	4	4.9	2.9	0.37	0.1	4.5	4.2	0.03	0.93	12	11	10	23	0.14	0.1	14	0.41	4.3	0.02	36
Mo	0.81	2.4	0.42	0.63	-	-	1.2	1.3	-	-	0.57	1.4	9.5	1.8	-	-	1.5	-	0.68	-	0.87
pH	7.8	8	8	8.1	8.0	8.0	7.8	8	7.8	7.8	7.9	8.1	7.3	8	7.7	7.9	7.8	7.7	8		7.6

*Master Thesis 2021. Forståelse av miljøutfordringer knyttet til bygging av vei i områder med svartskifer med potensiale for sur avrenning. Strømø, Tonje Katrin

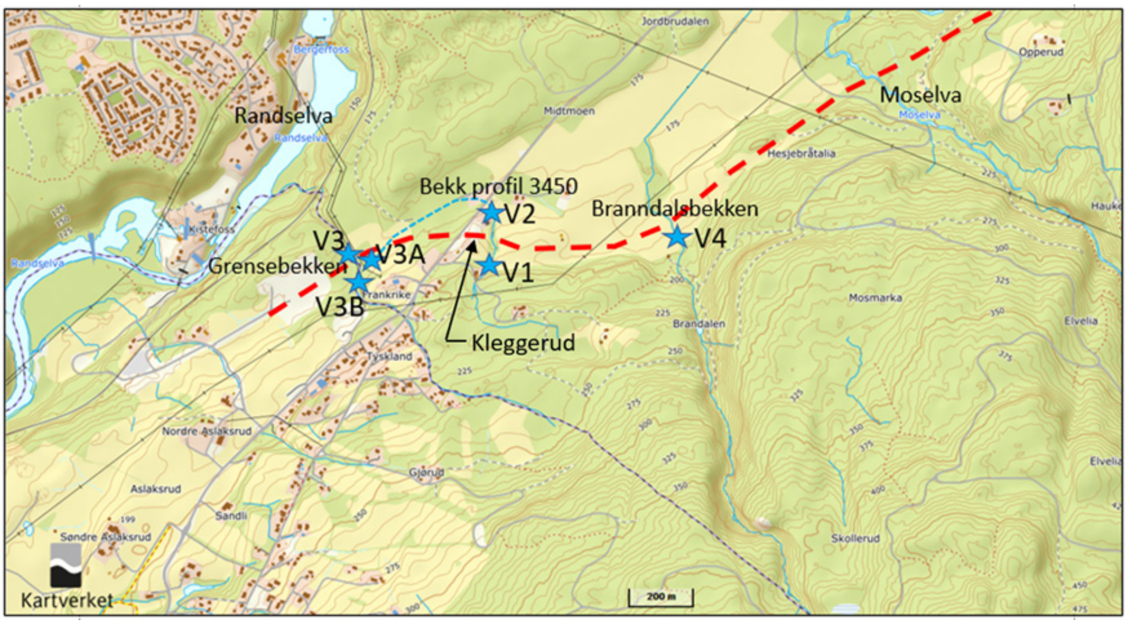

Figure 13 Sampling points for water sampling around the construction work at E16 Kleggerud January 2020.

A2 New road to Kistefos Museum

As preparatory work before starting the construction of new E16 from Eggemoen to Olum in Jevnaker, a new parking lot and access road to Kistefos museum were established in 2017. The surplus masses from the access road cutting consisted of a mixture of black shale, monzonite and syenite (the local version mænaite), see Figure 14 (Structor 2017). There was a deficiency of fill material for the planned E16 in the area. The rock masses from the access road cutting were therefore taken out and stored for later use in two stockpiles along the new road construction line, see Figure 15.

Figure 14 Road cutting in black shale (dark bottom parts) and syenite and monzonite for the local access road to Kistefos museum (from Structor 2017)

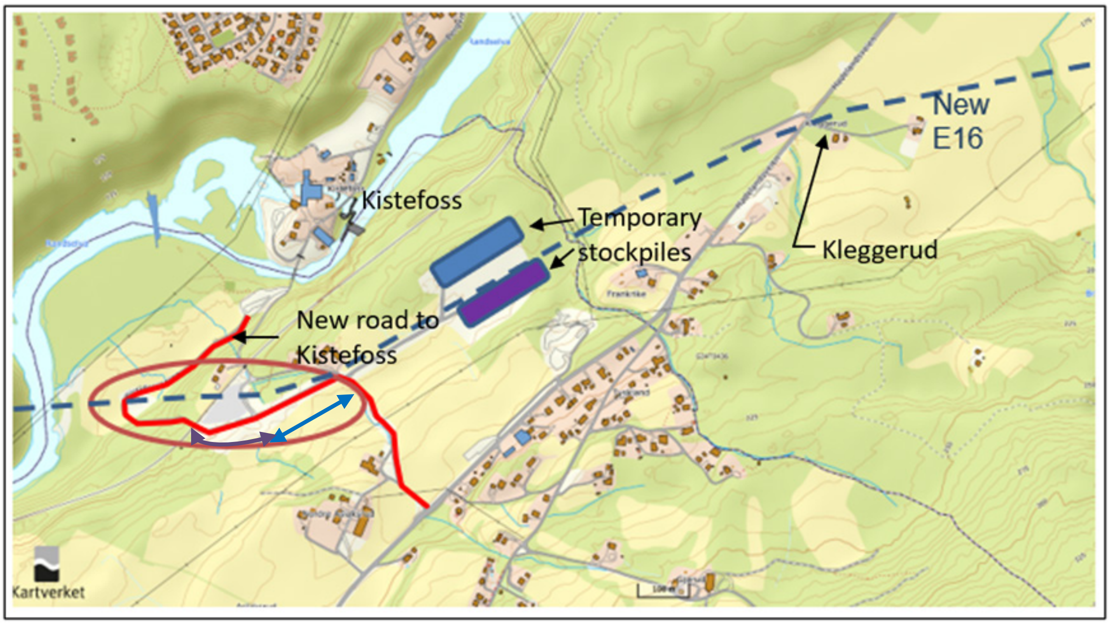

Figure 15 Initial road excavation for new entrance road to Kistefos Museum marked with red. The excavation area is in the orange circle. The temporary stockpiles are marked with blue and violet colour, and the rock masses originates within the area with same coloured arrows. The one marked violet is the one where the temperature rose, and self-heating started autumn 2019.

According to aerial photos and Structor's report (2017), the road cutting was taken out during the spring of 2017. The stockpiles were established and Structor quantified the content of black shales therein, fall 2017. NIBIO (2019) did a baseline assessment of the environmental condition in the creeks in the area in the spring and summer 2018, to look at the condition before the start of the major excavations in the E16 project. In the duration of the field campaign, the stockpiles were observed to be uncovered. NIBIO (2019) states that the piles were covered by the time of writing (January 2019). In the end of September 2019, the temperature 30 cm from the surface in one of the stockpiles was measured to around 380 °C (measured by Gabriel Ciur, Statens vegvesen). The heat was observed to occur in local spots. Nearby the points with high temperature, it was registered normal temperatures around 13 °C .

Stockpile 1, shown in blue in Figure 15: This stockpile has received blasted rock masses from the local road to chainage 630 (within the stretch of the blue arrow in Figure 15). The rock was estimated to mainly consist of syenite with minor contribution of black shale. The black shale content was estimated to be less than 5 % (Structor 2017). In the spring of 2020, Skanska controlled the black shale content of the stockpile by counting and measuring the different rock types. They found that that the content of black shale in the stockpile was >20 % (NGI 2020a).

Stockpile 2, shown in violet in Figure 15: This stockpile consists of rocks blasted out in the road construction line from chainage 630 and further on (within the stretch of the violet arrow in Figure 15). The rocks in this area mainly consist of monzonite and black shale. The content of black shale was estimated to be around 30 % (Structor 2017). Self-heating started in this pile, August 2019. This is discussed further in the main report.

The black shale in the area has been analysed and is classified as horizon 2 in the alum shale formation (Structor 2017). The content of Uranium in Stockpile 2 is between 50 – 80 mg/kg in the samples and Sulphur from 17000 to 43000 mg/kg, where the sample with 17000 mg/kg is considered to be mixed with monzonite. Two samples are also tested with XRD to detect minerals, and no pyrrhotite ($Fe_{1-x}S$) is detected (Structor, 2017). Analyses of rock samples are presented in Table 7.

Table 7 Chemical analysis of 5 rock samples from temporary storage at new road to Kistefos Museum. Only fine material was selected for analysis. The samples therefore have an unproportionally high content of black shale as monzonite is a harder rock type. Copied from Structor (2017).

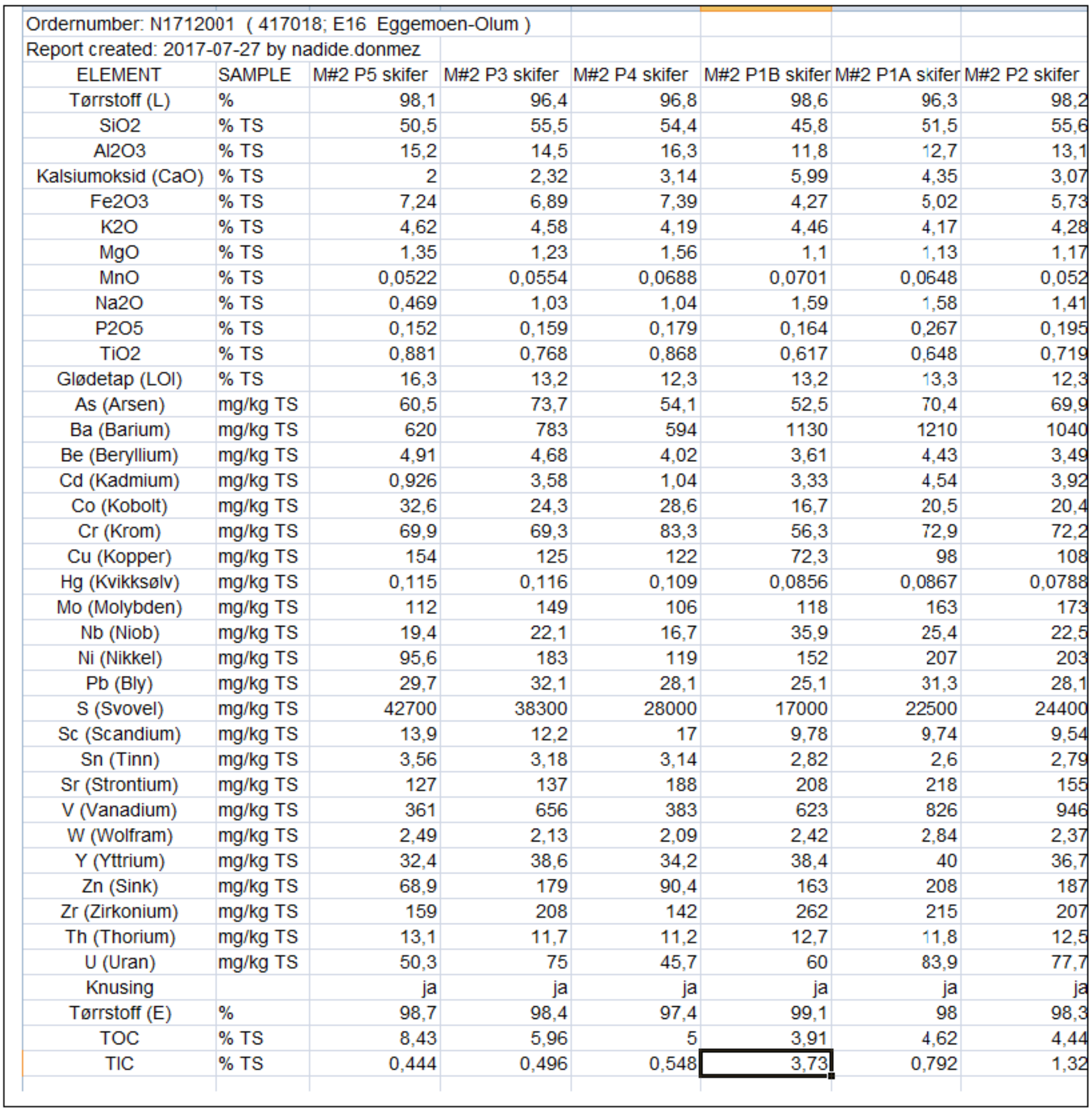

Ordernumber: N1712001 (417018; E16 Eggemoen-Olum)
Report created: 2017-07-27 by nadide.donmez

ELEMENT	SAMPLE	M#2 P5 skifer	M#2 P3 skifer	M#2 P4 skifer	M#2 P1B skifer	M#2 P1A skifer	M#2 P2 skifer
Tørrstoff (L)	%	98,1	96,4	96,8	98,6	96,3	98,2
SiO2	% TS	50,5	55,5	54,4	45,8	51,5	55,6
Al2O3	% TS	15,2	14,5	16,3	11,8	12,7	13,1
Kalsiumoksid (CaO)	% TS	2	2,32	3,14	5,99	4,35	3,07
Fe2O3	% TS	7,24	6,89	7,39	4,27	5,02	5,73
K2O	% TS	4,62	4,58	4,19	4,46	4,17	4,28
MgO	% TS	1,35	1,23	1,56	1,1	1,13	1,17
MnO	% TS	0,0522	0,0554	0,0688	0,0701	0,0648	0,052
Na2O	% TS	0,469	1,03	1,04	1,59	1,58	1,41
P2O5	% TS	0,152	0,159	0,179	0,164	0,267	0,195
TiO2	% TS	0,881	0,768	0,868	0,617	0,648	0,719
Glødetap (LOI)	% TS	16,3	13,2	12,3	13,2	13,3	12,3
As (Arsen)	mg/kg TS	60,5	73,7	54,1	52,5	70,4	69,9
Ba (Barium)	mg/kg TS	620	783	594	1130	1210	1040
Be (Beryllium)	mg/kg TS	4,91	4,68	4,02	3,61	4,43	3,49
Cd (Kadmium)	mg/kg TS	0,926	3,58	1,04	3,33	4,54	3,92
Co (Kobolt)	mg/kg TS	32,6	24,3	28,6	16,7	20,5	20,4
Cr (Krom)	mg/kg TS	69,9	69,3	83,3	56,3	72,9	72,2
Cu (Kopper)	mg/kg TS	154	125	122	72,3	98	108
Hg (Kvikksølv)	mg/kg TS	0,115	0,116	0,109	0,0856	0,0867	0,0788
Mo (Molybden)	mg/kg TS	112	149	106	118	163	173
Nb (Niob)	mg/kg TS	19,4	22,1	16,7	35,9	25,4	22,5
Ni (Nikkel)	mg/kg TS	95,6	183	119	152	207	203
Pb (Bly)	mg/kg TS	29,7	32,1	28,1	25,1	31,3	28,1
S (Svovel)	mg/kg TS	42700	38300	28000	17000	22500	24400
Sc (Scandium)	mg/kg TS	13,9	12,2	17	9,78	9,74	9,54
Sn (Tinn)	mg/kg TS	3,56	3,18	3,14	2,82	2,6	2,79
Sr (Strontium)	mg/kg TS	127	137	188	208	218	155
V (Vanadium)	mg/kg TS	361	656	383	623	826	946
W (Wolfram)	mg/kg TS	2,49	2,13	2,09	2,42	2,84	2,37
Y (Yttrium)	mg/kg TS	32,4	38,6	34,2	38,4	40	36,7
Zn (Sink)	mg/kg TS	68,9	179	90,4	163	208	187
Zr (Zirkonium)	mg/kg TS	159	208	142	262	215	207
Th (Thorium)	mg/kg TS	13,1	11,7	11,2	12,7	11,8	12,5
U (Uran)	mg/kg TS	50,3	75	45,7	60	83,9	77,7
Knusing		ja	ja	ja	ja	ja	ja
Tørrstoff (E)	%	98,7	98,4	97,4	99,1	98	98,3
TOC	% TS	8,43	5,96	5	3,91	4,62	4,44
TIC	% TS	0,444	0,496	0,548	3,73	0,792	1,32

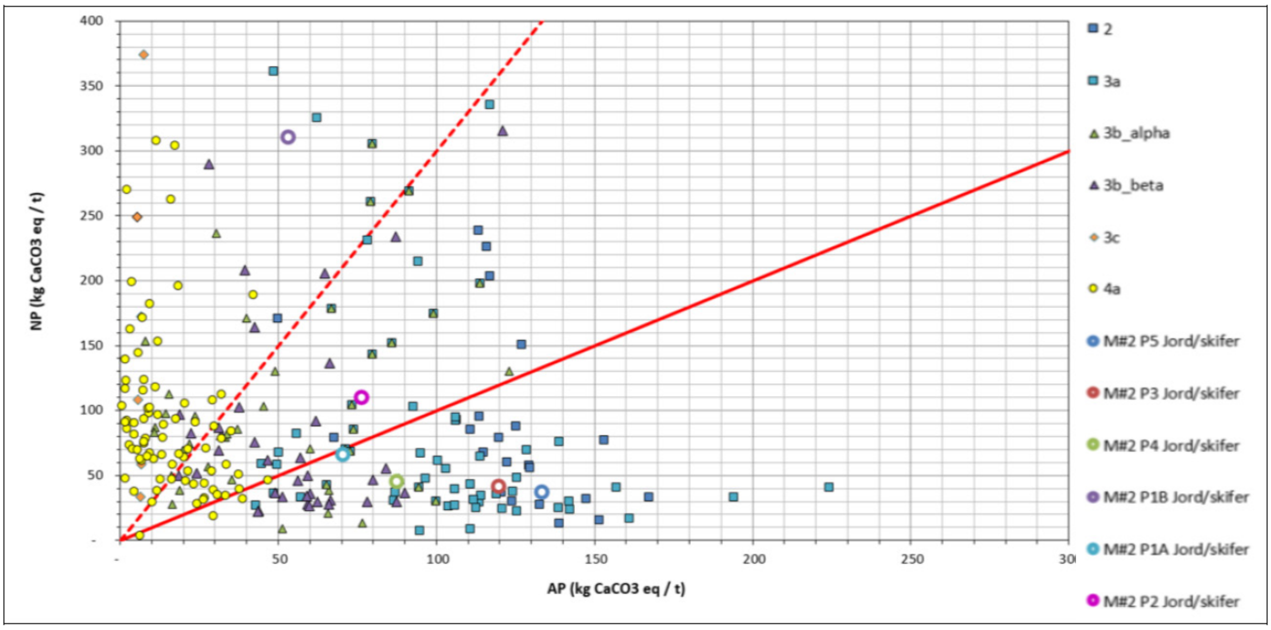

Figure 16 Diagram showing neutralizing potential (NP) versus acid-producing potential (AP) of six samples from the work with new road to Kistefos Museum. Copied from Structor (2017).

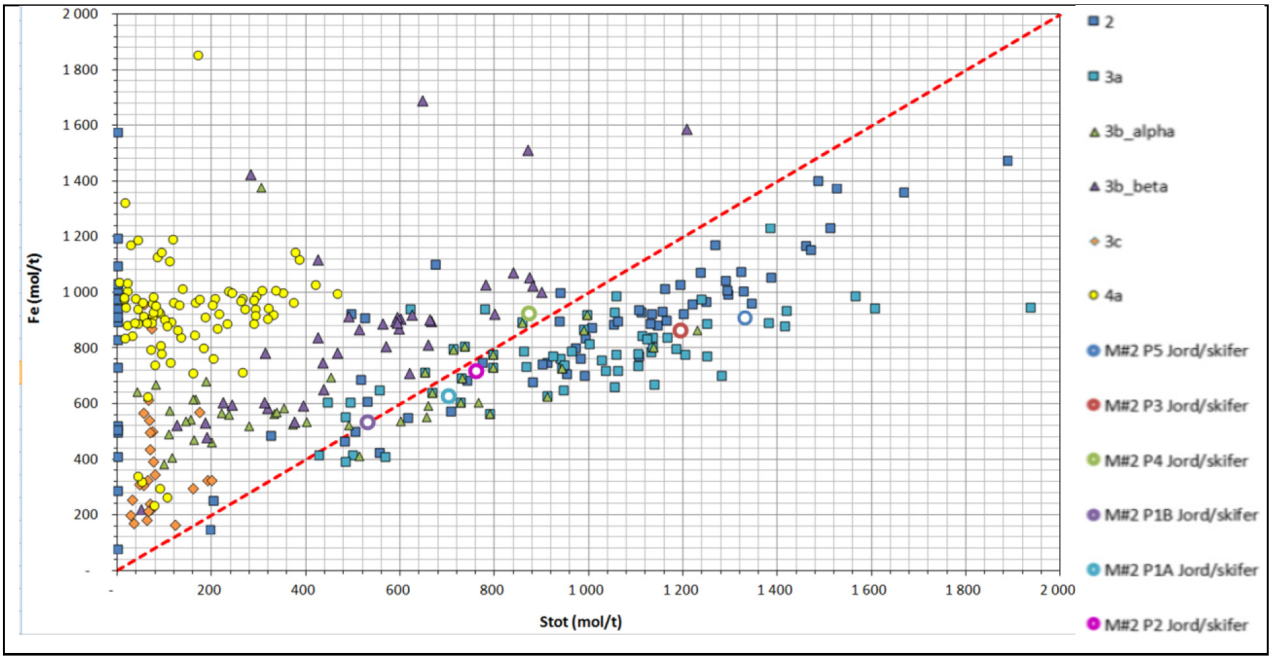

Figure 17 Diagram showing iron (Fe) versus total sulphur (Stot) of six samples from the work with new road to Kistefos Museum. Copied from Structor (2017).

A3 Rv. 4 Gran

A road tunnel was constructed at Gran, Hadeland in 2013-2015 to take Rv4 around Gran centre. The tunnel is cutting through the alum shale horizons. In Appendix C, selected parameters for the total rock content are shown.

Container leaching experiments with black shale was started by the Norwegian Public Road Authorities (SVV) in 2014 and 2015 with rock masses from the tunnel and from a road cutting north of the tunnel (Figure 18) (Statens vegvesen, 2017). The containers were sampled at irregular intervals until mid-2015. Experimental setup and results are described in Statens Vegvesen (2017). The sampling was resumed by two master students for a limited time in 2016, see Børresen (2017) and Erstad (2017).

Since 2016, the containers have been standing at Roa without any further sampling or other treatment (Figure 19). Five of the containers from these experiments were transferred to NGI 06.11.2020 (see Table 8), and sampling was started at NGI 11.11.2020. At this time, the containers were sprinkled with 20 L tap water due to dry weather. Another sampling was done a week later, after rain.

In addition to the sampling points noted in Table 8, where water samples were analysed for chemical components, field parameters (pH, conductivity, redox, temperature) were measured weekly in 2020 and monthly in 2021 and 2022. Note that the AT1 and AT2 containers were started in 2015 while the other three were started in 2014.

At NGI the containers were sampled together with the newly started container experiments with rock from E16 Kleggerud (see chapter A1.3) and will be sampled until 2028.

Table 8 The experimental set-up for container experiments started by SVV and continued by NGI.

Container	Rock	Source of rock	Start date	Experiment period reported by SVV [2]	Experiment period reported in master theses [3]	Sampling by NGI [4]
A1 [1]	Alum shale horizon 2	Blast from road cuttings north of tunnel at Gran	01.08.2014	Day 0-244 (19.05.2015)	Day 735-777	Days 2233-2494), 7, 8, 9, 10, 11, 12, 13, 14 years
A3	Alum shale horizon 2	Blast from road cutting north of tunnel at Gran	01.08.2014	Day 0-244 (19.05.2015)	Day 735-777	Days 2233-2494), 7, 8, 9, 10, 11, 12, 13, 14 years

Container	Rock	Source of rock	Start date	Experiment period reported by SVV 2)	Experiment period reported in master theses 3)	Sampling by NGI 4)
AT1	Alum shale horizon 3a	Blast from tunnel at Gran, chainage 9354	21.05.2015	Day 0-28 (18.06.2015)	Day 503-545	Days 2001-2310), 7, 8, 9, 10, 11, 12, 13, 14 years
AT2	Alum shale horizon 3a	Blast from tunnel at Gran, chainage 9354	21.05.2015	Day 0-28 (18.06.2015)	Day 503-545	Days 2001-2310), 7, 8, 9, 10, 11, 12, 13, 14 years
G2	Galgeberg shale horizon 3bβ	Mechanically excavated from tunnel at Gran, chainage 8514-8520 and 8586-8589	01.08.2014	Day 0-244 (19.05.2015)	Day 735-777	Days 2233-2494), 7, 8, 9, 10, 11, 12, 13, 14 years

1) Less fragmented alum shale
2) Statens vegvesen (2017)
3) Erstad (2017), Børresen (2017)
4) Sampling times in grey are planned but not yet executed

Figure 18 Container experiment set-up at Gran, for the first part of the experiment (Photo: SVV 2017).

Figure 19 Containers stored at Roa. Photo taken before they were brought to NGI at Ullevål, autumn 2020.

Figure 20 Content of container A1 (left) and A3 (right), taken 19.11.2020, after the containers were transported to NGI and 6 years after experiment start up.

Figure 21 Content of container AT1 (left) and AT2 (right) , taken 19.11.2020, after the containers were transported to NGI and 5 years after experiment start up.

Figure 22 Content of container G2, taken 19.11.2020, after the containers were transported to NGI and 6 years after experiment start up. Notice the plant growth at the surface of the rock masses.

The alum shale from the tunnel (chainage 9354) has also been used for batch leaching experiment under varying conditions (Wærsted, 2019, Wærsted et al., 2020) and earthworm uptake experiments (Schöpke, 2017).

The containers from SVV have been sampled at irregular intervals (see Table 8 for details), and we therefore do not know the leachate quality for the whole period of the experiment. Results for pH is presented in Figure 23. In the period that the containers were sampled by SVV (2017) and master students Erstad (2017) and Børresen (2017), all pH measurements were circumneutral. When measurements were resumed by NGI, 4 years after the master student measurements ended, pH had dropped in containers AT1, AT2 (AT = alum shale from tunnel) and G2 (Galgeberg shale). The A3 container (alum shale from road cut) seem to have a seasonal pattern, with lower pH during the summer, likely because the reaction rates are faster when temperatures are higher. The A1 container (larger pieces of alum shale from road cut) showed the first signs of pH drop autumn 2022, after 8 years of weathering.

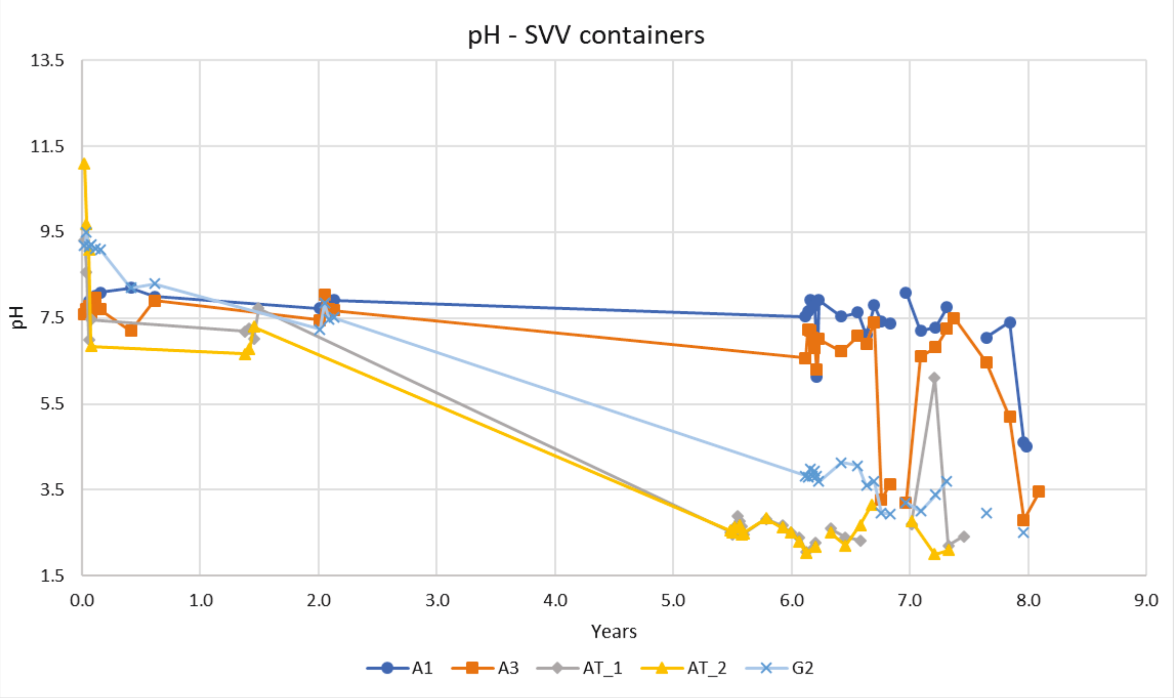

Figure 23 pH with time in leachate from the five containers from SVV.

Conductivity (Figure 24) was relatively high from the beginning in the leachate from all containers except the A1 container were larger rock pieces provided a smaller surface area for reaction. The conductivity has increased as pH dropped, but is lower in the A1 and A3 containers than in AT1, AT2 and G2.

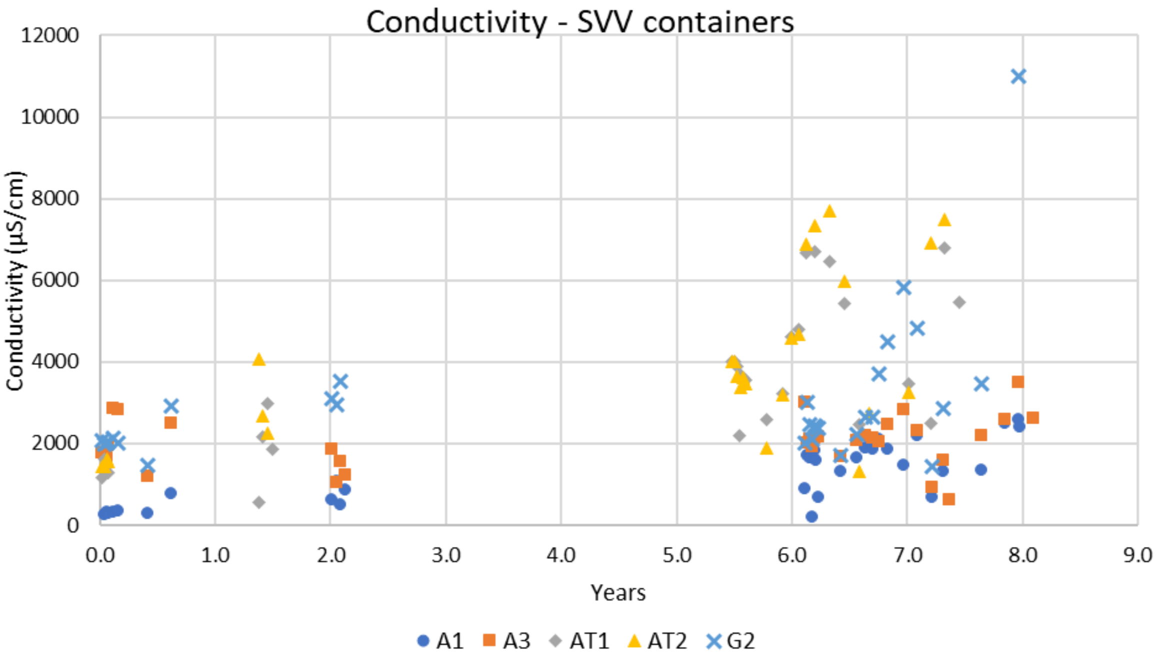

Figure 24 Conductivity with time in leachate from the five containers from SVV.

Sulphate (Figure 25) was higher in the containers with pH drop, which is expected as the reaction rates increased with lower pH. Measurement done by the master students autumn 2016 (1.5 or 2 y) were relatively high. One very high measurement for the Galgeberg shale is seen after 8 years, maybe related to the pH dropping below 3 in this container.

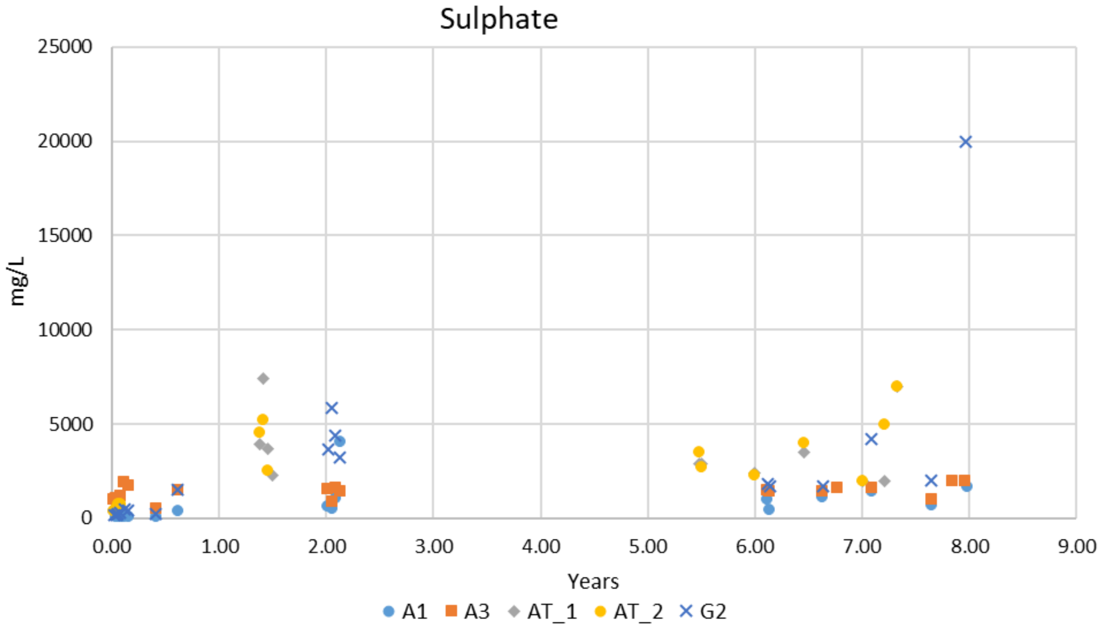

Figure 25 Sulphate with time in leachate from the five containers from SVV.

Alkalinity (Figure 26) and calcium (Figure 27) are both expected to originate from calcite in the rock masses, but the high alkalinity values for G2 in the first year are not reflected in the calcium concentrations. Alkalinity will be 0 as pH drops below 4.5, while Ca may still be leached from calcite or other sources. The A3 container had the highest Ca leaching from the beginning, likely reflecting high calcite content. AT containers has increased to similar levels as pH dropped. The two AT containers follow each other very closely in the last measurements, with AT1 measurements disappearing behind AT2.

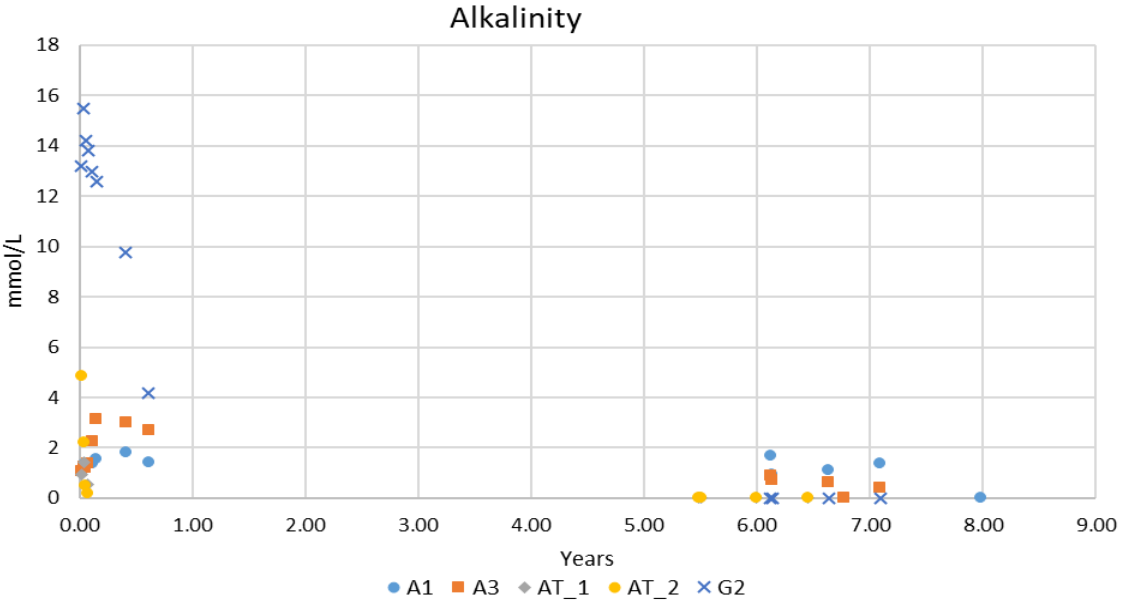

Figure 26 Alkalinity with time in leachate from the five containers from SVV (AT1 measurements disappearing behind AT2).

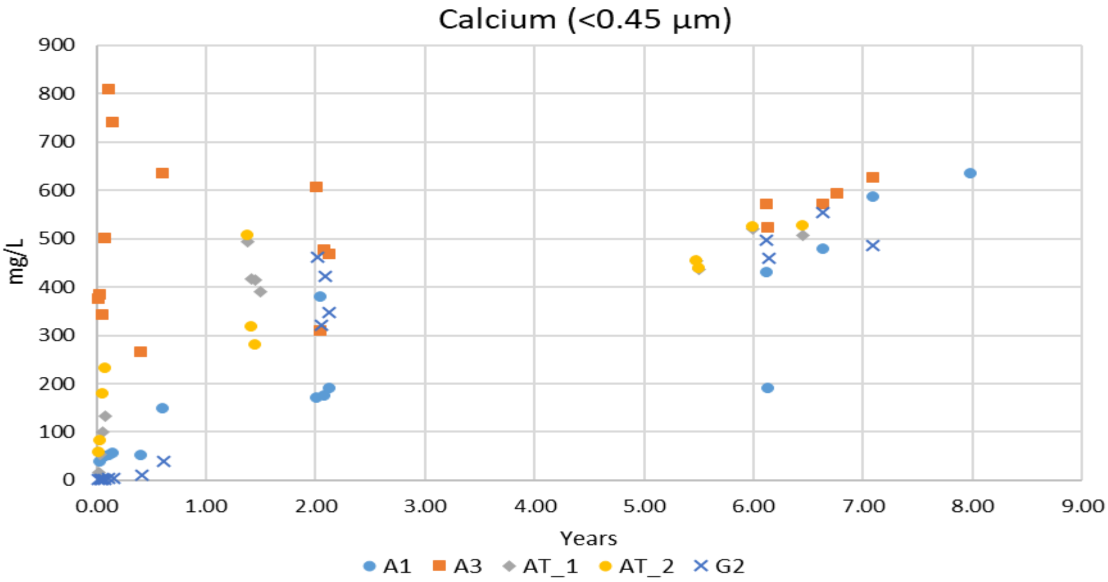

Figure 27 Calcium measurements with time in filtered (0.45 µm) leachate samples from the five SVV containers (AT1 measurements disappearing behind AT2).

Iron (Figure 28) and aluminium (Figure 29) concentrations increased as pH dropped.

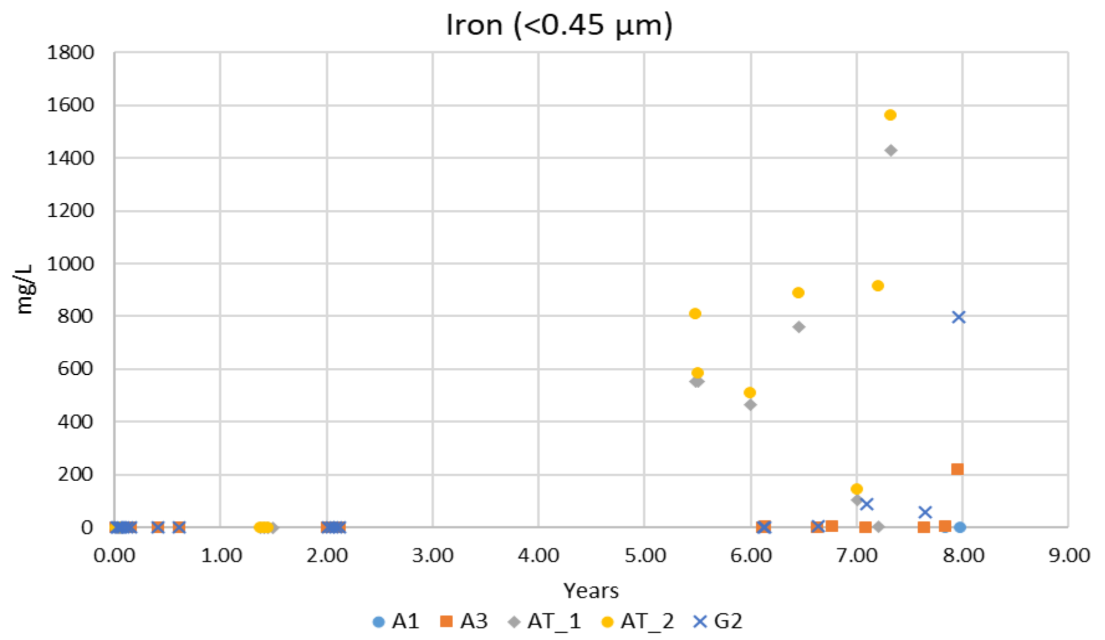

Figure 28 Iron measurements with time in filtered (0.45 µm) leachate samples from the five SVV containers

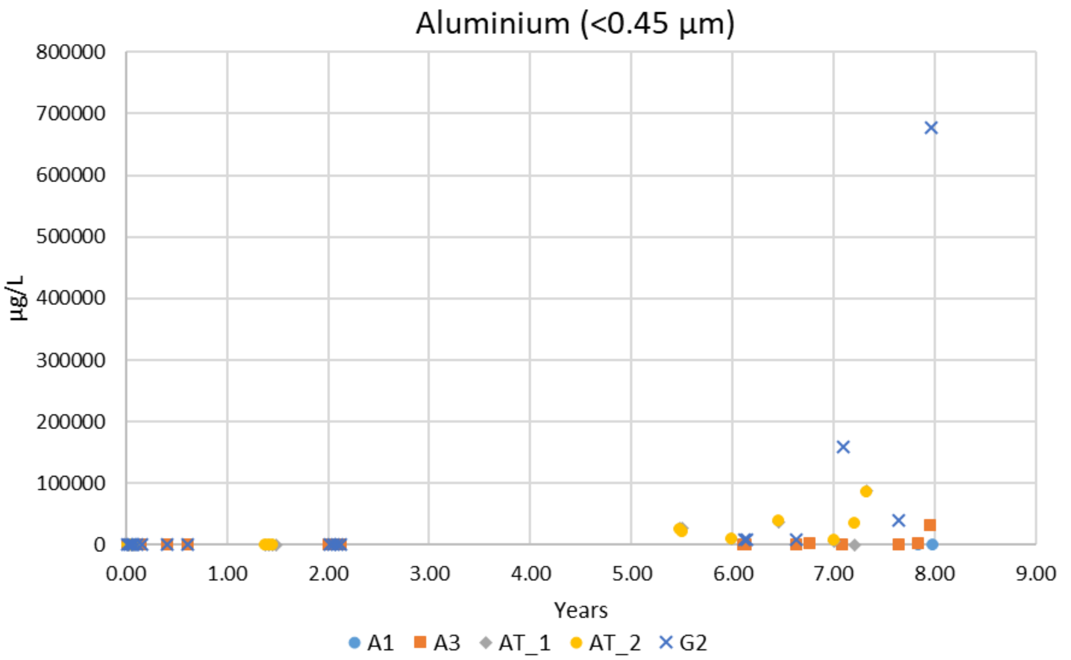

Figure 29 Aluminium measurements with time in filtered (0.45 µm) leachate samples from the five SVV containers.

Concentrations of cadmium (Figure 30) were the highest in the AT1 and AT2 container leachates when sampled by the master students autumn 2016 (Erstad, 2017; Børresen, 2017), while when sampled by NGI, the concentrations have been highest in the G2 leachate. Uranium (Figure 31) concentrations were high from the beginning, especially in the alum shale from the road cut (A3 and A1), and later also in leachate from the alum shale from tunnel (AT containers) and Galgeberg shale.

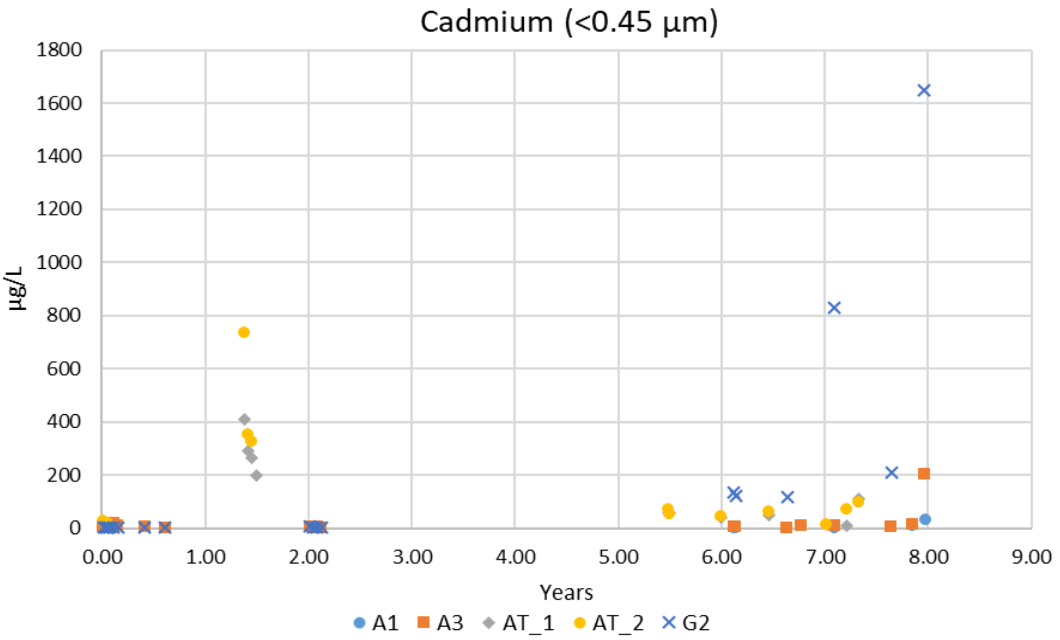

Figure 30 Cadmium measurements with time in filtered (0.45 µm) leachate samples from the five SVV containers

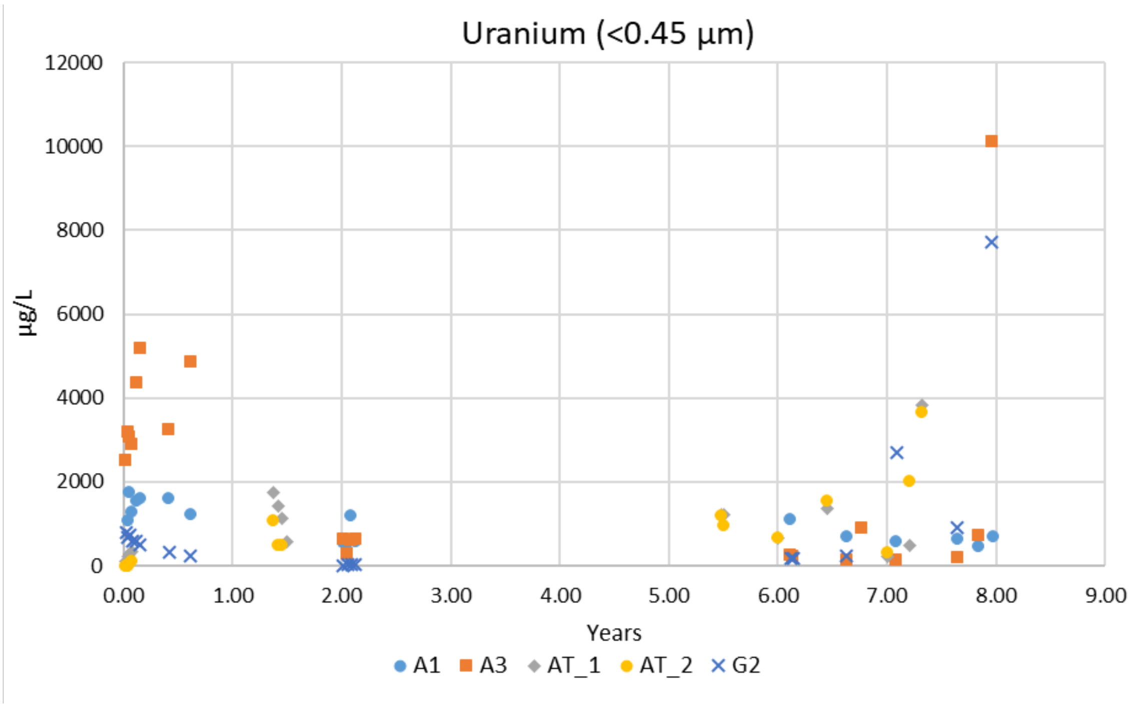

Figure 31 Uranium measurements with time in filtered (0.45 µm) leachate samples from the five SVV containers.

A4 E6 Uthus-Kåterud

Not far from Hamar at Hedmark, between Kolomoen and Arnkvern, Nye Veier AS built a new four-lane highway to accommodate the increase in traffic at E6. The road project led to excess excavation masses, especially due to a deep road cutting through Uthus intersection. The road goes through bedrock with different formation age, among others from the Cambro-Ordovician age.

It is taken core samples of moraine from the road cutting at Uthus, and from both moraine and rock at Kåterud bridge, further north. The bedrock of black shale in the area was mostly classified as alum shale in horizon 3a (NGI, 2017a). For the moraine and soil masses, only the acid formation potential and radioactivity were considered. Three of nineteen samples of soil were found to be in the acid producing zone (see chapter 4 in the main report for explanation). The other soil samples were not found to have a net potential for acid formation. None of the samples were found to be above the limit for radioactive waste (NGI, 2017b).

Black shale from bedrock was deposited at a landfill, while for moraine and top soil masses with fractions of black shale, local solutions for mass storage were found. For local solutions, risk assessments were done to consider the potential harm to the environment. The risk assessment was based on one stage batch leaching tests performed on soil masses with a fraction of black shale, calculating the potential concentrations of

Al, As, Cu, Ni, Zn and U that, in worst case, could be found in the local waterways after establishing the local solutions. The concentrations were assessed against established threshold values (Rambøll, 2018).

The results from the one stage batch leaching tests are shown in Table 9. The results show that concentrations for some metals are higher than the threshold values, but these values are higher than the concentrations that would be seen in nature, due to dilution with precipitation into the local waterways.

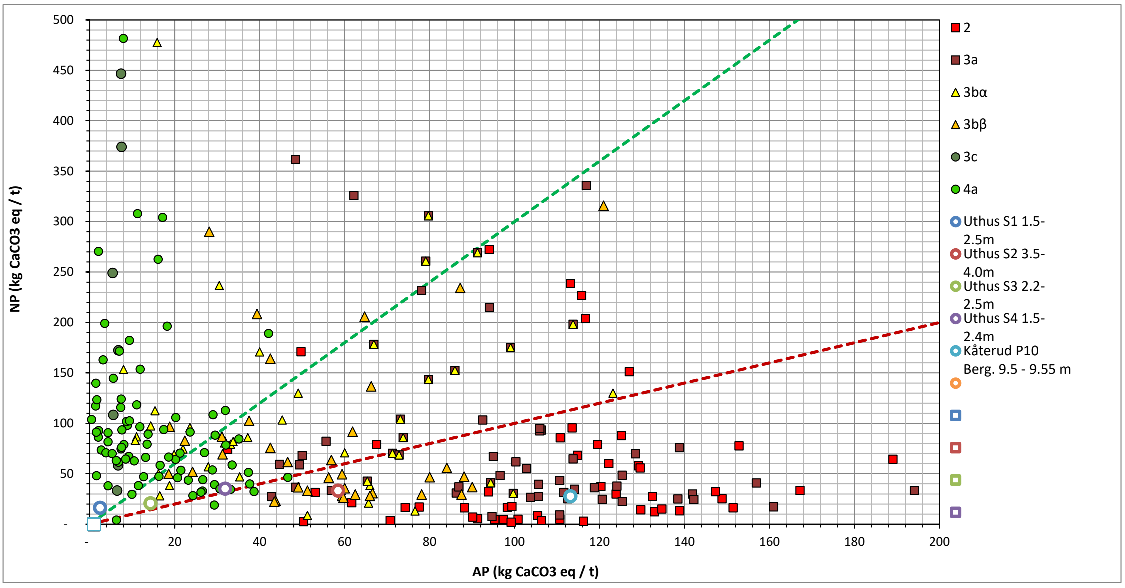

Figure 32 Neutralizing potential plotted against acidification potential, for the samples of soil with shale from Uthus and for one rock sample at Kåterud (open symbols, named Uthus and Kåterud…) and reference samples (2, 3a, 3bα, 3bβ, 3c and 4a).

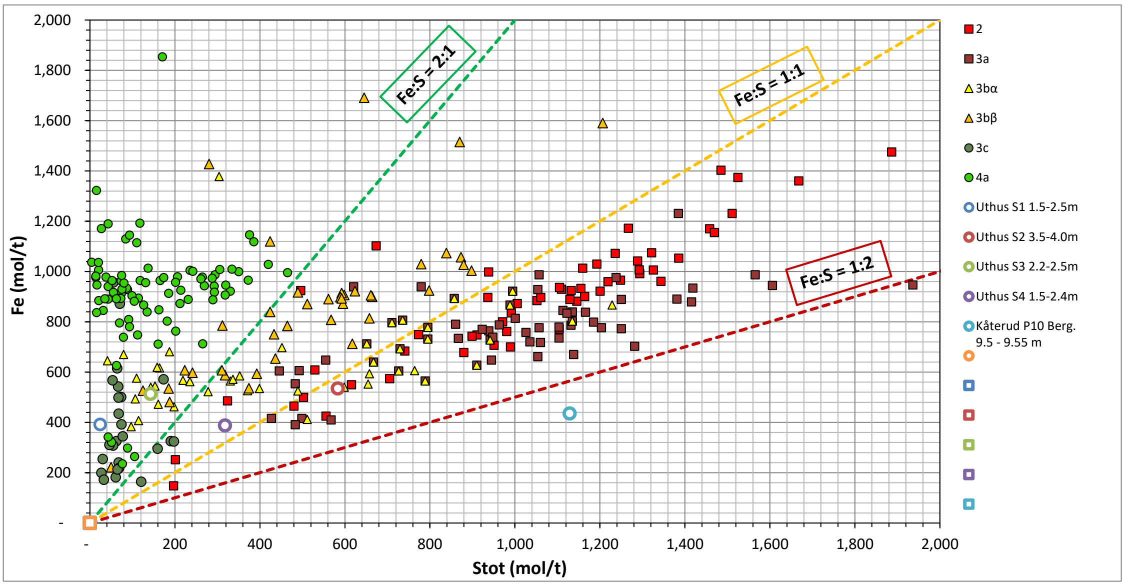

Figure 33 Total content of Sulphur plotted against iron content for the samples of soil with shale from Uthus and for one rock sample at Kåterud (open symbols, named Uthus and Kåterud…) and reference samples (2, 3a, 3bα, 3bβ, 3c and 4a).

Table 9 Results from one stage batch leaching tests of masses with a potential for acidification at E6 Kolomoen-Arnkvern. The concentrations are in µg/L and are compared to threshold values for the elements. Concentrations exceeding the threshold values are marked with grey colour.

Parameter	Soil		Rock	Threshold-values
	Sjakt 2 08b	Sjakt 4 08d	Prøve 10: 9,5-9,55m, 08e Eluat	
Al	8,41	17,7	12	200*
As	0,553	0,674	1.35	0,5**
Cu	5,3	3,71	2.1	7,8**
Ni	12,5	2,12	830	4**
Zn	23	9,25	18.9	11**
U	57,4	16,7	146	30***

* Norwegian guidelines for drinking water, limit for measures
** AA-EQS after M-608
*** WHO (2012)

An additional control program was introduced in the area, to reduce the impact further and to verify the risk assessment:

- All masses that were handled locally was tested to determine the acid formation potential.
- The masses were compacted at site to reduce porosity to a minimum and thereby hinder water and air intrusion, which would further reduce the acid drainage formation from the fraction of black shale in the masses due to little contact between black shale fractions and water and oxygen in the compressed masses.
- The local waterways were sampled regularly.

A5 NOAH Langøya

In 2015, NOAH was considering the possibility to deposit alum shale as ordinary waste at their waste deposit site at Langøya, outside Holmestrand. Alum shale had for numerous years been deposited as hazardous waste at the site. In advance to the deposition, NOAH wanted to investigate possible measures to reduce the acid drainage and also to look at the possibility of self-heating in the waste.

To reduce acid drainage in the operating phase, NOAH wanted to combine alum shale with waste of a basic pH. This was tested using column tests with alum shale and a variety of wastes. To study the risk of self-heating, NOAH constructed an *in-situ* test cell, to better study the effect of natural conditions occurring while temporary storing the alum shale under open air. NGI helped NOAH in planning the experimental setup (NGI, 2015). In the following chapters, some of the results from the experiments are shown.

A5.1 Characterization of alum shale

Alum shale for both the column tests and the test cell was taken out at a construction site in Oslo city centre. The shale was characterized by measuring the total concentration with an XRF in all batches received at NOAH Langøya, as well as performing a one stage batch leaching test on some deliveries of shale. For this study alum shale received between 13th and 28th of April 2015 have been included. This alum shale was used to build the columns and the test cell.

According to the classification tool M-310 (Norwegian Environment Agency, 2015a), the samples are mostly associated with reference samples from horizon 2. Three of the samples (D-62517, D-62545 and D-62546) possibly originates from the transition between horizon 2 and 3a, since the samples mostly lie in a zone of overlap between the reference materials of these horizons. The triangular diagrams used for the classification are shown in Appendix B.

Using the concentrations found in the XRF-analysis, one can say something about the potential of acidic runoff from the shale through looking at the neutralization potential together with the acidification potential. For the samples from NOAH there are no results for TIC, and therefore results for Ca are used to estimate NP by assuming all Ca originates from carbonates. As can be seen in Figure 34, all samples are in the acidic zone, which give the alum shale a potential for acidic runoff when exposed to precipitation and air.

The Fe:S ratio is around 1:1 indicating that the sulphur is mainly present as sulphides, resulting in an elevated potential for acidic run-off and leaching of metals (Figure 35).

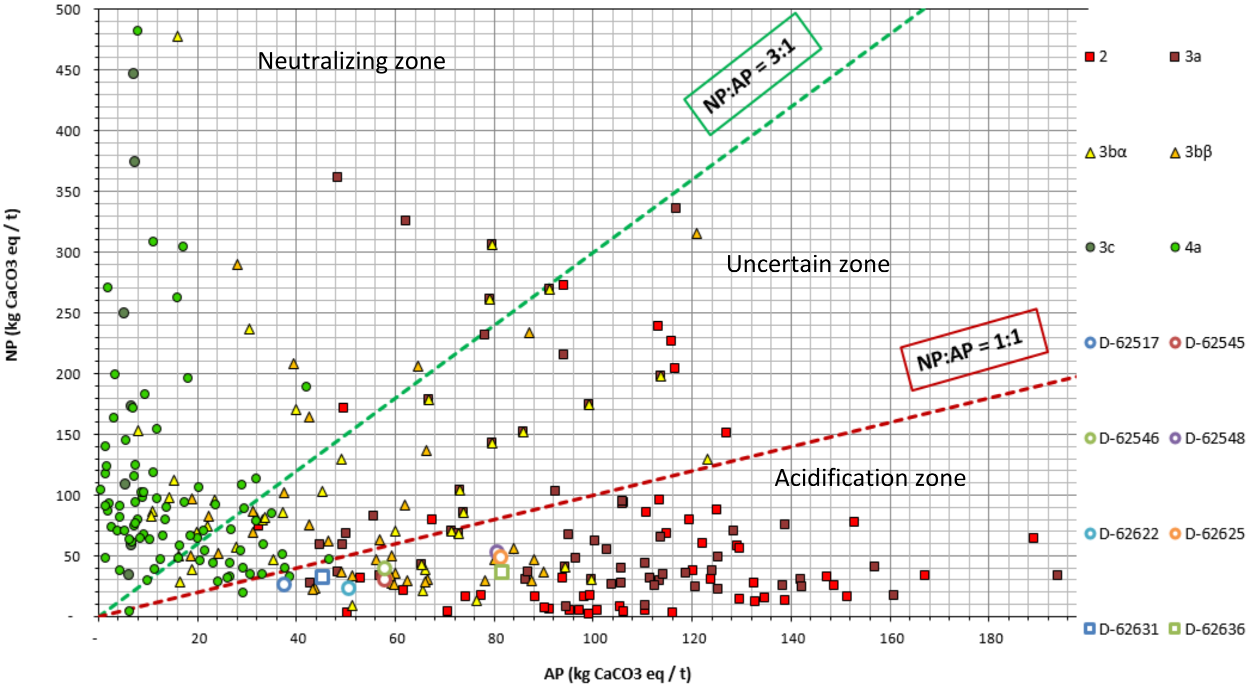

Figure 34 Neutralizing potential plotted against acidification potential, both for the samples of shale deposited at NOAH Langøya (open symbols, named D-62…) and reference samples (2, 3a, 3bα, 3bβ, 3c and 4a).

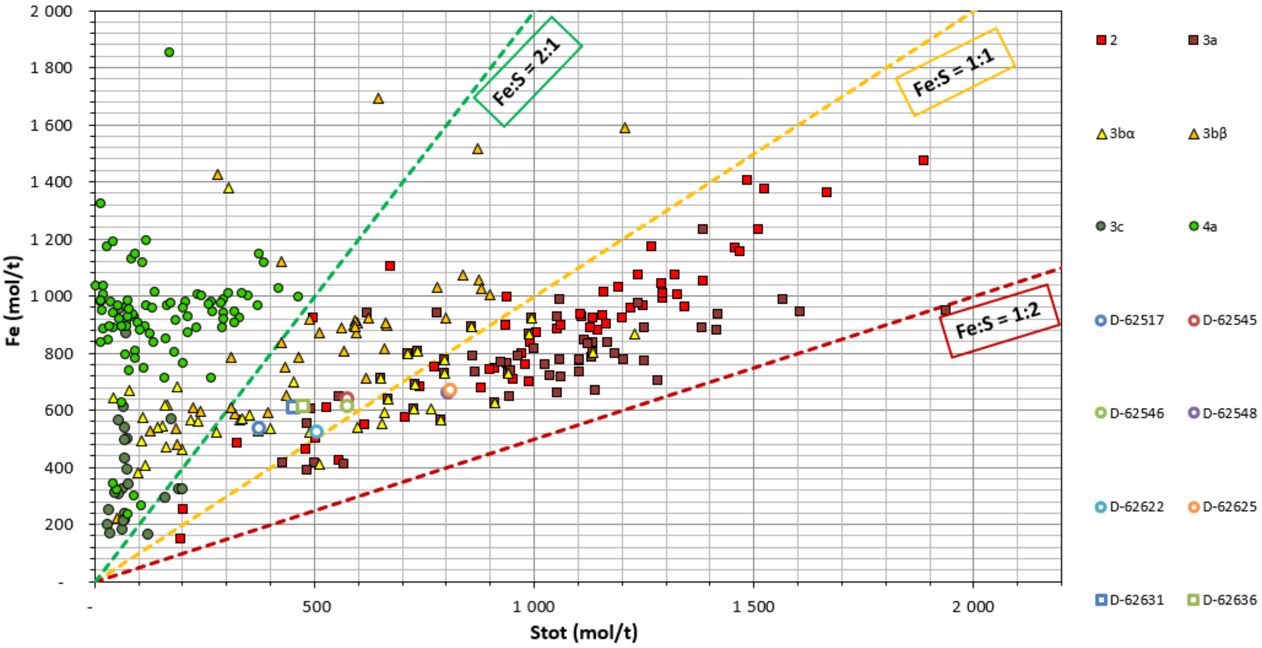

Figure 35 Total content of Sulphur plotted against iron content for the samples of shale deposited at NOAH Langøya (open symbols, named D-62…) and reference samples (2, 3a, 3bα, 3bβ, 3c and 4a).

A5.2 Column experiments

The alum shale was placed in columns to look at leaching from the shale over time. The amount of water added the first four months was equal to a year of precipitation in the area (typically between 850 to 1100 mm per year). Another important goal for the experiment was to determine the best material to use as a top layer over deposited alum shale, to prevent and/or neutralize the acidic drainage that is expected when precipitation and oxygen will facilitate the oxidation reactions in the shale.

Seven columns were built, using 30 cm of compressed alum shale and 15 cm of another waste material as topping in six of the columns. One column consisted of alum shale only, to function as a reference without top layer, and also to be able to compare with the results from the *in-situ* test cell (test cell west). The different waste materials used were limestone, gypsum, ash and bottom ash. Two of the columns were added waste with a basic pH, called waste X and waste Y. Waste y is not reported here, due to only four sampling points from the column.

Figure 36 Column experiment set-up (Photo NOAH).

The column with only alum shale showed a similar trend to what was seen in the test cell (Figure 37). For instance, the pH was quite high (above 7) before it suddenly dropped to around pH 3. The pH-drop was followed by increasing concentrations of metals. For instance, the concentrations of aluminium, cobber and uranium (U is seen in Figure 37) increased after the pH drops. The drop happened around 350 days into the column experiment. The sudden release of the metals was probably connected to both the dissolution of minerals in the shale (the concentration of iron also rose in the same period (Figure 38), indicating dissolution of iron sulphides and sulphates in the shale), but also that metal speciation changes with pH. The metals that increase will probably be present in a more mobile form at a lower pH-value. Uranium had the highest leached concentrations in the start of the experiment, showing that some species of uranium also can be released from the shale at higher pH values.

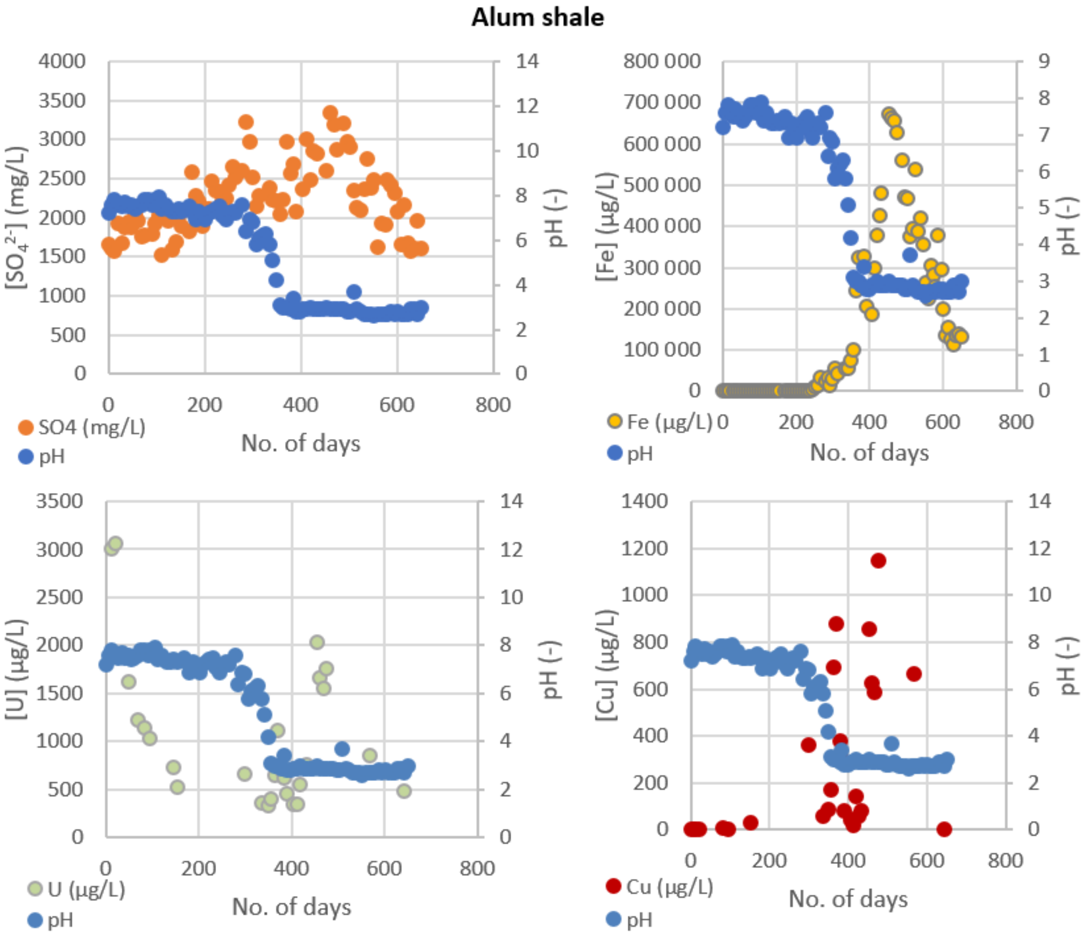

Figure 37 Column test with only alum shale; From top left sulphate, iron, uranium and copper plotted together with pH (all) in leachate

Column test results for the columns built with a top cover is shown in Figure 38 and Figure 39. As can be seen, some of the waste had a buffering effect, preventing the pH to drop, resulting in less release of metals into the leachate. Especially adding limestone, bottom ash and ash had this effect. In the following, examples of leaching from columns with alum shale together with different materials are compared. Figures for the column added limestone are presented in the main text (see chapter 4.4)

For the ashes in the experiment (Figure 38) it is evident the basic ash will have capacity to stabilize the pH at a high level for a long time. For bottom ash, the pH of the leachate was around 8 for the whole period, while for ash the pH dropped from pH around 12 to a pH around 8 after about 380 days. This drop happened at about the same time as the pH drop for the pure alum shale (350 days), see figure 24. It is possible to observe a corresponding increase in sulphate at the same time. The ability for the ash to stabilize the alum shale is also evident from the detected concentrations of metals in the leachate, here visualized for iron and uranium. The concentrations are much lower than what was detected from the leachate from alum shale alone, and much lower than for the other materials tested. For waste X and gypsum (Figure 39) one can see an increase in metal concentrations in the leachate as the pH drops. This is especially evident for the gypsum, where for instance the copper concentrations increase with a factor 100 when the pH drops (from around 70 µg/L to 7000 µg/L).

For the materials used as a top cover over the alum shale, the ash (both ash and bottom ash) is the most successful to decrease the leaching from the alum shale. Also, limestone has some effect. The leaching of some elements, for instance uranium and nickel, are still quite high from the column containing alum shale and limestone. In the column containing alum shale and waste X, one can see that the waste does not have the same neutralizing capacity as the ash, as the pH is down to around 3 in the same time (about 350 days) as the column with alum shale only. It seems like adding the material has little effect on stabilizing the alum shale. Also, the same can be seen for adding gypsum. The trends for leaching in the column containing alum shale and gypsum correspond to the leaching seen in the column with alum shale only.

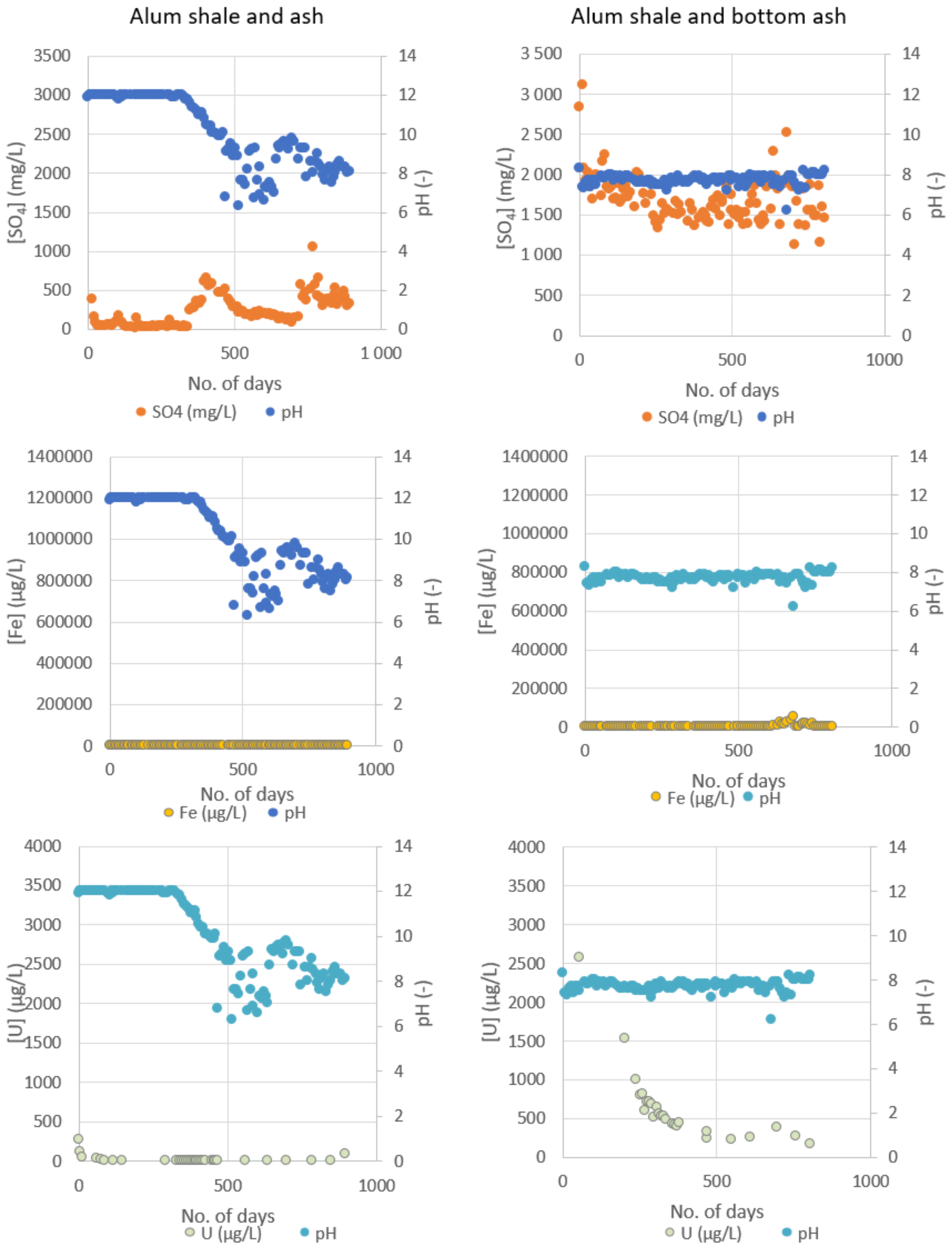

Figure 38 Column test with alum shale and ash (left) and alum shale and bottom ash (right); From top down: sulphate (SO_4), iron (Fe) and uranium (U) concentrations and pH (all) in the leachate.

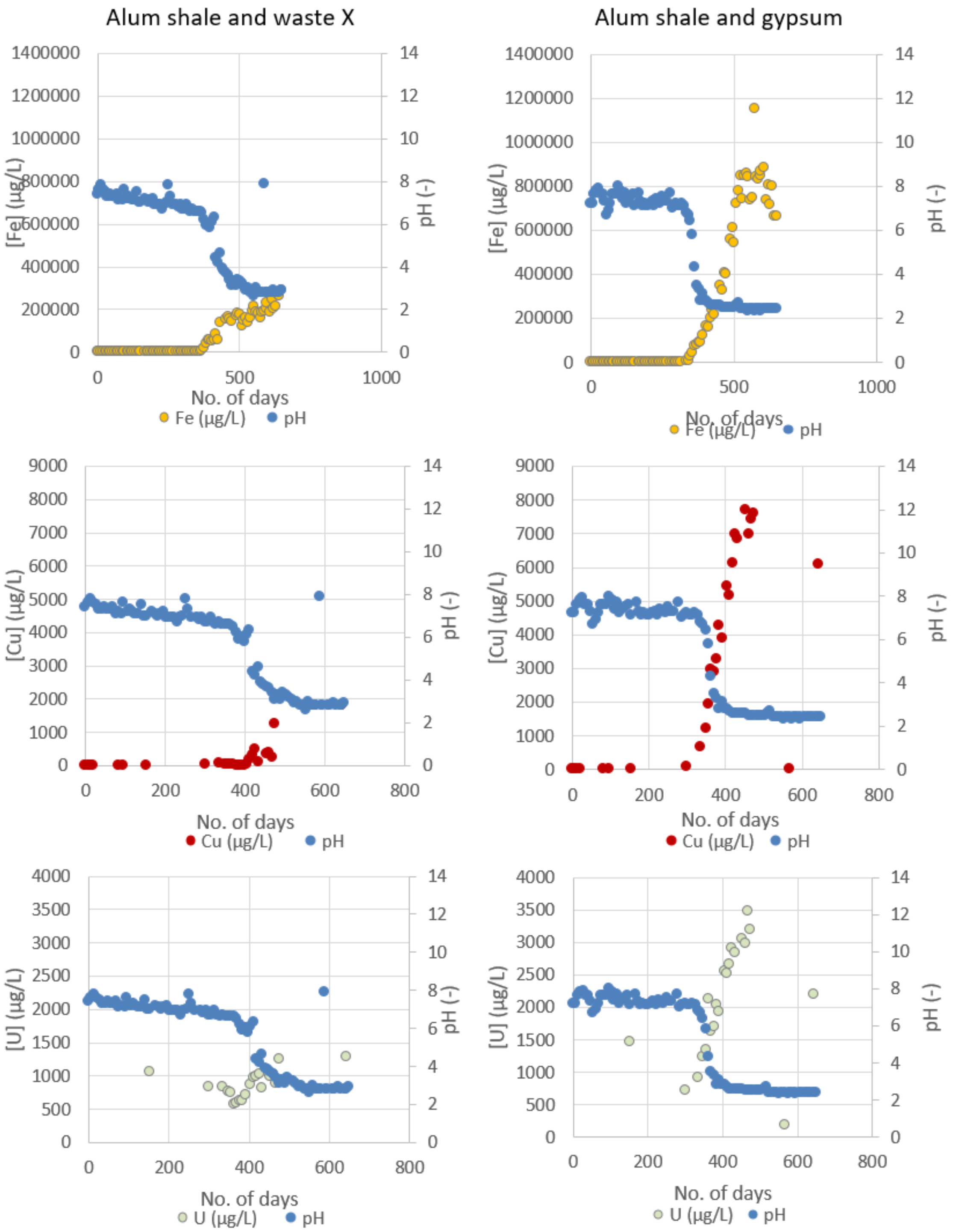

Figure 39 Column test with alum shale and waste X (left) and alum shale and gypsum (right). From top down: iron (Fe), copper (Cu) and uranium (U) concentrations and pH (all) in the leachate.

A5.3 Test cell experiment

The alum shale deposited in the test cell (test cell west) originated from horizon 2 and 3. The shale was newly received at NOAH Langøya, when deposited at 24th and 28th of April 2015. NGI does not have any information of the time from blasting at the construction site to reception at Langøya. Considering the time horizon for the cell being open for weathering at Langøya (519 days), it is considered of little significance. Also, when looking at the pH-values (Figure 42), all samples are basic at the start of the experiments, and there has likely been little exposure of O_2 and H_2O before deposition at Langøya.

The cell consisted of a little over 400 tons of alum shale and was left open for weathering. A temperature logger was installed for continuous monitoring of the temperature development. The leachate from the cell was collected, for chemical analysis for the following parameters: pH, conductivity, Fe, SO_4^{2-}, Ca, K, Mg, Ca, Mn, Al, Zn, Ni, Na, Si, Pb, Cu, Cd, Co and U. See Figure 40 for picture of the test cell.

Figure 40 Test cell experiment (Photo: NOAH)

The test cell experiment was started 7th of May 2015 and covered 6th of October 2016 (518 days, see black vertical line in Figure 41). The 6th of October, the test cell was flushed with anoxic water with basic pH (8,5). This was done to slow down the reactions in the alum shale. After flushing, the cell was capped with a low-permeable, basic waste to prevent oxygen and water coming through the shale. The temperature measurements and sampling of leachate was continued after the closure of the cell, though the amount of water was limited (not quantified).

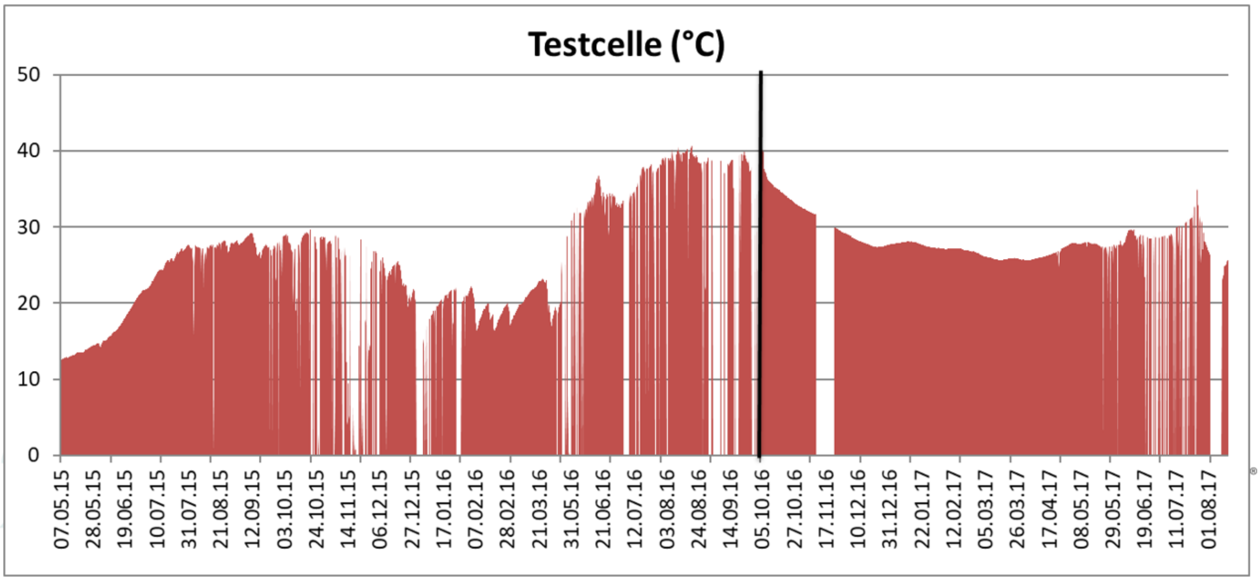

Figure 41 Temperature measurements in test cell (from NOAH). Black vertical line shows when the test cell was flushed with basic, anoxic water and capped to prevent further intrusion of water and oxygen.

About a year into the experiment (end of May in 2016), there was a rise in temperature in the test cell (Figure 41). This is followed by a significant drop in pH from 7,9 on the 1st of August to 4,4 on the 9th of August. Simultaneously, metals present in the shale were mobilized, as seen by a large increase in all analysed metals in the leachate (see examples for detected concentrations for uranium, copper, aluminium and cadmium in Figure 43, plotted together with the pH in the leachate).

For uranium, there were also quite high concentrations in the leachate before the pH-drop. This corresponds to theory, where uranium can be leachable under near neutral conditions. The concentrations of the other elements in the figure show that their mobility is highly pH-dependent.

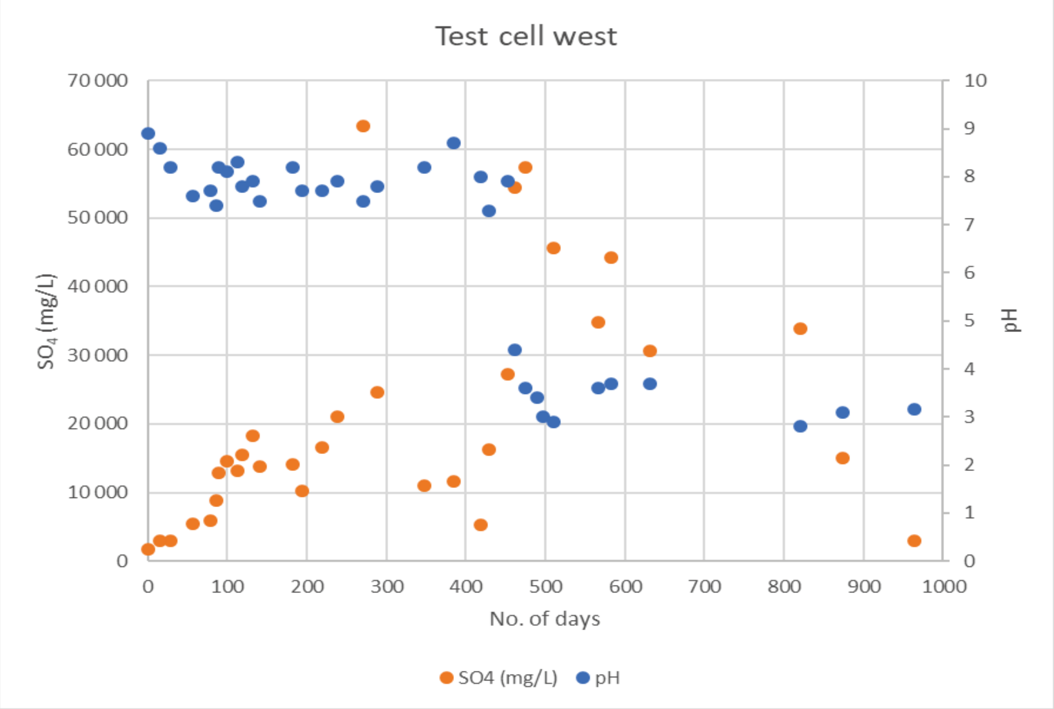

Figure 42 Test cell with alum shale; pH and sulphate (SO_4) in leachate.

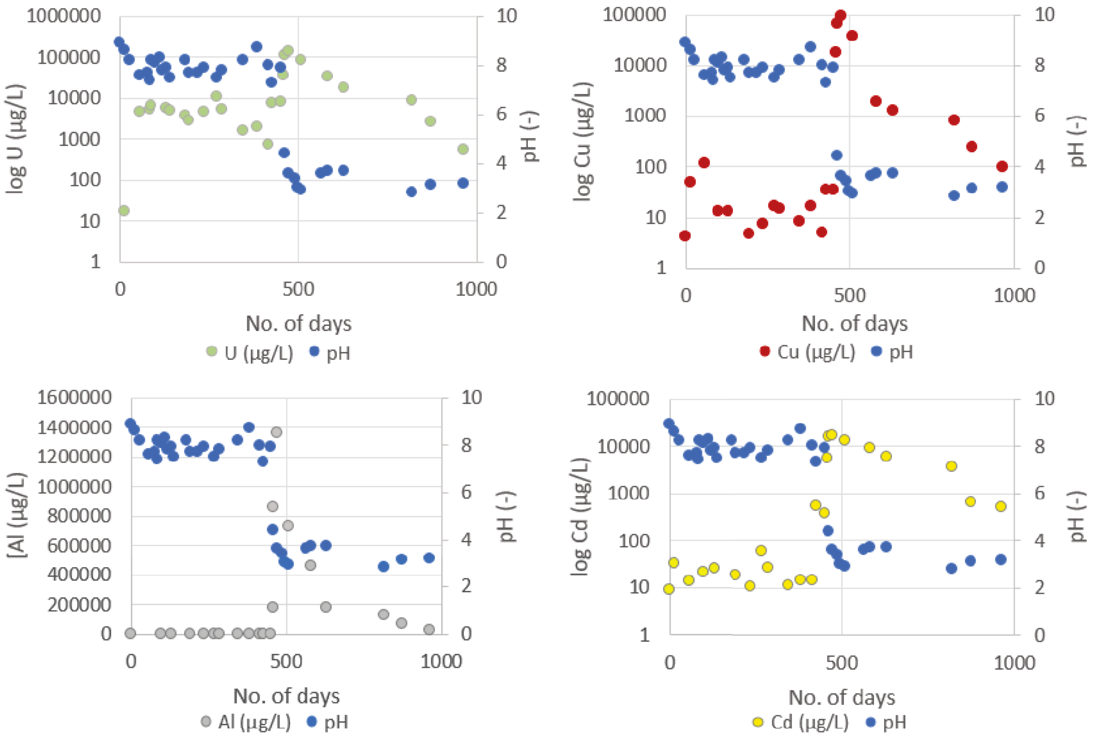

Figure 43 Detected concentrations of uranium (U), copper (Cu), aluminium (Al) and cadmium (Cd), plotted with pH in the leachate from the test cell. Note that element concentrations for uranium, copper and cadmium are on a logarithmic scale.

A6 Høvik

As a part of the preliminary work on the infrastructure project E18 between Lysaker and Ramstadsletta, the rocks along the future road line have been mapped. The rocks belong to horizon 4 in the Oslo-Asker formation (from the Cambro-Ordovician period), consisting of mudrocks (shales) with interbedded calcareous rocks and some intrusive rocks of Permian age, Figure 44.

Figure 44 Picture of typical shale samples from horizon 4 in the Oslo-Asker formation.

It was a concern in the project that the rocks could be a source of acid rock drainage, and thus negatively affecting concrete installations and water mains and sewage. To clarify if the dark shales in the formations have the potential of generating acid rock drainage, geochemical rock analyses and one stage batch leaching tests were performed on rock samples taken from bore hole cores (unweathered samples).

According to the classification tool (M-310, Norwegian Environment Agency, 2015a), the samples representing the bedrock in the area, will not be generating acid rock drainage, as they all fall in the area above NP:AP of 3:1 (see Figure 45). The Fe:S ratio is well over 2:1, indicating that iron and other metals mainly are combined as silicate minerals in the rock, and not as sulphides (Figure 46). This means that the metals are strongly tied and not mobile and that the rocks have a low potential for leaching metals (NGI 2020b).

From the one stage batch tests it was found that the leachate from the samples had high pH and low levels of heavy metals and sulphate. Uranium was not detected in the leachate, see Table 10.

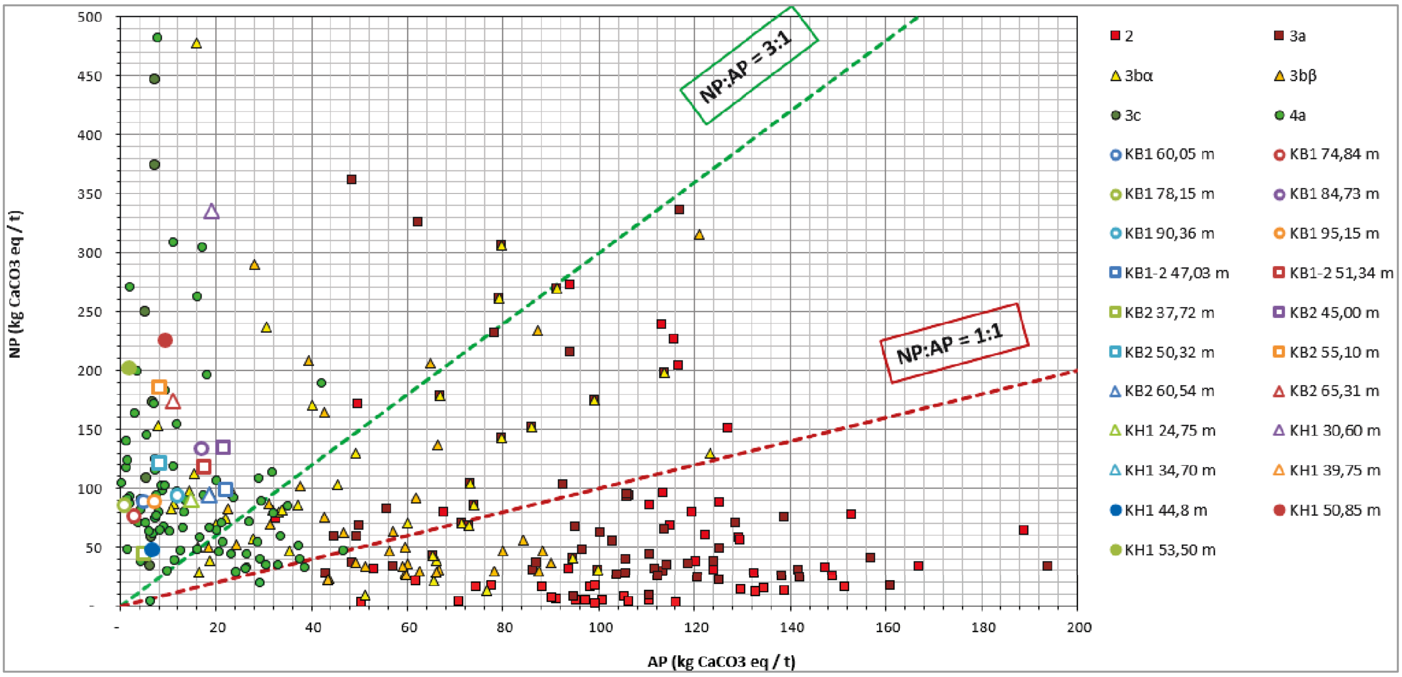

Figure 45 Acidification potential plotted against neutralizing potential for the Høvik shales and reference samples (2, 3a, 3bα, 3bβ, 3c and 4a).

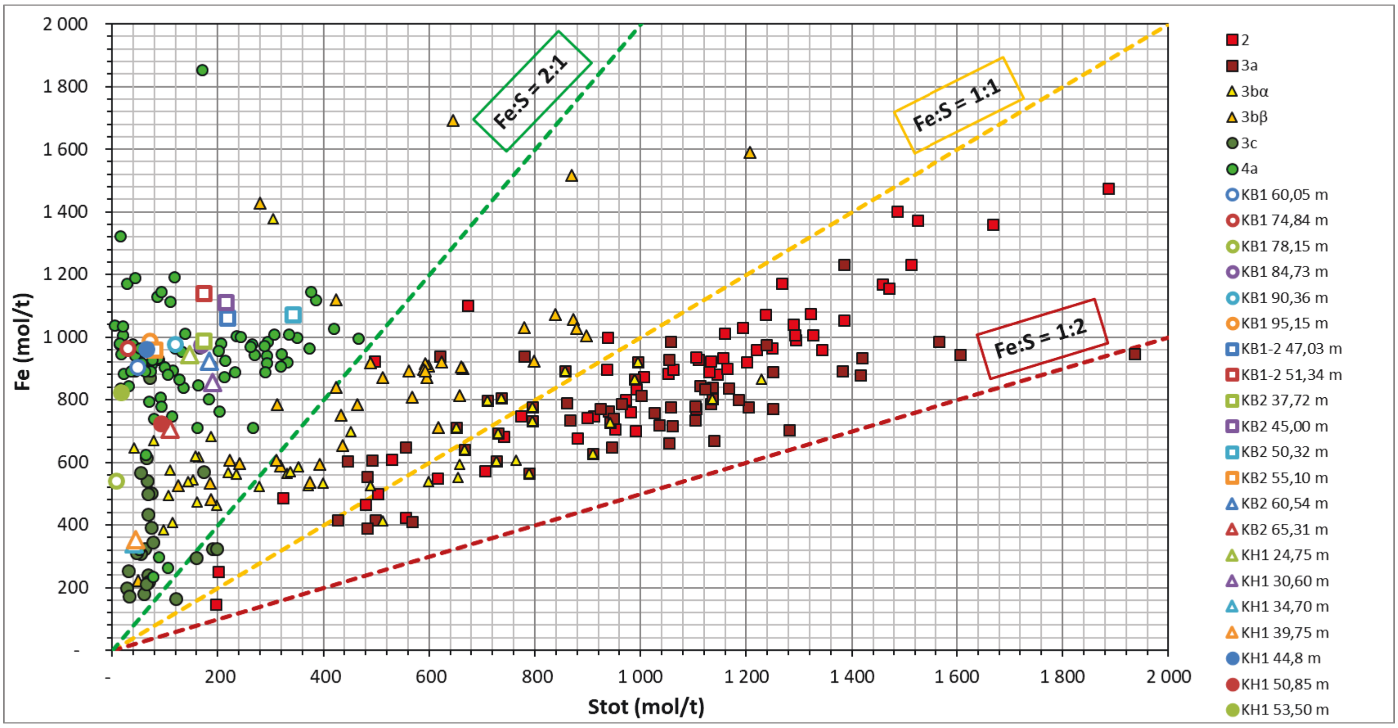

Figure 46 Total content of sulphur plotted against iron for the Høvik shales and reference samples (2, 3a, 3bα, 3bβ, 3c and 4a).

Table 10 Results from one stage batch leachate tests on Høvik shales compared with guidelines for deposition of waste (mg/kg) (NGI 2020c).

	KB1	**KB1-2**	**KB2**	**KH1**	**Inert waste (L/S=10) (mg/kg)**	**Ordinary waste (L/S=10) (mg/kg)**	**Hazardous waste (L/S=10) (mg/kg)**
As	0,067	0,033	<0,020	<0,020	0,5	2	25
Ba	0,78	0,89	0,54	1,61	20	100	300
Cd	<0,0050	<0,0050	<0,0050	<0,0050	0,04	1	5
Cr	0,07	<0,050	<0,050	<0,050	0,5	10	70
Cu	<0,100	<0,100	<0,100	<0,100	2	50	100
Hg	<0,00010	<0,00010	<0,00010	<0,00010	0,01	0,2	2
Mo	0,11	<0,100	<0,100	<0,100	0,5	10	30
Ni	0,054	<0,030	<0,030	<0,030	0,4	10	40
Pb	0,013	<0,010	<0,010	<0,010	0,5	10	50
Sb	0,015	0,012	0,015	<0,010	0,06	0,7	5
Se	<0,050	<0,050	<0,050	<0,050	0,1	0,5	7
Zn	0,77	0,29	0,64	0,6	4	50	50
Cl^- (Chloride)	13	6,4	6,9	6,4	800	15 000	25 000
F^- (fluoride)	2,3	2,1	1,9	1,6	10	150	500
SO_4 (sulfate)	64	56	39	52	1 000	20 000	50 000
DOC	82	75	67	42	500	800	1 000
Fenol index	<0,05	<0,05	<0,05	<0,05	1	-	-
TDS	<50	<50	<50	<50	4 000	60 000	100 000
pH	9,8	9,4	9,6	9,2	-	-	-
Uranium	<0,01	<0,01	<0,01	<0,01	-	-	-
Conductivity (mS/m)	23,8	13,3	17,5	8,1	-	-	-

A7 Taraldrud

Next to E6 in Ski commune, close to the Taraldrud exit, black shales were deposited for levelling purposes in the 1980s and 1990s. The rock masses originated from excavation projects connected to some identified projects in Oslo city centre. The rock masses in the area of excavation are mainly categorized as horizon 2 and 3a alum shales. In 2017, NGI estimated the volume of black shales to be around 51 250 m^3, covered by approximately 64 000 m^3 of other inert rock masses (NGI 2017c). The extent and thickness of alum shale is shown in Figure 47.

The shales in parts of the area have had access to oxygen and water for many years and were visibly weathered. Weathering of the black shales have led to acid rock drainage with low pH and high concentrations of heavy metals and uranium in the nearby creek. To limit the run-off from the deposited rock masses, a treatment dam was installed in 2008. Limestone has been added to the dams to increase the pH value and thereby precipitate (and co-precipitate) metals and uranium.

The deposited masses have been examined multiple times (Bioforsk in 2007-2009, NGI in 2015-2017). Water sampling from the nearby creek, treatment dams and pits were performed by NGI in 2015 (NGI 2016a).

In 2017 NGI dug 16 pits to evaluate the extent and volume of the black shale. It was performed geochemical analyses of black shale samples and water samples were taken from the pits with water intrusion. The placement of the sampling points in 2017 is given in Figure 47.

From the geochemical analyses the deposited black shales were classified to mainly consist of alum shale stage 2 and 3a, with elements of Hagastrand-/Galgeberg stage 3bα and 3bβ, Elnes shale stage 4a and calcareous clay shale. The acid potential and neutralization potential are plotted in Figure 48, showing that the alum shale samples are in the acid-producing zone. The Fe:S ratio is around 1:1 indicating that sulphur mainly is present as sulphides, resulting in an elevated potential for acidic run-off and leaching of metals from the alum shales (Figure 49).

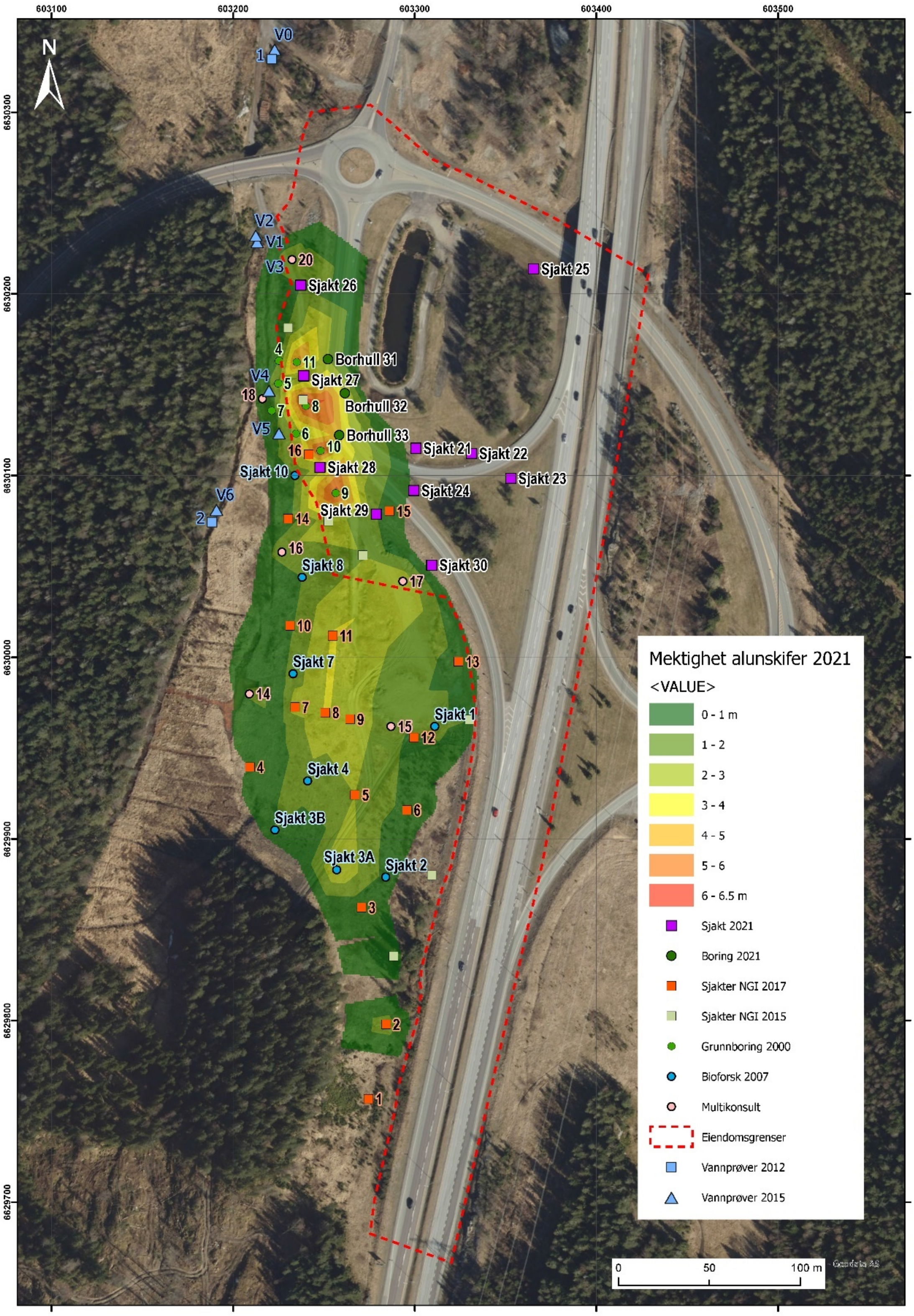

Figure 47 Taraldrud, map indicating the thickness of alum shale layer and sampling points (NGI, 2022c).

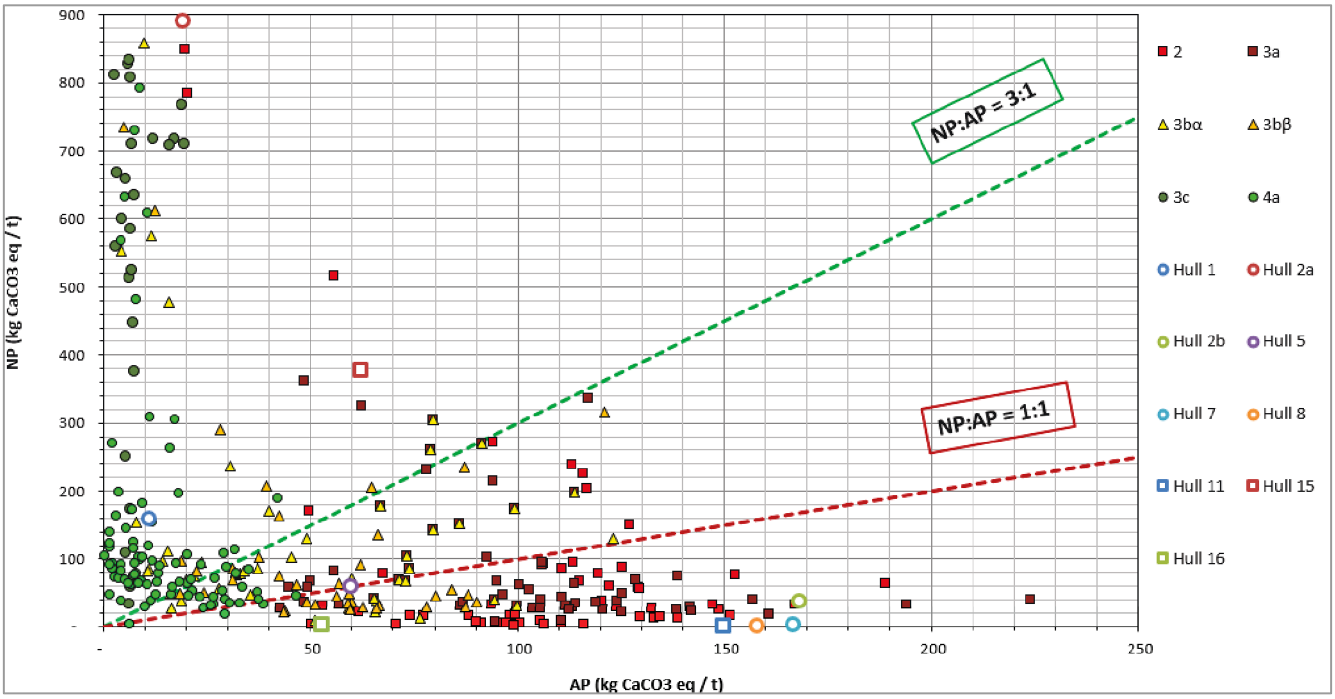

Figure 48 Acidification potential plotted against neutralizing potential for the Taraldrud shales and reference samples (2, 3a, 3bα, 3bβ, 3c and 4a) (NGI, 2017c).

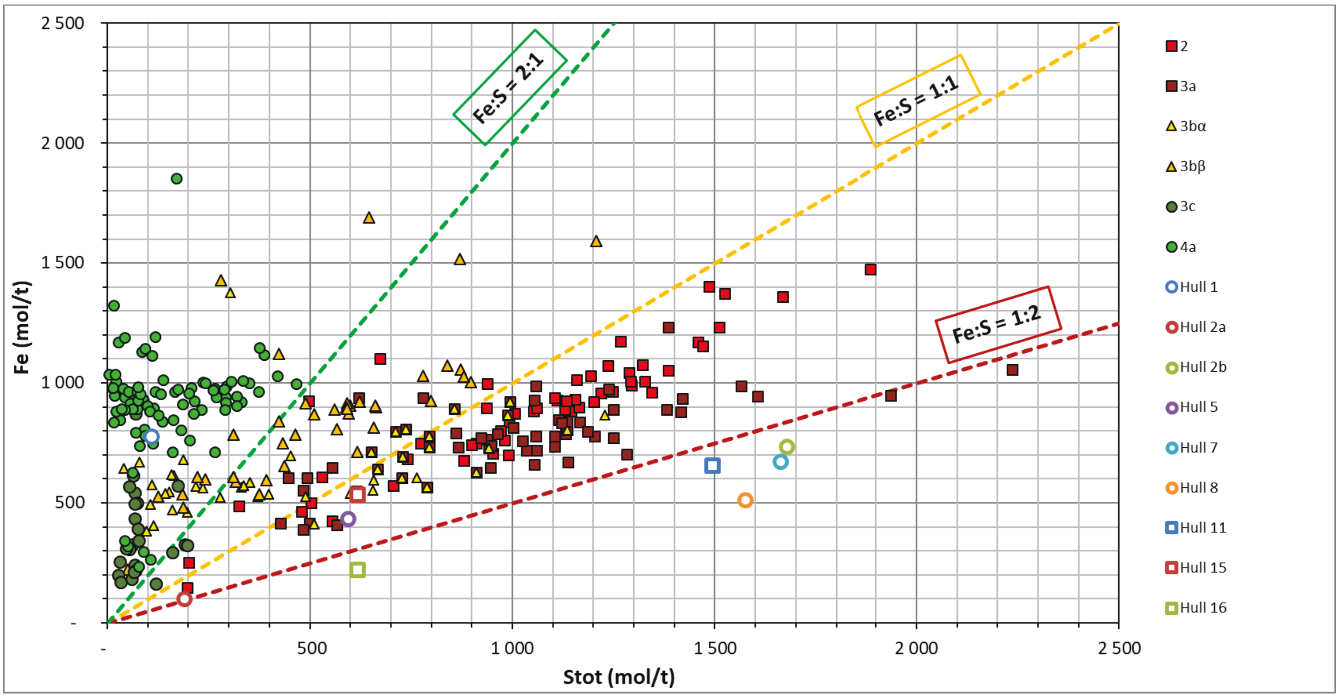

Figure 49 Total content of sulphur plotted against iron content for the Taraldrud shales and reference samples (2, 3a, 3bα, 3bβ, 3c and 4a) (NGI, 2017c).

The uranium concentration in the samples from Taraldrud was measured both with total chemical analyses of the rock samples with ICP-MS at an accredited laboratory, and with pXRF calibrated specifically for use with black shales at NGI's laboratory. The results are given in Table 11. For the samples that were measured with both techniques, linear regression gives an R^2 of 0.97 and the slope 1.1, indicating that the two methods give very similar results.

Table 11 Concentrations of uranium (mg/kg) in samples from Taraldrud measured with pXRF and total chemical analyses with ICP-MS (NGI 2017c).

Sampling point	Uranium content measured with ICP-MS (mg/kg)	Uranium content measured with pXRF (mg/kg)	Horizon
1	6,4	3,0	Elnes fm. (4a)
2a	48	47	Calcareous shale
2b	145	159	Alum shale fm. (2 and 3a)
3	-	91	-
5	52	39	Galgeberg-/Hagastrand fm. (3bα/3bβ)
6	-	59	-
7	145	152	Alum shale fm. (2 and 3a)
8	113	126	Alum shale fm. (2 and 3a)
9	-	106	-
10	-	90	-
11	130	144	Alum shale fm. (2 and 3a)
12	-	131	-
13	-	109	-
14	-	164	-
15	92	70	Galgeberg-/Hagastrand fm. (3bα/3bβ)
16	44	41	Alum shale fm. (2 and 3a)

- total chemical analysis has not been performed on this sample

Of the 17 sampling points, 4 had intruding water that was sampled and analysed (Table 12). Water sample from hole 1 represents the least contaminated sample and has a neutral pH. The content of metals is moderate, corresponding to the classification of the rocks from this hole. The black shale is classified to have a high neutralisation potential and it is therefore not expected to find elevated heavy metal concentrations (Table 12).

The sample from point 16 represent the opposite, with an acidic pH of 3 and elevated metal concentrations. The classification of the black shale from this hole shows high risk of ARD and the data is a good example of a relatively mature and extensive weathering process of black shales.

With a pH of 5.7-5.9 the water samples from hole 7 and 14 are not as acidic as in hole 16, but also here the content of heavy metals is elevated compared to hole 1. The shale in hole 7 and 14 are classified as alum shale with high risk of acid rock drainage (ARD). The differences in the water analyses are thought to be caused by local variations in the grain size distribution of the rocks, combined with the availability of oxygen and water in the deposited masses. The uranium concentrations in the water samples are also varying with the assumed degree of weathering, from high concentrations in hole 16 (6980 µg U/L) to intermediate in hole 7 and 14 (110 and 200 µg U/L), and low in hole 1 (2.9 µg U/L).

Table 12 Results from analyses of filtrated water samples from sampling points (pits) from Taraldrud (NGI 2017c)

Parameter		1	7	14	16
pH		7,0	5,7	5,9	3,0
Conductivity	mS/m	101	293	338	513
Ca	mg/l	167	529	518	483
Fe	mg/l	0,02	38	127	334
K	mg/l	15	4,8	4,6	<3
Mg	mg/l	19	146	123	196
Na	mg/l	14	23	89	129
Al	µg/l	8,9	12	530	182 000
As	µg/l	1,9	<0,5	<0,5	<30
Ba	µg/l	121	15	15	<10
Cd	µg/l	0,16	15	4,5	306
Co	µg/l	3,2	177	185	1030
Cr	µg/l	<0,5	<0,5	<0,5	122
Cu	µg/l	11	<1	<1	9880
Hg	µg/l	<0,02	<0,02	<0,02	<0,02
Mn	µg/l	4030	10 100	9270	9420
Mo	µg/l	4,1	0,866	3,44	<30
Ni	µg/l	4,72	1350	1390	7760
Pb	µg/l	0,381	<0,2	<0,2	<10
Zn	µg/l	80	305	515	9900
V	µg/l	1,1	<0,05	<0,05	93,8
Th	µg/l	<0,2	<0,2	<0,2	21,9
U	µg/l	2,9	110	200	6980
DOC	mg/l	15	1,7	1,8	2,3

Parameter		1	7	14	16
Sulphate (SO_4)	mg/l	24	1980	2140	4500
Nitrate (NO_3)	mg/l	<2,0	<2,0	<2,0	<2,0
Chloride (Cl^-)	mg/l	20	16	170	210

The recipient (Snipetjernsbekken, a small stream draining to Gjersjøen) was sampled in 2015 and the results are given in Table 13 (V0, V2, V6) together with some more samples from porewater seeping into shafts during sampling (P4-P7) as well as water samples taken in treatment dams (V3-V5). V1 is water from a storm water pipe that enters the stream between V0 and V2. Sampling points are given in the map in Figure 47.

Table 13 Results from water sampling in nearby recipient performed at Taraldrud in 2015 (NGI 2016a). Samples with P are from pits, V is from the creak or from the treatment dams.

		P4	**P5**	**P6**	**P7**	**V0**	**V1**	**V2**	**V3**	**V3 filtr.**	**V4**	**V4 filtr.**	**V5**	**V5 filtr.**	**V6**
		Pore	**Pore**	**Pore**	**Pore**	**Up**	**Storm**	**Up**	**Treat**	**Treat**	**Treat**	**Treat**	**Treat**	**Treat**	**Down**
pH		6,09	7,08	-	2,68	7,43	7,64	7,47	6,66	-	3,38	-	3,16	-	7,3
Conductivity	mS/m	99,8	147	-	400	21,6	82,1	22,4	180	-	227	-	293	-	25,5
Ca	mg/l	134	333	642	557	24,4	36,7	24,2	285	275	354	328	467	440	27,8
Fe	mg/l	156	59,7	487	278	0,995	1,28	1,01	33,9	4,53	41,4	20,3	81,1	44,8	1,18
K	mg/l	4,46	19	14,5	7,42	2,37	4,33	2,41	7,35	7,45	2,51	<3	2,37	<3	2,56
Mg	mg/l	45,7	44,5	90,4	122	2,44	3,76	2,53	56,2	59,3	75,8	78,4	94,7	98,7	3,21
Na	mg/l	13,4	14,5	11,8	74	16,2	123	17,1	63,2	61,5	50,9	47,8	71,7	66,5	20,7
Al	µg/l	215	32 900	101 000	70 600	1230	1300	1290	1590	36,6	21 500	20 700	30 000	29 400	1510
As	µg/l	4,11	34,3	102	149	0,526	0,672	0,638	0,837	<1	<0,5	<1	0,686	<1	0,688
Ba	µg/l	116	674	762	610	27,1	39,3	29,2	89,2	75,1	17,8	16,5	12,9	12,6	28
Cd	µg/l	<0,1	1,75	132	53,8	<0,05	<0,05	<0,05	6,88	5,88	20	19	27,5	29	0,278
Co	µg/l	10,9	39	678	408	0,402	0,525	0,371	87,6	82,4	194	183	285	268	1,93
Cr	µg/l	1,99	69,6	168	80,6	1,6	1,91	1,75	<0,9	<0,5	8,17	2,41	14	9,35	1,54
Cu	µg/l	<2	193	1850	2250	1,6	7,36	1,6	76,3	6,59	350	347	623	580	6,24
Hg	µg/l	<0,02	0,667	0,295	0,152	<0,02	<0,02	<0,02	<0,02	<0,02	<0,02	<0,02	<0,02	<0,02	<0,02
Mn	µg/l	21700	1230	8630	4090	53,3	72,4	51,6	2980	2920	2850	2710	4010	3830	76,9
Mo	µg/l	<1	43,8	83,4	318	0,552	3,33	0,547	2,05	1,3	0,759	<0,5	1,66	<0,5	0,789
Ni	µg/l	2,21	134	4610	3340	1,9	3,31	2,13	657	615	1610	1450	2350	2110	12,6
Pb	µg/l	<1	171	118	66,8	0,733	1,03	0,74	<0,5	<0,2	2,21	1,92	2,11	2,05	0,971
Zn	µg/l	<8	590	3430	1920	4,07	11,1	5,07	342	304	891	799	1230	1120	14,2
V	µg/l	7,13	91,1	252	91,6	2,42	2,88	2,4	0,561	<0,05	1,57	<0,05	4,89	<0,05	2,06

		P4	**P5**	**P6**	**P7**	**V0**	**V1**	**V2**	**V3**	**V3 filtr.**	**V4**	**V4 filtr.**	**V5**	**V5 filtr.**	**V6**
		Pore	**Pore**	**Pore**	**Pore**	**Up**	**Storm**	**Up**	**Treat**	**Treat**	**Treat**	**Treat**	**Treat**	**Treat**	**Down**
U	µg/l	1,1	52,1	3210	1580	0,734	3,52	0,932	87,6	69,7	483	455	799	795	3,54
Si	mg/l	6,71	54,3	97,7	51,1	5,81	5,83	5,82	10,2	9,13	16,1	15,9	19,2	19,3	6,15
DOC	mg/l	34,4	1,9	-	1,68	11,5	8,11	10,3	5,95	-	1,48	-	1,45	-	9,66
Sulphate	mg/l	14,5	650	-	2730	12,5	31,2	12,6	787	-	1420	-	1900	-	23,4
Nitrate	mg/l	<2,00	11,2	-	<2,00	2,16	3,99	2,18	<2,00	-	<2,00	-	<2,00	-	2,24
Chloride	mg/l	5,61	3,13	-	124	22,4	194	24,8	87,7	-	75,1	-	102	-	29,4

- analysis was not performed on this sample. Pore = porewater from excavated shafts. Up = Upstream. Storm = water from storm water pipe. Treat = treatment dam. Down = downstream

A8 Vilberg

In 2007, a total quantity of approximately 34 515 ton of black shales were deposited in an old gravel pit at Vilberg in Ullensaker commune (NGI 2016b). The rocks were encapsulated in clay to keep the oxidation to a minimum. The shales came from different locations in the Oslo area, see Table 14. The shale from Konows gate, Alunverket and Gran are thought to be exposed to rain and air for longer periods before they were deposited and are thus considered to be weathered.

Table 14 Rock masses received at Vilberg

Date of deposition	Mass (ton)	Origin
09.02 – 19.03.2007	12 000	Konows gate 7, Oslo
06.02 – 02.03.2007	8106	Sofies Hage, step 2 (Freia-park), Københavngata and Karlstadgata, Oslo
06.03 – 12.04.2007	698	Backfill from Alunverket, Grønlia, Oslo
06.02 – 21.02.2007	13 711 (shale mixed with clay)	Gran, Enebakk (originally from Oslo city center)

It has been performed geochemical analyses of rock samples from the landfill (samples taken in 2016). The shales have been classified to be alum shale from horizon 2 and 3a, Galgeberg shale 3bβ and Hagastrand shale 3bα.

The shales mainly have a NP:AP ratio under 1:1, indicating a potential to generate acid rock drainage, while some of the samples were classified to be in the uncertainty zone, see Figure 50.

The Fe:S ratio is around 1:1 indicating that the sulphur mainly is present as sulphide, resulting in an elevated potential for acidic run-off and leaching of metals (Figure 51).

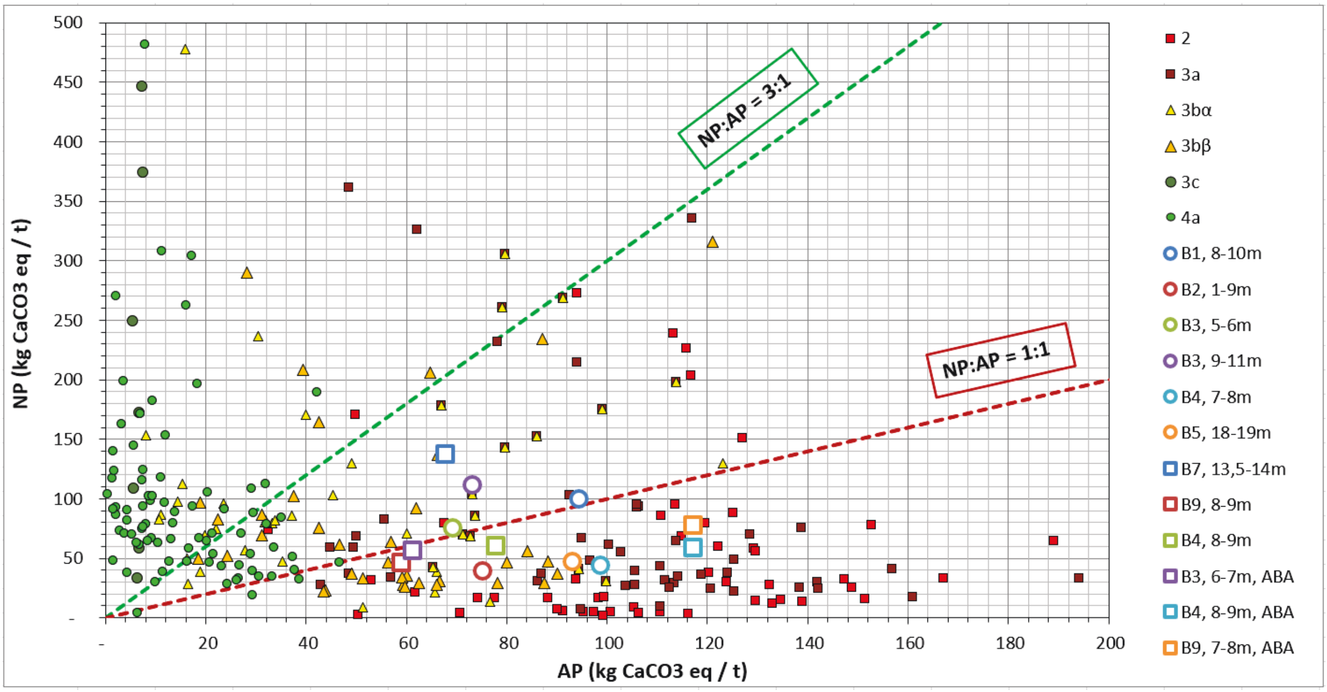

Figure 50 Acidification potential plotted against neutralizing potential for the Vilberg shales and reference samples (2, 3a, 3bα, 3bβ, 3c and 4a) (NGI, 2020d).

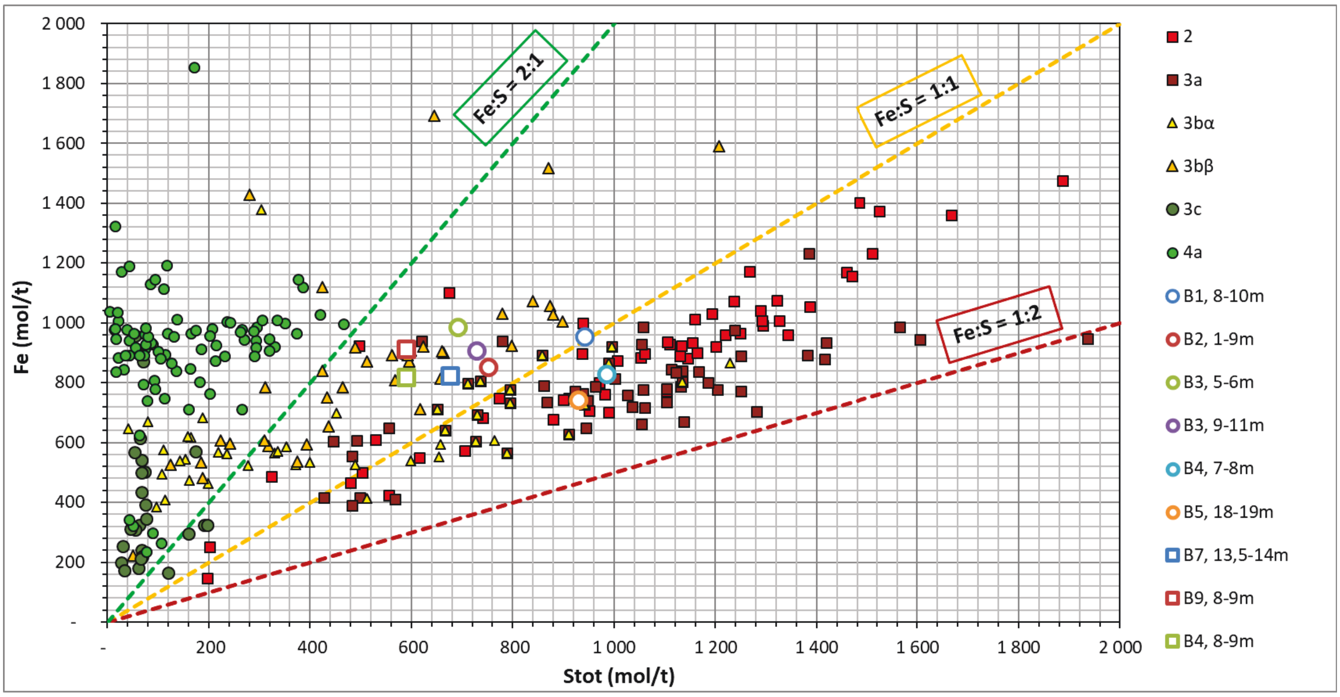

Figure 51 Total content of sulphur plotted against iron content for the Vilberg shales and reference samples (2, 3a, 3bα, 3bβ, 3c and 4a) (NGI, 2020d).

The shales from Vilberg were tested with ABA tests (Acid-Base Accounting) and the results are given in Table 15. The following can be noted from the tests:

- All pH values are above 7.
- Two samples are in the uncertainty zone and 8 have net acid-forming potential.
- Compared with AP-NP diagram in Figure 50, the ratio of NP:AP is approximately the same, indicating a similar risk of acid rock drainage (ARD).
- The measured AP and NP in both tests (geochemical and ABA) are of the same magnitude, but the NP is in average a little lower in the ABA tests.
- Testing of the clay did not show that the clay has neutralising effects. The neutralising ability is based on the content of carbonates in both ABA tests and in the M-310 classification tool.
- The ABA test was unsuitable for classifying mixed samples of clay and shale.

It should be remarked that the tests are not performed on the same shale samples, but from samples taken from different depths in the boreholes. Results for the chemical analysis and the ABA test are therefore not directly comparable.

Table 15 Results from ABA-tests on samples of black shale, clay and a mixture of black shale and clay (NGI 2016b, 20160342-01-R).

	Paste pH	**TIC %**	**CaCO$_3$ NP**	**S(T) %**	**S(SO$_4$) %**	**S(S$_2$) %**	**Insol-uble S %**	**AP** kg CaCO$_3$ eq/ t	**Modified NP** kg CaCO$_3$ eq/ t	**NP: AP**	**Fizz Test**	**Sample type**
B1 (8-9m)	7,66	0,35	29,2	2,73	0,04	2,44	0,25	76,3	33,2	0,44	Slight	Shale and clay
B2 (8-9m)	7,18	0,26	21,7	2,38	0,19	1,98	0,21	61,9	20,7	0,33	None	Shale and clay
B2 (12-12.5m)	7,43	0,21	17,5	0,80	0,07	0,69	0,04	21,6	20,1	0,93	None	Clay
B3 (6-7m)	7,43	0,68	56,7	2,34	0,08	1,96	0,30	61,3	56,2	0,92	Slight	Shale
B3 (8-9m)	7,27	0,49	40,8	1,79	0,14	1,53	0,12	47,8	39,2	0,82	Slight	Shale and clay
B3 (14-15m)	7,50	0,22	18,3	0,57	0,05	0,48	0,04	15,0	19,8	1,32	None	Clay
B4 (8-9m)	7,50	0,74	61,7	2,79	0,09	2,41	0,29	75,3	58,4	0,78	Moderate	Shale
B5 (17-18m)	8,04	0,21	17,5	0,82	0,05	0,7	0,07	21,9	22,7	1,04	None	Shale and clay
B7 (13.5-14m)	7,58	0,76	63,3	2,21	0,07	1,92	0,22	60,0	58,5	0,98	Slight	Shale and clay
B9 (7-8m)	7,29	0,93	77,5	3,94	0,07	3,75	0,12	117,2	77,3	0,66	Moderate	Shale

To follow up on the groundwater around the deposit, five groundwater wells have been installed up- and downstream the disposal site to detect a potential leakage of heavy metals, uranium, sulphur and a lowering of pH values. Placement of the wells is given in Figure 52.The groundwater has been monitored from 2016 to 2020. The development of the pH and conductivity is given in Figure 53 and the content of uranium and sulphur is given in Figure 54.

No negative effects have been proven so far and the values in the wells downstream varies as the well upstream (BR4/Ny BR4) the deposited shales. pH vales are between

7 and 8 and uranium concentrations are low and well under WHO guidelines of 30 µg U/L.

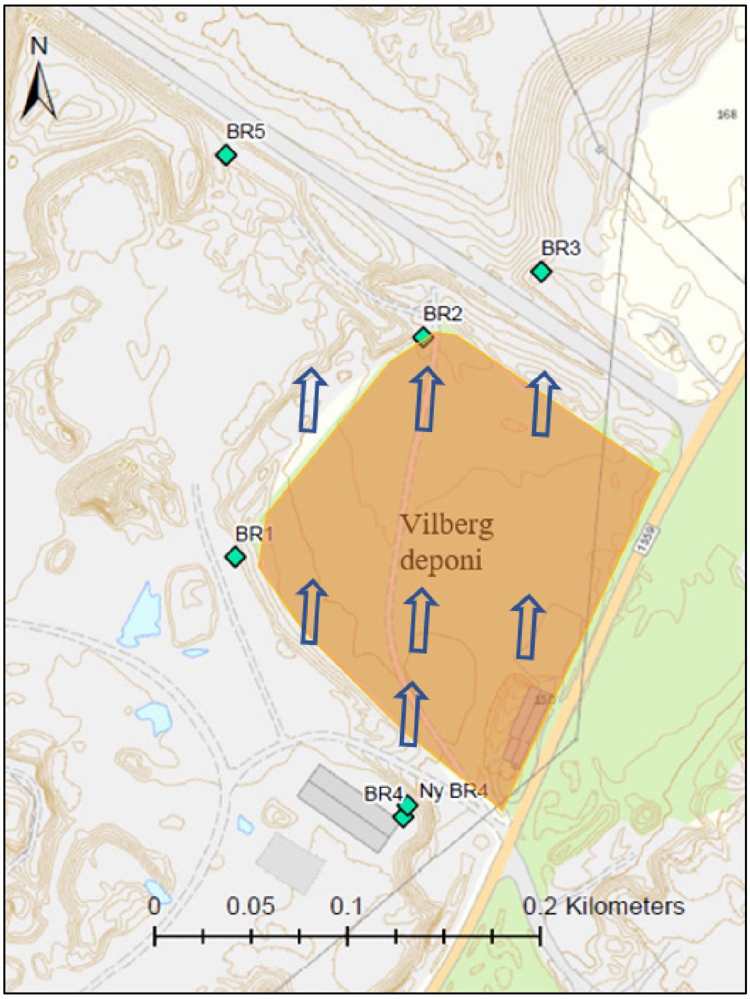

Figure 52 Map over the disposal site at Vilberg, with groundwater wells marked by green diamonds and groundwater flow indicated by blue arrows (NGI, 2020d).

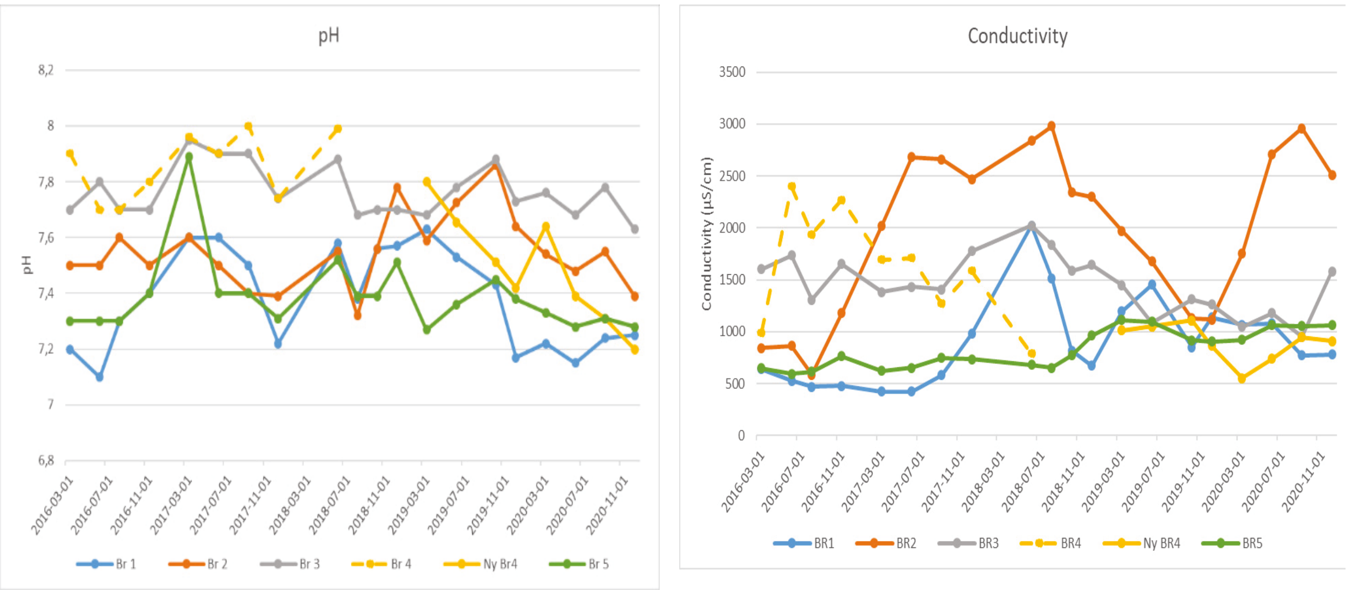

Figure 53 pH and conductivity in groundwater wells 2016-2020, Vilberg (NGI 2020d).

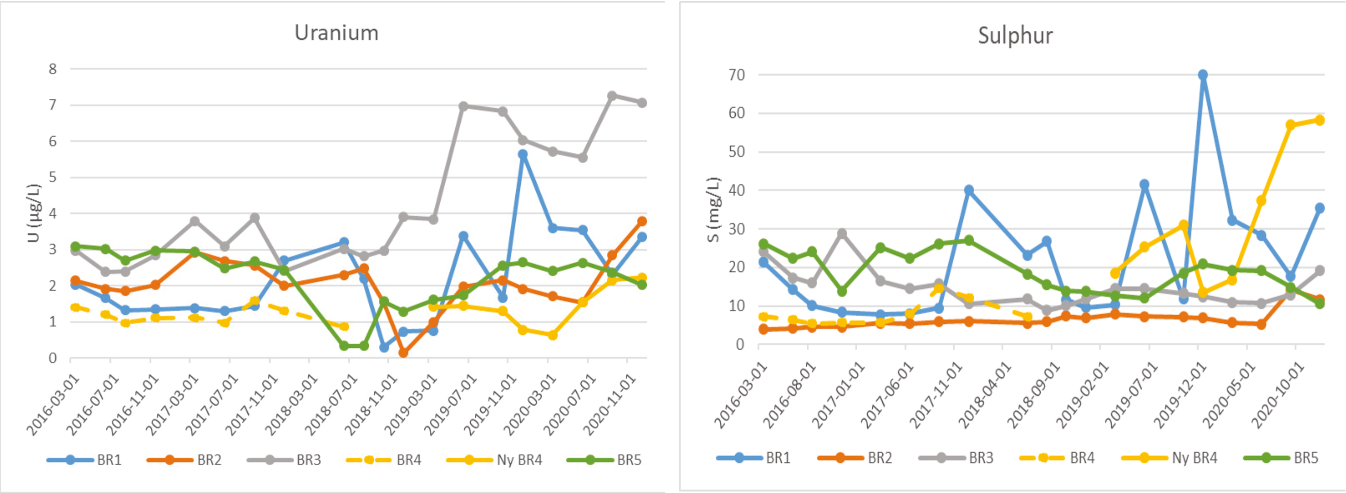

Figure 54 Uranium and sulphur concentrations in groundwater wells 2016-2020, Vilberg (NGI 2020d).

A9 References

Børresen, H. S. 2017. Geochemical and mineralogical evaluation of mineral-water reactions and leaching potential in a black shale depot. Weathering and transport of Ni, Zn, Cd, Sr and Co from Alum- and Black shale. Master thesis, Department of Geosciences, University of Oslo.

Erstad, L. A. 2017. Leaching of uranium and heavy metals from acid producing black shales. Experiments and modeling study. Master thesis, Department of Geosciences, University of Oslo.

Mamen, 2022. Oslo (klima). https://snl.no/Oslo_-_klima. Accessed 12.10.2022.

Miljødirektoratet 2019. Tillatelse til virksomhet etter forurensningsloven for NOAH AS. Tillatelsenummer: 2009.121.T, sist endret: 2019-09-27.

NGI 2022a. Under Oslo. WP1 – Container experiments - Yearly report 2021. NGI report 20200436-09-R.

NGI 2022b. Under Oslo. WP1 – Naturally mixed fractions of black shale and rhomb porphyry. NGI report 20200436-02-R.

NGI 2022c E6 Taraldrud alunskifer tiltaksplan. Koordinert tiltaksplan for forurenset grunn på eiendommene gnr./bnr. 105/4 og 157/2 på Taraldrud. NGI rapport 20210283-02-R

NGI 2020a. E16 Åsbygda – Olum. Prøvegraving ved Kleggerud – Datarapport. NGI report 20190261-01-R.

NGI 2020b. E18 Vestkorridoren, Lysaker – Ramstadsletta, Byggeplan. Klassifisering av mørk leirskifer. Report 11850 X_691 rev 01.

NGI 2020c. E18 Vestkorridoren, Lysaker – Ramstadsletta, Byggeplan. Basiskarakterisering av mørk leirskifer. Report 11850 X_692 rev 01.

NGI 2020d. Vilberg deponi. Grunnvannsovervåking 2019 – datarapport. NGI report 20170284-03-R.

NGI 2017a. E6 Kolomoen – Arnkvern. pXRF-karakterisering av svart leirskifer fra kjerneboring med Sonic Core på Kåterud. NGI technical note 20160890-11-TN.

NGI 2017b. E6 Kolomoen – Arnkvern. pXRF-karakterisering av løsmasser fra sjakting på Uthus. NGI technical note 20160890-12-TN.

NGI 2017c. Taraldrud – Grunnforurensning svartskifer. Geokjemisk kartlegging og volumestimat av svartskifer. NGI report 20160766-01-R.

NGI 2016b. Vilberg, Ullensaker kommune. Kartlegging av deponi for svartskifer. NGI report 20160342-01-R.

NGI 2016a. Taraldrud deponi. Kartlegging av utbredelse av alunskifer. NGI Technical Note 20150875-01-T.

NGI 2015. NOAH Langøya – Alunskifertesting. Kinetiske tester i kolonner og i feltceller. NGI technical note 20150271-01-TN, draft.

NGI 2013. Tunnel Gran-Jaren. Identifisering og karakterisering av skiferhorisonter i tunneltrasé. NGI report 20120110-01-R rev 1.

NIBIO 2019. E16 Eggemoen-Olum. Vannkjemiske og biologiske undersøkelser 2018. NIBIO rapport nr. 4/2018.

Norwegian Environment Agency 2016. Quality standards for water, sediment and biota – revised 2020.10.30. M-608.

Norwegian Environment Agency (Miljødirektoratet) 2015a. Identifisering og karakterisering av syredannende bergarter. Veileder M-310.

Rambøll 2018. E6 Kolomoen-Arnkvern. Risikovurdering for masseutfylling. Rambøll note, dated: 2018-01-05.

Schöpke, C. 2017. Uranium and toxic metal uptake by the earthworm Eisenia hortensis in contaminated soils. (MSc), Norwegian University of Life Sciences, Ås.

Statens vegvesen (Norwegian Public Roads Administration) 2017. Utlekkingsforsøk med svartskifer fra Rv. 4, Hadeland. SVV report no. 665.

Statens vegvesen (Norwegian Public Roads Administration) Region Øst, 2019. E16 Eggemoen – Olum. Åsbygda – Olum. Bergartsforekomster pr. 3250 – 4000. Tegning V902. Vedlegg til D2.6 Geologisk samlerapport. Dok nr. E16-GE-5530. Datert 2019-01-07.

Structor 2017. Vurdering av gjenbruk sprengstein i to tipper ved Kistefos. Report E16-GE-5516.

Strømø, T. K. 2021. Forståelse av miljøutfordringer knyttet til bygging av vei i områder med svartskifer med potensial for sur avrenning. Masteroppgave 60 ECTS. Norwegian University of Life Sciences, Ås.

WHO 2012. Uranium in drinking water. Background document for development of WHO guidelines for drinking water. World Health Organization.

Wærsted, F.M., 2019. Mobility of Naturally Occurring Radionuclides and Stable Elements in Alum Shale: A Case Study of Gran, Highway 4, Norway (PhD). Norwegian University of Life Sciences. https: //nmbu.brage.unit.no/nmbu-xmlui/handle/11250/2651558.

Wærsted, F.M., Riss, P.J., Skipperud L., 2020. The effect of water exchange on the leaching of alum shale. Applied Geochemistry; 119: 104610.

Appendix B

TRIANGULAR PLOTS OF BLACK SHALES

Contents

B1 E16 Kleggerud (Container experiments at NGI)

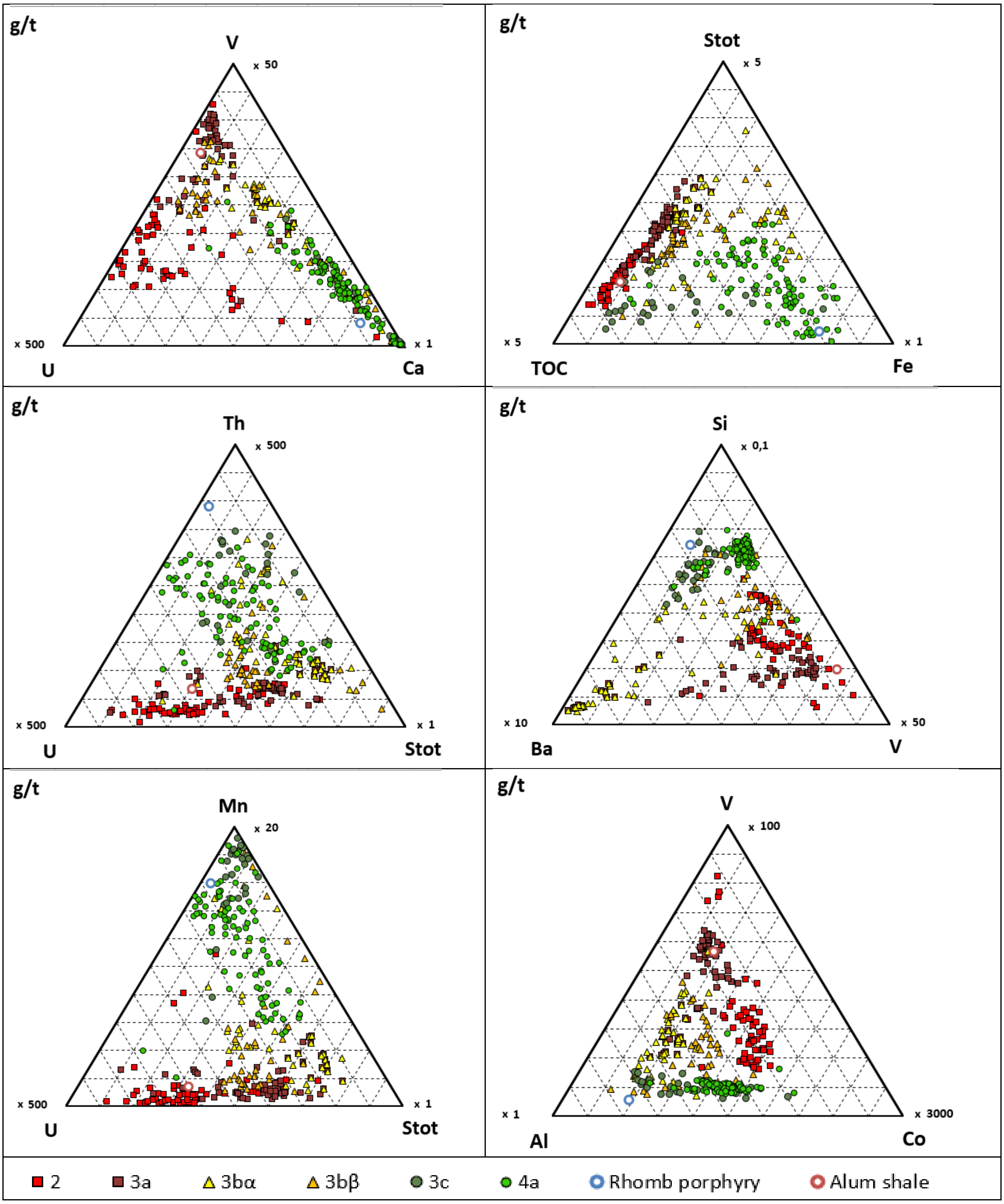

Figure 1 E16 Kleggerud (NGI), relative content in alum shale 2/3a and rhomb porphyry, compared with reference samples from black shales in the Oslo area (2, 3a, 3b, 3c and 4a).

B2 E16 Kleggerud (samples from road construction)

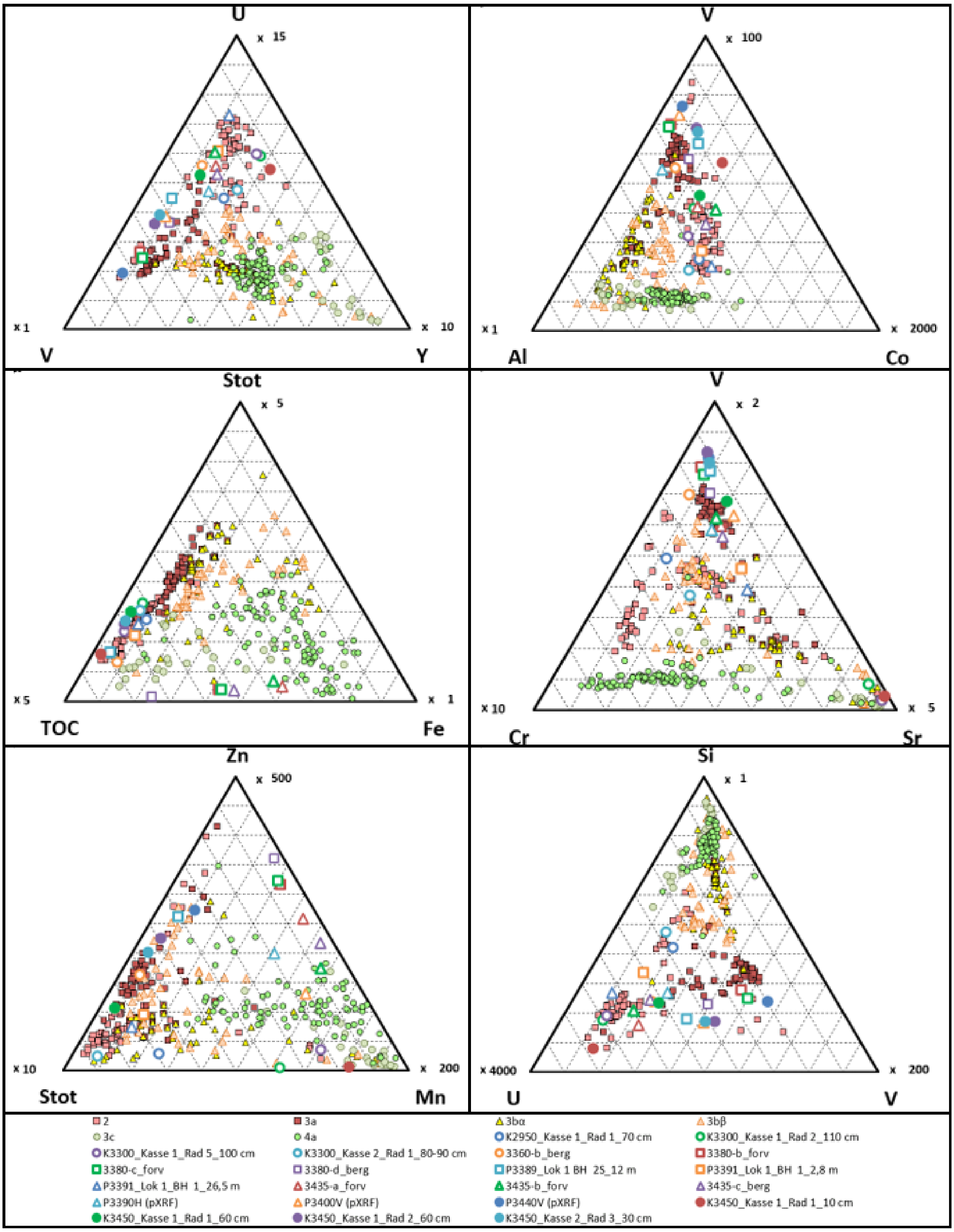

Figure 2 E16 Kleggerud, relative content in the samples (profile 2950-3450), Alum shale 2 or 3a, compared with reference samples from black shales in the Oslo area (2, 3a, 3b, 3c and 4a).

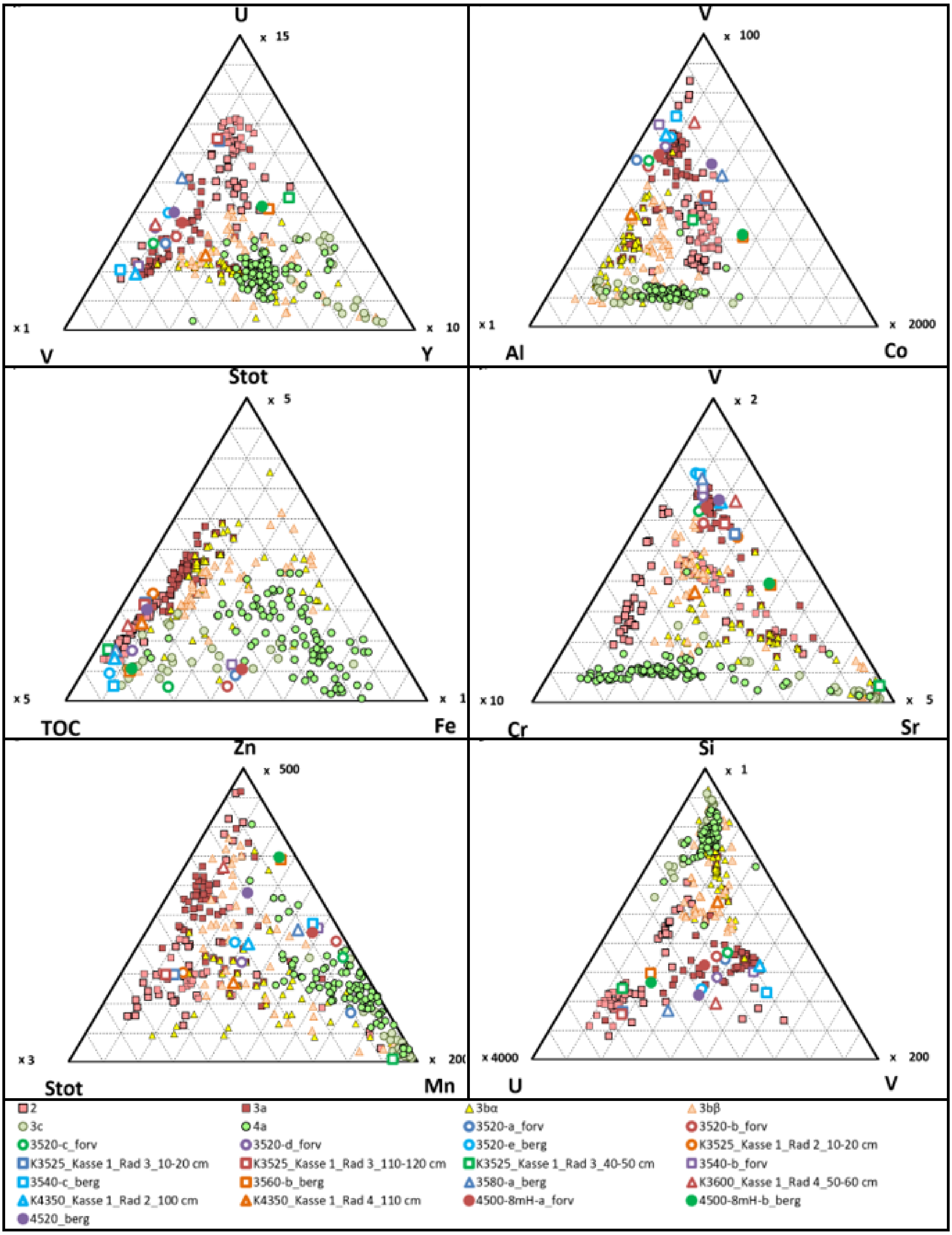

Figure 3 E16 Kleggerud, relative content in the samples (profile 3500-4520), Alum shale 2 or 3a, compared with reference samples from black shales in the Oslo area (2, 3a, 3b, 3c and 4a).

B3 New road to Kistefos Museum

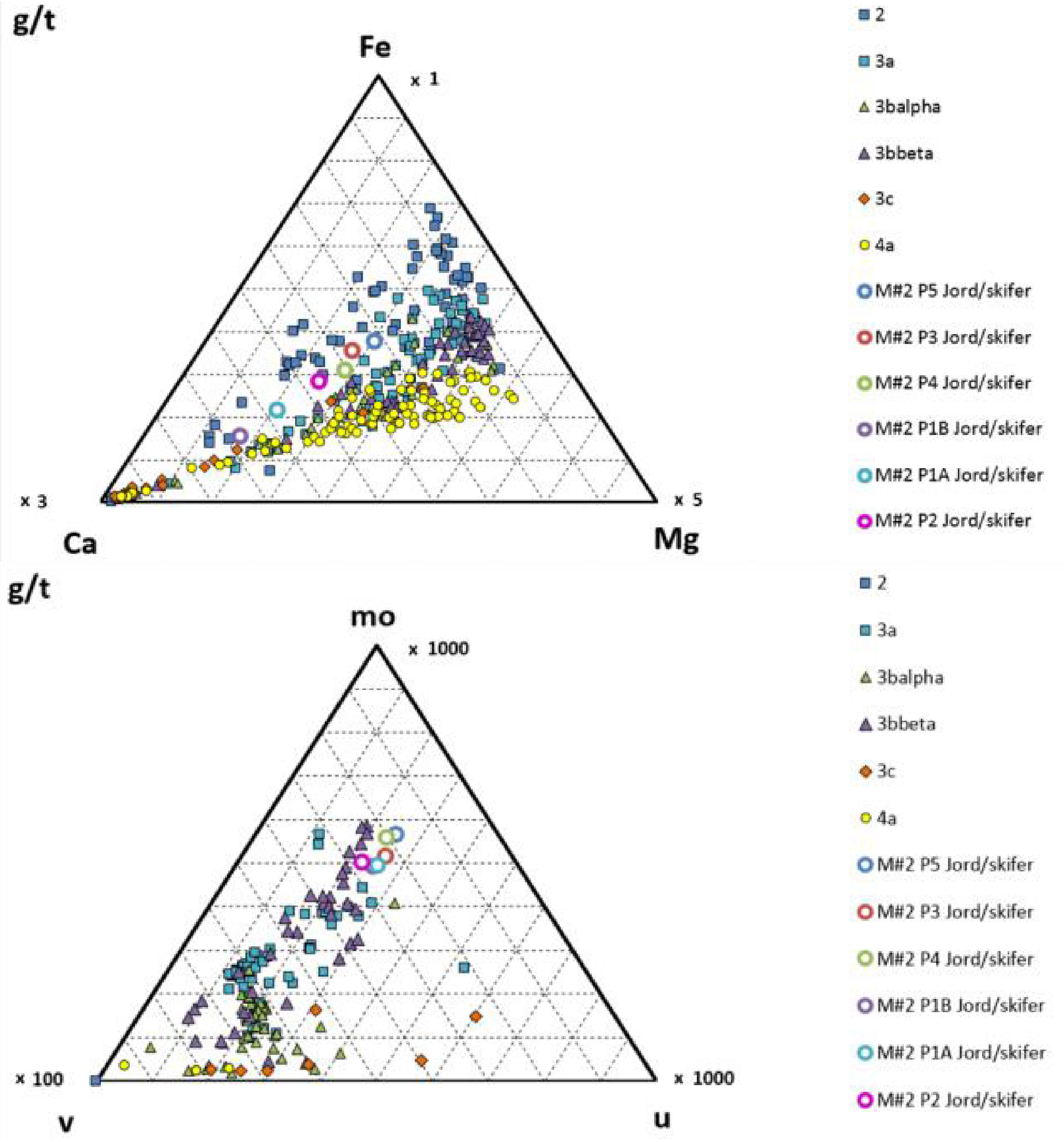

Figure 4 Chemical fingerprint together with evaluation of Fe:S and AP:NP places the black shale in the alum shale formation. The upper triangular diagram fits with the alum shale formation, while the lower figure fits with Galgeberg shale. (Copied from: Structor 2017. Vurdering av gjenbruk sprengstein i to tipper ved Kistefos. Report E16-GE-5516).

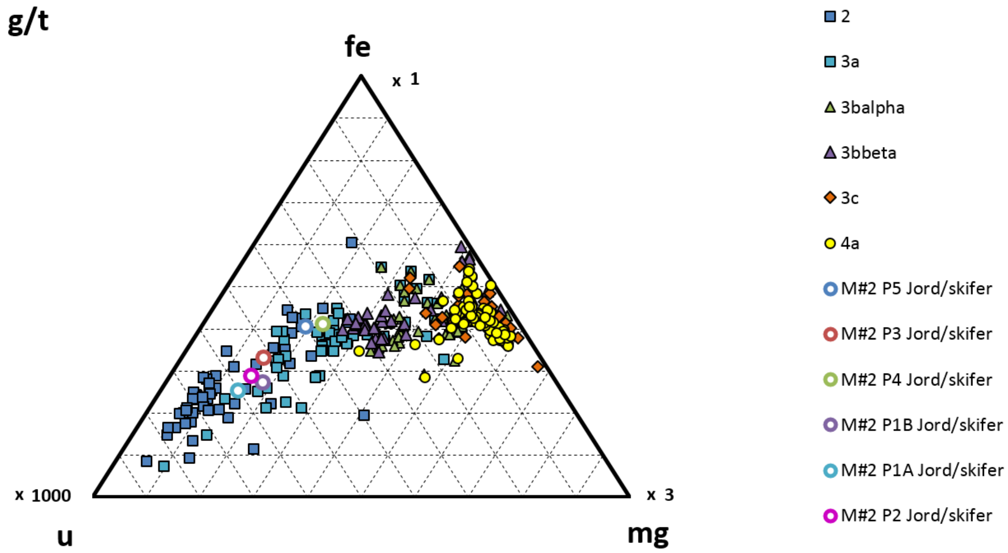

Figure 5 Chemical fingerprint together with evaluation of Fe:S and AP:NP places the black shale in the alum shale formation. The triangular diagram fits with the alum shale formation. (Copied from: Structor 2017. Vurdering av gjenbruk sprengstein i to tipper ved Kistefos. Report E16-GE-5516).

B4 Rv. 4 Gran

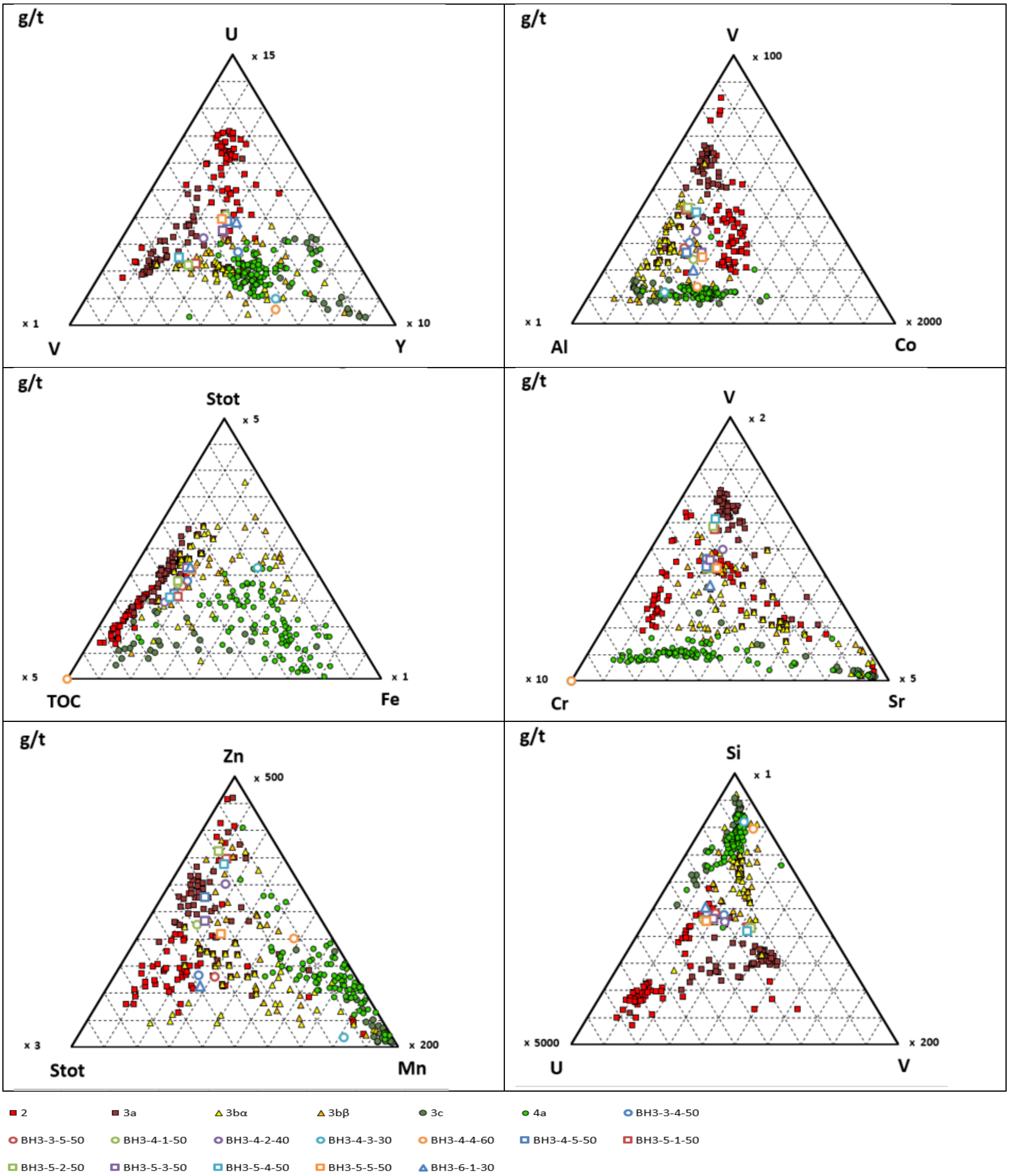

Figure 6 Rv. 4 Gran, relative content of elements in the samples, horizon 3bβ (Galgeberg fm), compared with reference samples from black shales in the Oslo area (2, 3a, 3b, 3c and 4a) (From NGI report 20120110-01-R).

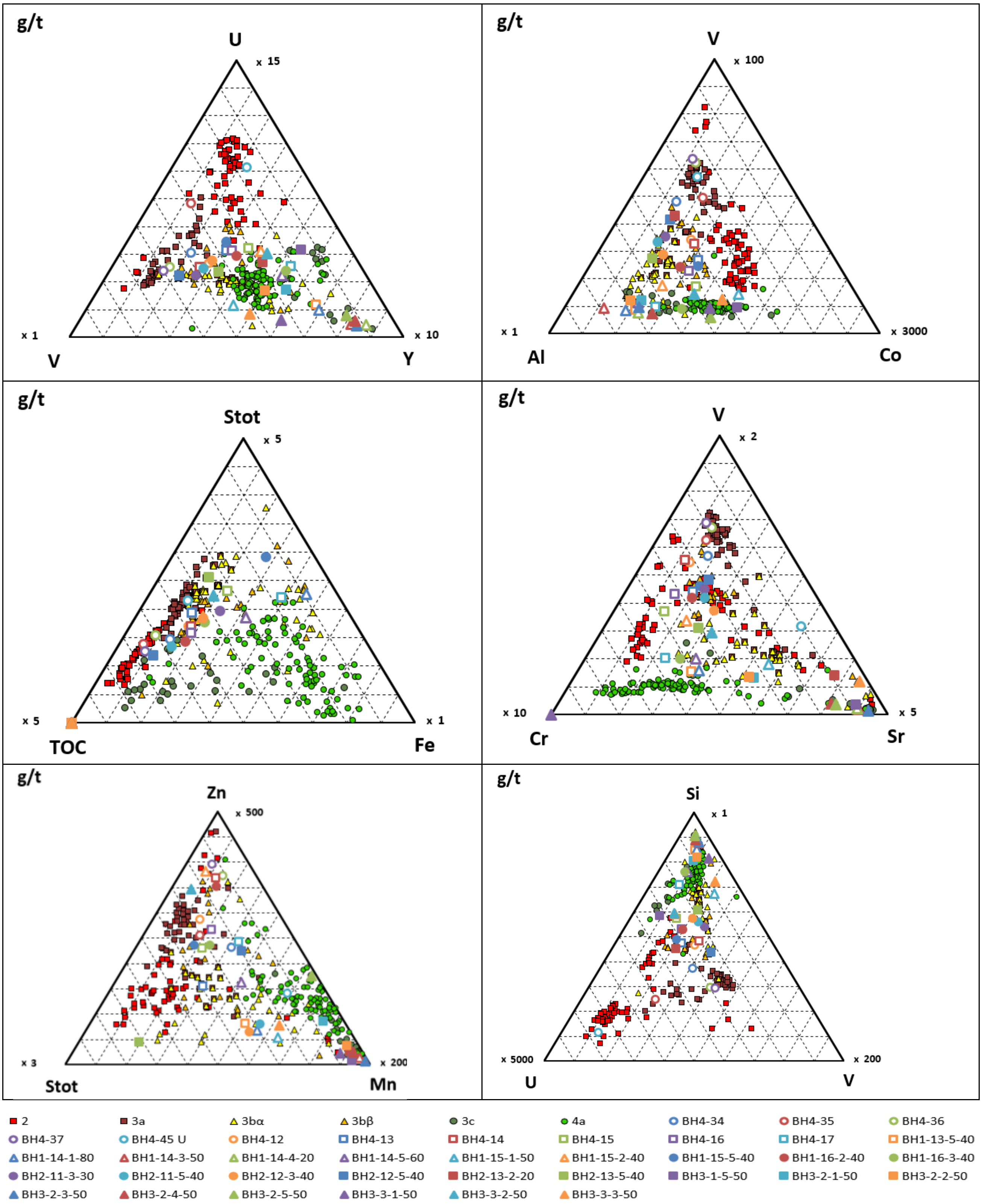

Figure 7 Gran Rv. 4, relative content of elements in the samples, horizon 2, 3a and 3bβ (Alun shale and Galgeberg fm), compared with reference samples from black shales in the Oslo area (2, 3a, 3b, 3c and 4a). (From NGI report 20120110-01-R).

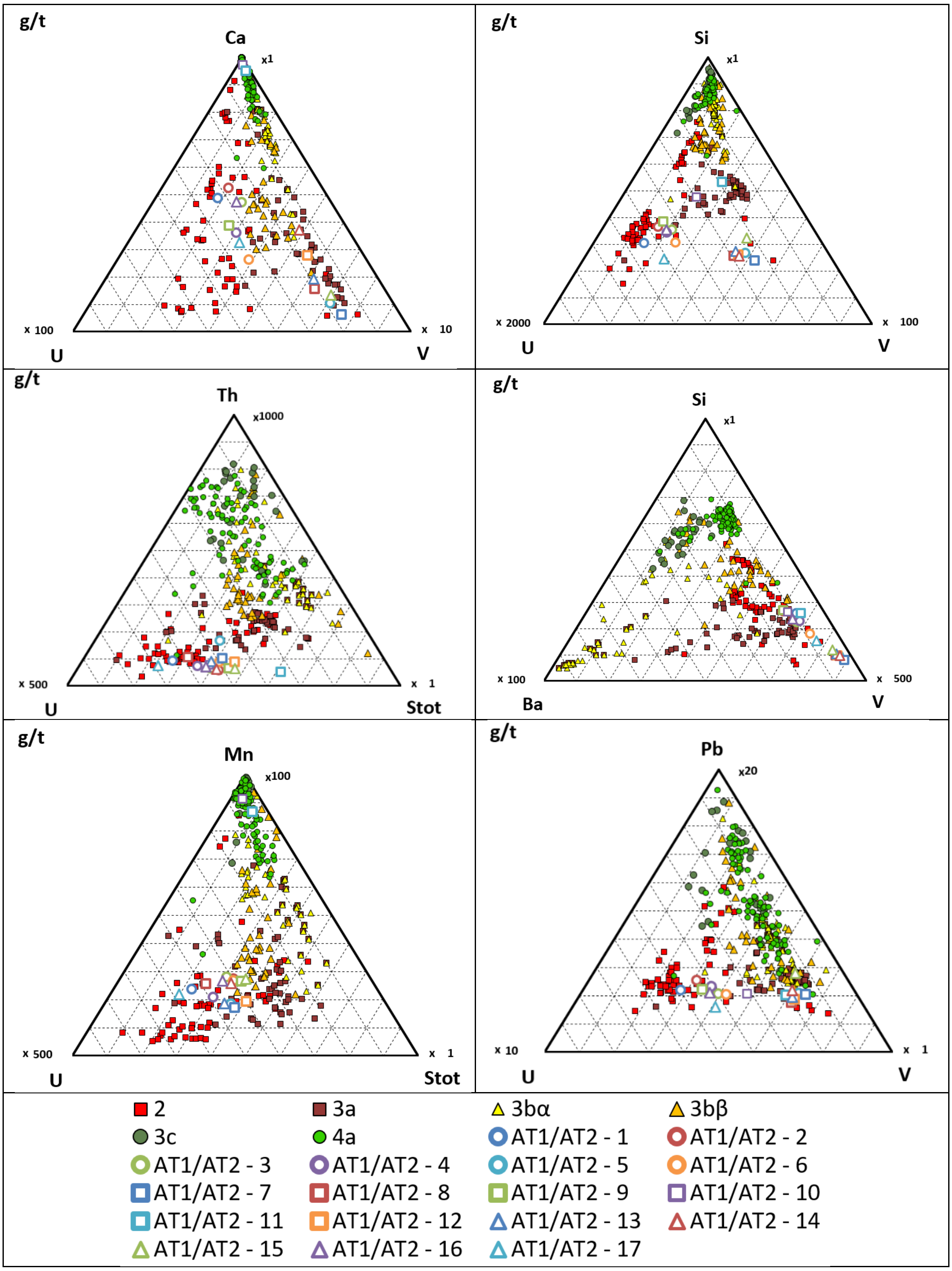

Figure 8 Relative content of elements in Gran samples related to the containers AT1 and AT2 (alum shale, 2 and 3a) in container experiments at Gran, later transferred to NGI, compared with reference samples from black shales in the Oslo area (2, 3a, 3b, 3c and 4a). The sampling is done with XRF by the Norwegian Road Authorities.

Table 1 Summary of the interpretation of the horizon of the samples analysed with XRF at Rv. 4 Gran (part 1).

Sample	**1**	**2**	**3**	**4**	**5**	**6**	**7**	**8**
U, Ca, V	2	2	2	2	3a	2	3a	3a
U, V, Si	2	2	2	2	2	2	2	2
U, Stot, Th	2	2	2	2	2/3a	2	2	2
Ba, V, Si	2/3a	2/3a	2/3a	2/3a	2	2	2	2
U, Stot, Mn	2	2/3a	2/3a	2	2/3a	2/3a	2/3a	2
U, V, Pb	2	2	2	2	3a	2	3a	2/3a
Horizon	**2**	**2**	**2**	**2**	**2/3a**	**2**	**2**	**2**

Table 2 Summary of the interpretation of the horizon of the samples analysed with XRF at Rv. 4 Gran (part 2).

Sample	**9**	**10**	**11**	**12**	**13**	**14**	**15**	**16**	**17**
U, Ca, V	2	4a	4a	3a	3a	3a	3a	2	2
U, V, Si	2	3a	3a	2	2	2	2	2	2
U, Stot, Th	2			2	2	2	2	2	2
Ba, V, Si	2/3a	2/3a	2/3a	2	2	2	2	2/3a	2
U, Stot, Mn	2/3a	4a	4a	2/3a	2/3a	2/3a	2/3a	2/3a	2
U, V, Pb	2	3a	3a	2/3a	2/3a	2/3a	3a	2	2
Horizon	**2**	**3a**	**3a**	**2/3a**	**2**	**2**	**2**	**2**	**2**

B5 E6 Uthus - Kåterud

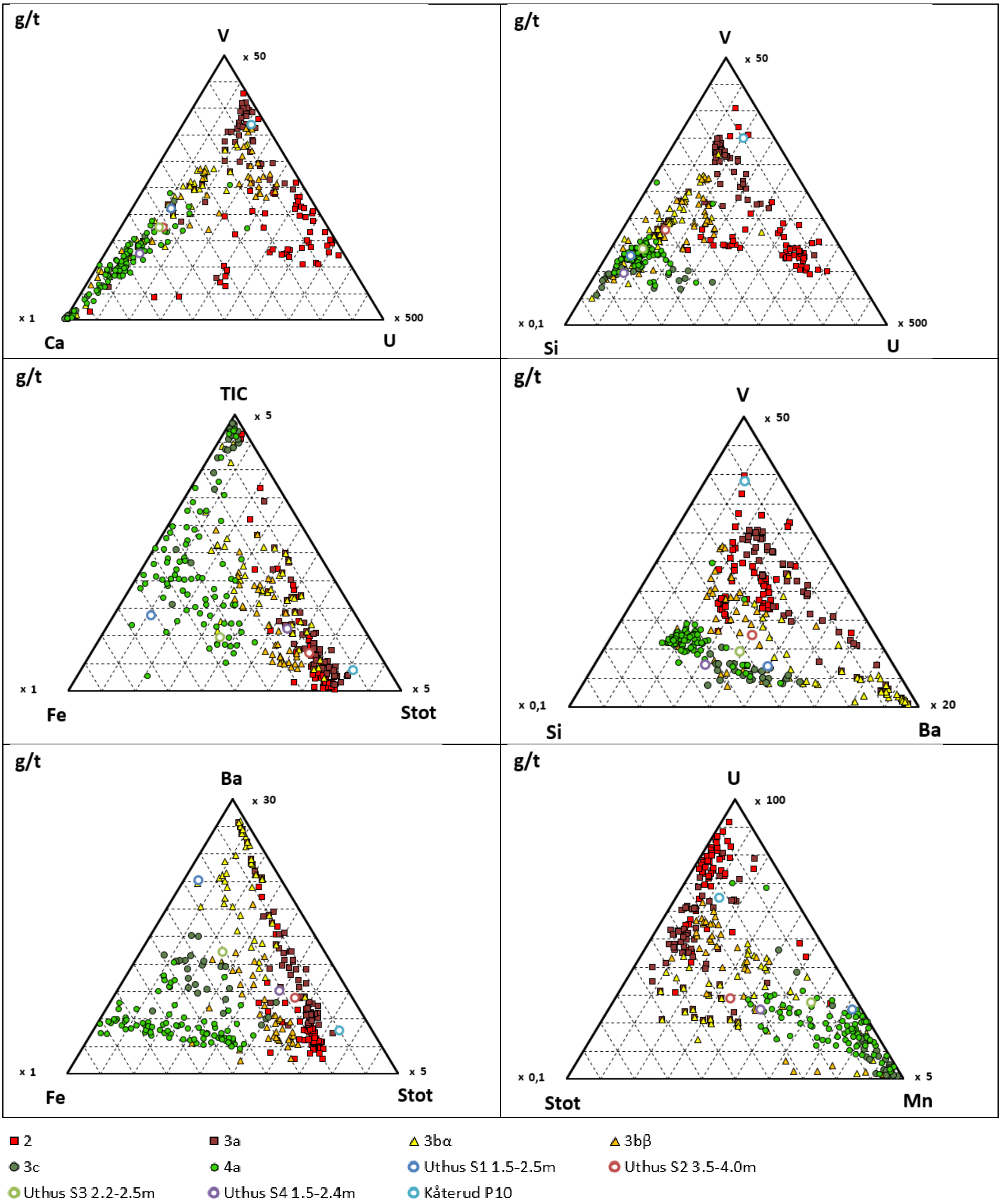

Figure 9 E6 Kåterud and Uthus, relative content of elements in the samples, compared with reference samples from black shales in the Oslo area (2, 3a, 3b, 3c and 4a).

B6 NOAH Langøya

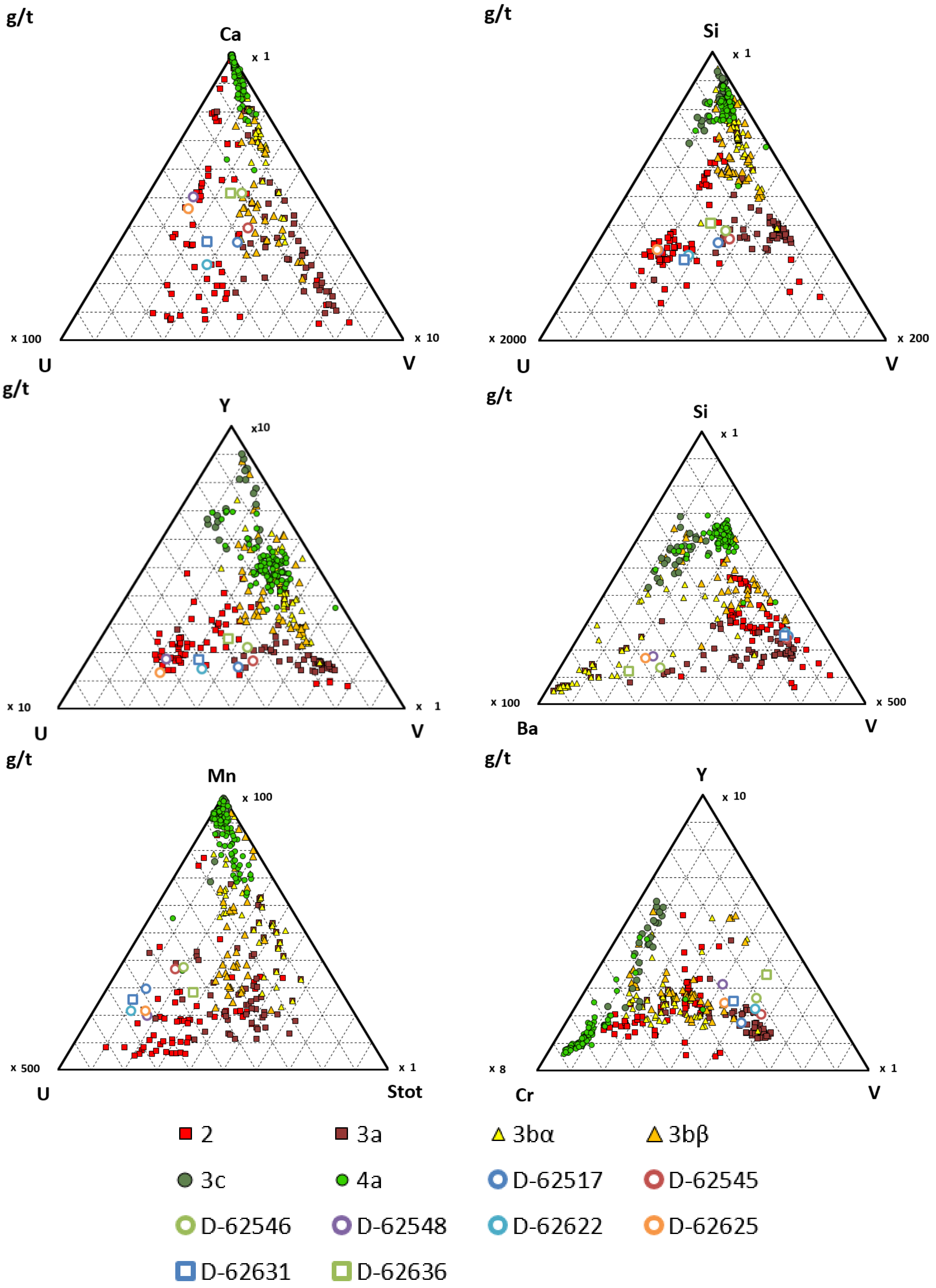

Figure 10 Relative content of elements in the samples of shales deposited at NOAH Langøya, alum shale (mostly horizon 2), compared with reference samples from black shales in the Oslo area (2, 3a, 3b, 3c and 4a).

Table 3 Summary of the interpretation of the horizon of the samples analysed with XRF at NOAH

Elements	D..517	D..545	D..546	D..548	D..622	D..625	D..631	D..636
U, Ca, V	2/3a	3a/3bβ	2/3bβ	2	2	2	2	2
U, V, Si	2/3a	3a	3a	2	2	2	2	2
U, V, Y	2/3a	3a	2/3a	2	2	2	2	2
Ba, V, Si	2	2/3a	3a	3a/3bα	2	3a/3bα	2/3a	3a/3bα
U, Stot, Mn	2	2/3a	2/3a	2	2	2	2	2/3a
Cr, V, Y	3a	3a	3a	3a/2	3a	3a	3a	?
Horizon	**2**	**3a**	**2/3a**	**2**	**2**	**2**	**2**	**2**

B7 Høvik

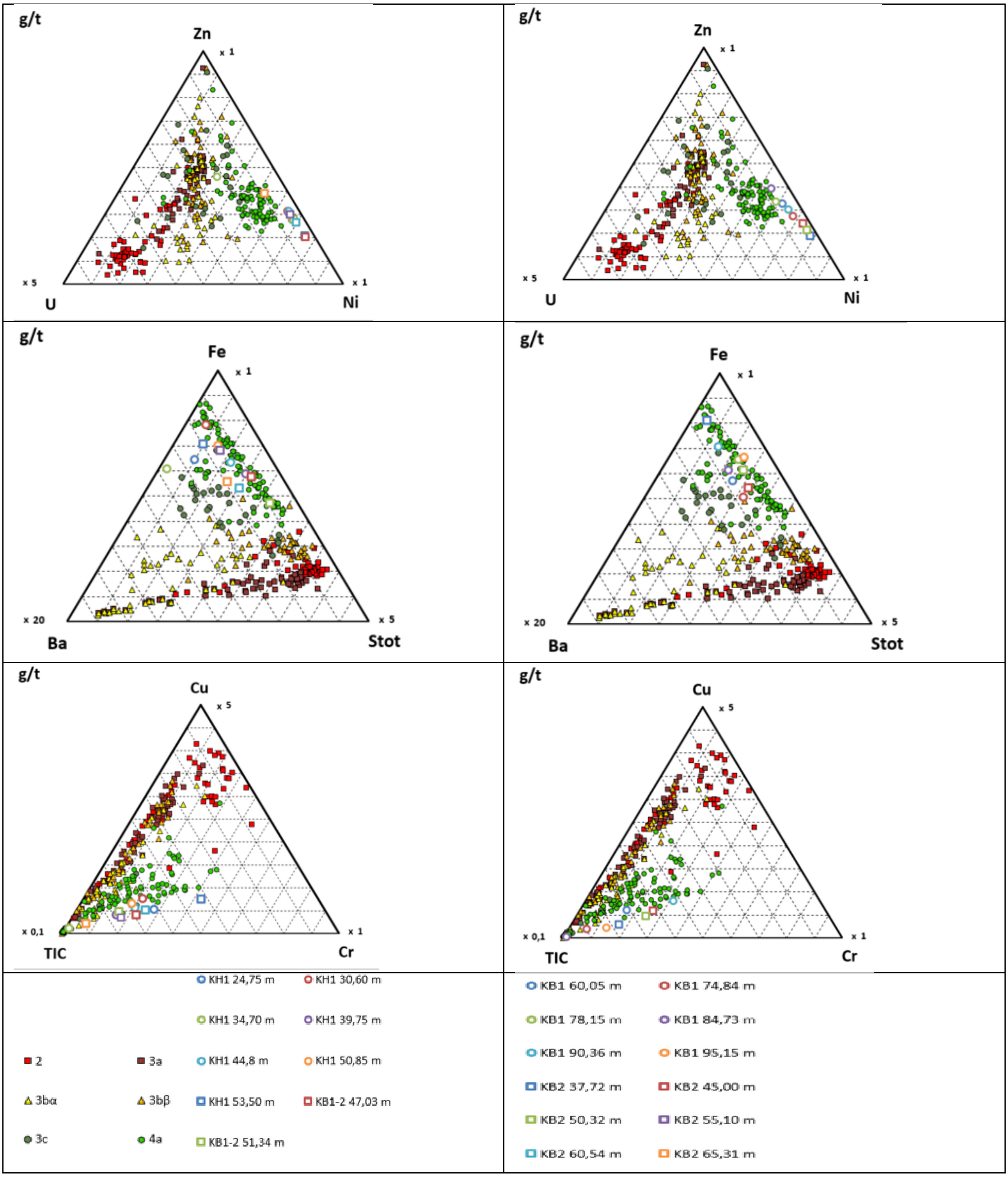

Figure 11 Høvik, relative content of elements in the samples, horizon 4 (Venstøp, Nakkholmen and Arnestad fm), compared with reference samples from black shales in the Oslo area (2, 3a, 3b, 3c and 4a).

B8 Taraldrud

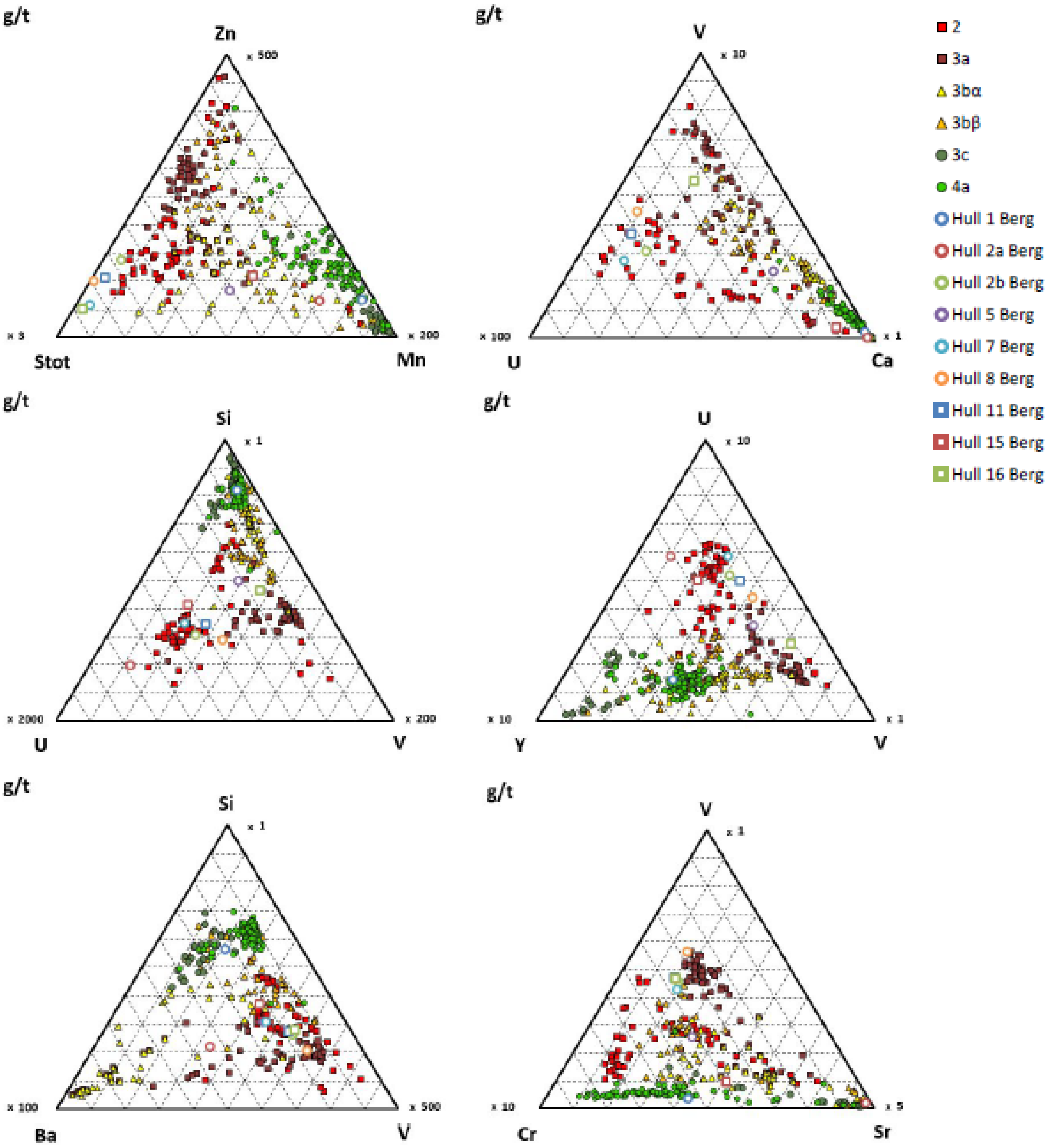

Figure 12 Taraldrud, relative content of elements in the samples. Shales are mainly classified as alum shale stage 2 and 3a, with elements of Hagaberg-/Galgeberg stage 3bα and 3bβ, Elnes shale stage 4a and calcareous clay shale, compared with reference samples from black shales in the Oslo area (2, 3a, 3b, 3c and 4a).

B9 Vilberg

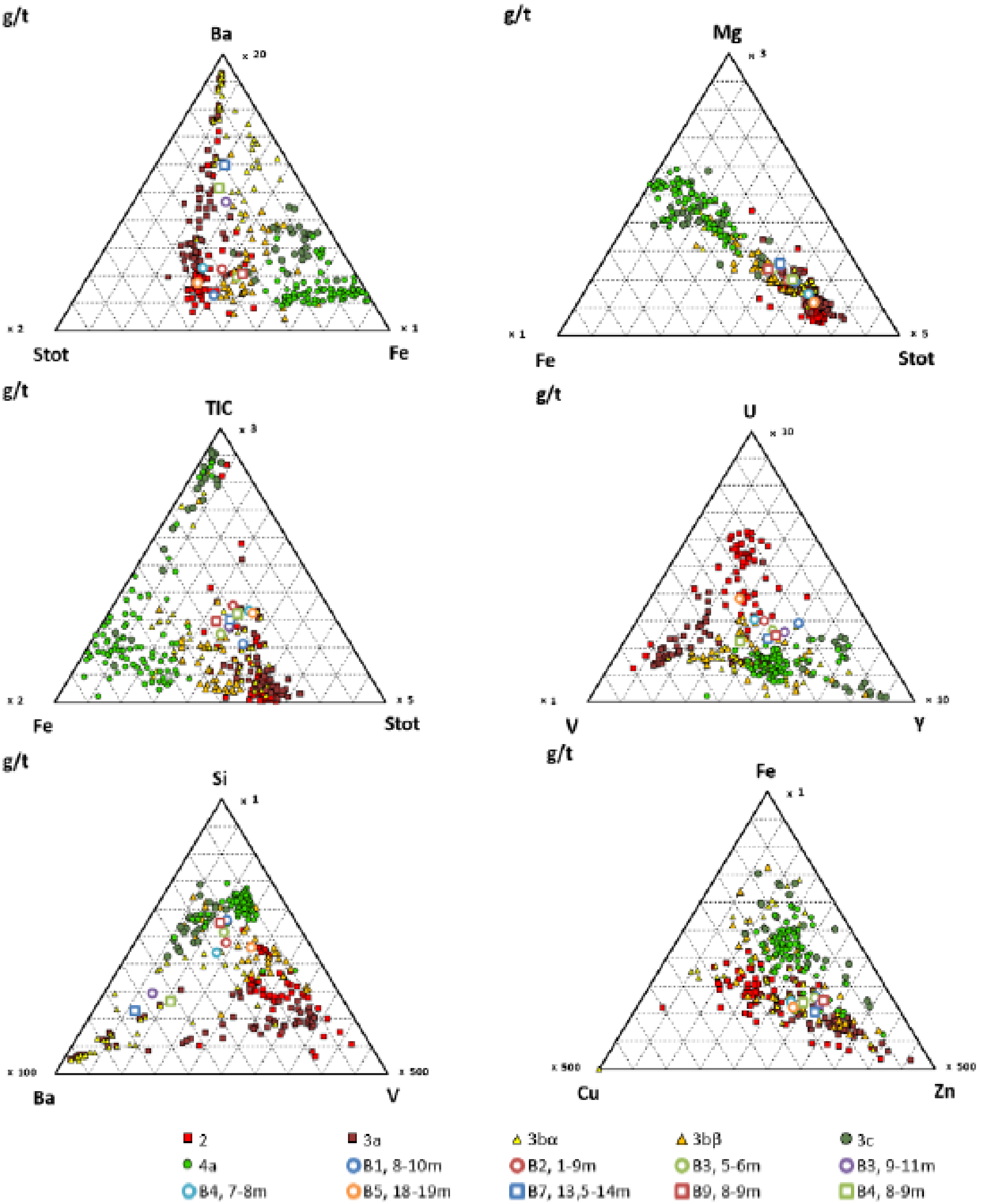

Figure 13 Vilberg, relative content of elements in the samples, mainly Alum shale horizon 2 and 3a and some Galgeberg shale 3bβ and Hagaberg shale 3bα, compared with reference samples from black shales in the Oslo area (2, 3a, 3b, 3c and 4a).

Appendix C

GEOCHEMICAL ANALYSES OF ROCK SAMPLES

E16 Kleggerud	**S (%)**	**TIC (%)**	**TOC (%)**	**AP (kg $CaCO_3$ eq/t)**	**NP (kg $CaCO_3$ eq/t)**	**NP:AP**	**U (mg/kg)**	**Horizon**
E16 Kleggerud (NGI)	1.89	0.27	5.9	59	22	0.4	69	2/3a
K2950_Kasse 1_Rad 1_70 cm	3.59	1.12	8.19	112	93	0.8	47	2
K3300_Kasse 1_Rad 2_110 cm	1.33	10.5	2.48	42	875	21	44	2
K3300_Kasse 1_Rad 5_100 cm	0.64	10.6	1.94	20	883	44	26	2
K3300_Kasse 2_Rad 1_80-90 cm	4.62	0.89	9.59	144	74	0.5	45	2
K3450_Kasse 1_Rad 1_10 cm	0.38	10.8	1.94	12	900	76	28	2
K3450_Kasse 1_Rad 1_60 cm	4.74	0.70	10.4	148	58	0.4	107	3a
K3450_Kasse 1_Rad 2_60 cm	3.77	0.58	10.2	118	49	0.4	116	3a
K3450_Kasse 2_Rad 3_30 cm	4.25	0.30	10.9	133	25	0.2	122	3a
K3450_Kasse 2_Rad 3_30 cm	1.04	0.33	5.82	33	28	0.9	37	3a
K3525_Kasse 1_Rad 2_10-20 cm	5.87	0.85	9.59	183	71	0.4	196	2/3a
K3525_Kasse 1_Rad 3_10-20 cm	6.06	1.14	11.5	189	95	0.5	194	2
K3525_Kasse 1_Rad 3_110-120 cm	6.38	1.17	12.5	199	97	0.5	197	2
K3525_Kasse 1_Rad 3_40-50 cm	0.48	11.0	2.25	15	917	61	17	2
K3600_Kasse 1_Rad 4_50-60 cm	3.38	1.28	9.51	106	107	1.0	107	3a
K4350_Kasse 1_Rad 2_100 cm	1.04	0.33	5.82	33	28	0.9	37	3a
K4350_Kasse 1_Rad 4_110 cm	1.36	0.10	3.47	43	8.5	0.2	22	3a/3bβ
P3389_Lok 1 BH 2S_12 m	2.42	0.85	11.5	76	71	0.9	130	3a
P3391_Lok 1_BH 1_2,8 m	2.12	2.20	6.56	66	183	2.8	77	2
P3391_Lok 1_BH 1_26,5 m	2.84	1.63	7.22	89	136	1.5	123	2
3360-b	1.60	<0.1	9.5	50	4.2*	0.1	150	2/3a
3380-b	<0.11	<0.1	0.7	1.7*	4.2*	2.4	68	3a
3380-c	<0.11	<0.1	0.7	1.7*	4.2*	2.4	60	3a
3380-d	<0.11	0.3	2.4	1.7*	25.0	14.5	85	3a

E16 Kleggerud	S (%)	TIC (%)	TOC (%)	AP (kg $CaCO_3$ eq/t)	NP (kg $CaCO_3$ eq/t)	NP:AP	U (mg/kg)	Horizon
3435-a	0.13	<0.1	0.9	4.1	4.2*	1.0	170	2
3435-b	0.15	<0.1	0.8	4.7	4.2*	0.9	200	2
3435-c	0.11	0.1	1.4	3.4	8.3	2.42	120	2
3520-a	0.14	<0.1	0.8	4.4	4.2*	1.0	49	3a
3520-b	<0.11	<0.1	0.6	1.7*	4.2*	2.42	57	3a
3520-c	<0.11	<0.1	0.8	1.7*	4.2*	2.42	46	3a
3520-d	1.10	<0.1	4.8	34.4	4.2*	0.1	74	3a
3520-e	1.10	<0.1	9.9	34.4	4.2*	0.1	100	3a
3540-b	0.15	<0.1	0.6	4.7	4.2*	0.9	47	3a
3540-c	0.30	0.1	5	9.4	8.3	0.9	52	3a
3560-b	0.95	3.00	7.5	29.7	250.0	8.4	73	2
3580-a	2.00	<0.1	9.3	62.5	4.2*	0.1	170	2
4310-0	<0.11	<0.1	< 0.2	1.7*	4.2*	2.4	13	4a
4310-2	<0.11	<0.1	0.3	1.7*	4.2*	2.4	14	4a
4500-8mH-a	0.16	<0.1	0.7	5.0	4.2*	0.8	76	3a
4500-8mH-b	1.10	2.7	7.8	34.4	225.0	6.5	79	2
4520	4.20	<0.1	8.7	131.3	4.2*	0.0	110	3a

Rv. 4 Gran (cont. AT1 and AT2)	S (%)	TIC(%)**	TOC (%)	AP (kg $CaCO_3$ eq/t)	NP (kg $CaCO_3$ eq/t)	NP:AP	U (mg/kg)	Horizon
A1A3 - 1	4.10	0.69		128	58	0.5	194	2
A1A3 - 2	5.80	0.64		181	53	0.3	141	2
A1A3 - 3	4.88	0.57		153	47	0.3	132	2
A1A3 - 4	4.38	0.37		137	31	0.2	142	2
A1A3 - 5	4.23	0.14		132	12	0.1	104	2, 3a

Rv. 4 Gran (cont. AT1 and AT2)	**S (%)**	**TIC (%)**	**TOC (%)**	**AP (kg $CaCO_3$ eq/t)**	**NP (kg $CaCO_3$ eq/t)**	**NP:AP**	**U (mg/kg)**	**Horizon**
A1A3 - 6	6.06	0.27		189	22	0.1	147	2
A1A3 - 7	4.23	0.09		132	7	0.1	99	2
A1A3 - 8	3.04	0.21		95	17	0.2	115	2
A1A3 - 9	6.50	0.38		203	31	0.2	139	2
A1A3 - 10	1.25	7.41		39	618	15.8	34	3a
A1A3 - 11	2.91	5.76		91	480	5.3	32	3a
A1A3 - 12	6.04	0.48		189	40	0.2	120	2, 3a
A1A3 - 13	4.54	0.30		142	25	0.2	123	2
A1A3 - 14	4.62	0.71		145	59	0.4	115	2
A1A3 - 15	4.73	0.18		148	15	0.1	94	2
A1A3 - 16	5.33	0.62		167	52	0.3	153	2
A1A3 - 17	3.99	0.53		125	44	0.4	233	2
Rv. 4 Gran 2012	**S (%)**	**TIC (%)**	**TOC (%)**	**AP (kg $CaCO_3$ eq/t)**	**NP (kg $CaCO_3$ eq/t)**	**NP:AP**	**U (mg/kg)**	**Horizon**
BH4-34	1.43	0.71	2.77	45	59	1.3	51	3a
BH4-35	1.82	0.40	4.3	57	34	0.6	110	3a
BH4-36	1.60	0.82	3.12	50	68	1.4	55	3a
BH4-37	1.37	0.33	3.59	43	27	0.6	54	3a
BH4-45 U	1.55	4.34	1.61	48	362	7.5	244	2
BH4-12	1.82	0.76	2.62	57	64	1.1	33	3bβ
BH4-13	1.98	1.1	2.34	62	92	1.5	32	3bβ
BH4-14	1.90	0.59	2.72	59	49	0.8	29	3bβ
BH4-15	2.12	1.64	1.44	66	137	2.1	26.5	3bβ
BH4-16	1.49	0.74	2.32	47	62	1.3	30	3bβ

Rv. 4 Gran 2012	S (%)	TIC (%)	TOC (%)	AP (kg $CaCO_3$ eq/t)	NP (kg $CaCO_3$ eq/t)	NP:AP	U (mg/kg)	Horizon
BH4-17	1.00	0.83	0.384	31	69	2.2	15	3bβ
BH1-13-5-40	0.60	1.16	<0.21	19	97	5.1	5.5	3bβ
BH1-14-1-80	0.59	0.60	0.121	19	50	2.7	4.6	3bβ
BH1-14-3-50	0.16	8.83	<1.27	5	736	147.2	0.8	3bβ
BH1-14-4-20	0.40	7.34	<1.06	13	612	48.8	1.2	3bβ
BH1-14-5-60	0.78	0.62	0.643	24	52	2.1	11	3bβ
BH1-15-1-50	2.79	2.81	<0.42	87	234	2.7	5.8	3bβ
BH1-15-2-40	1.40	0.28	1.62	44	23	0.5	26	3bβ
BH1-15-5-40	2.13	0.37	0.527	67	31	0.5	37	3bβ
BH1-16-2-40	1.57	0.44	2.9	49	37	0.7	29	3bβ
BH1-16-3-40	1.64	0.40	2.02	51	33	0.6	12	3bβ
BH2-11-3-30	1.06	0.95	0.995	33	79	2.4	21	3bβ
BH2-11-5-40	1.13	0.56	2.43	35	47	1.3	22	3bβ
BH2-12-3-40	1.45	1.24	1.71	45	103	2.3	23	3bβ
BH2-12-5-40	1.19	1.03	3.24	37	86	2.3	26	3bβ
BH2-13-2-20	0.51	5.73	<0.85	16	477	30.1	17	3bβ
BH2-13-5-40	2.45	0.16	1.65	77	13	0.2	18	3bβ
BH3-1-5-50	0.56	8.6	<1.27	17	717	41.2	9.0	3bβ
BH3-2-1-50	0.22	2.07	<0.35	7	172	25.6	7.0	3bβ
BH3-2-2-50	0.17	2.99	<0.42	5	249	46.4	5.2	3bβ
BH3-2-3-50	0.09	9.73	<1.41	3	811	295.8	0.6	3bβ
BH3-2-4-50	0.22	7.02	<1.06	7	585	85.9	1.6	3bβ
BH3-2-5-50	0.23	6.29	<0.92	7	524	74.2	1.9	3bβ
BH3-3-1-50	0.90	3.48	<0.49	28	290	10.3	2.3	3bβ

Rv. 4 Gran 2012	**S (%)**	**TIC (%)**	**TOC (%)**	**AP (kg $CaCO_3$ eq/t)**	**NP (kg $CaCO_3$ eq/t)**	**NP:AP**	**U (mg/kg)**	**Horizon**
BH3-3-2-50	2.80	0.35	2.28	88	29	0.3	26	3bβ
BH3-3-3-50	3.87	3.79	<0.57	121	316	2.6	3.4	3bβ
BH3-3-4-50	2.00	0.35	2.3	63	29	0.5	36	3bβ
BH3-3-5-50	1.92	0.43	2.46	60	36	0.6	37	3bβ
BH3-4-1-50	2.50	0.35	3.18	78	29	0.4	43	3bβ
BH3-4-2-40	1.80	0.56	3.32	56	46	0.8	39	3bβ
BH3-4-3-30	1.36	1.97	0.579	43	164	3.9	3.6	3bβ
BH3-4-4-60	2.07	2.47	<0.35	65	206	3.2	2.5	3bβ
BH3-4-5-50	1.90	0.34	2.89	59	28	0.5	43	3bβ
BH3-5-1-50	1.39	0.27	2.15	43	22	0.5	32	3bβ
BH3-5-2-50	2.11	0.34	2.57	66	28	0.4	31	3bβ
BH3-5-3-50	2.88	0.44	2.75	90	37	0.4	41	3bβ
BH3-5-4-50	1.89	0.41	3.11	59	34	0.6	35	3bβ
BH3-5-5-50	2.69	0.70	2.53	84	56	0.7	41	3bβ
BH3-6-1-30	2.82	0.57	2.58	88	47	0.5	35	3bβ
Uthus - Kåterud	**S (%)**	**TIC (%)**	**TOC (%)**	**AP (kg $CaCO_3$ eq/t)**	**NP (kg $CaCO_3$ eq/t)**	**NP:AP**	**U (mg/kg)**	**Horizon**
Kåterud P10 9.5-9.55 m (rock)	3.62	0.33	10.8	113	28	0.2	105	2
Uthus S1 1.5-2.5m (soil)	0.08	0.20	1.6	2	16	6.7	6.6	2, 3a
Uthus S2 3.5-4.0m (soil)	1.87	0.4	4.0	58	33	0.6	15	2, 3a
Uthus S3 2.2-2.5m (soil)	0.46	0.25	2.3	14	21	1.4	9.2	2, 3a
Uthus S4 1.5-2.4m (soil)	1.02	0.42	2.1	32	35	1.1	8.4	2, 3a

NOAH	**S (%)**	**TIC(%)****	**TOC (%)**	**AP (kg $CaCO_3$ eq/t)**	**NP (kg $CaCO_3$ eq/t)**	**NP:AP**	**U (mg/kg)**	**Horizon**
D-62517	1.20	0.32		38	26	0.7	120	2
D-62545	1.85	0.37		58	31	0.5	100	3a
D-62546	1.85	0.48		58	40	0.7	83	2, 3a
D-62548	2.58	0.64		81	53	0.7	190	2
D-62622	1.62	0.28		51	23	0.5	190	2
D-62625	2.60	0.59		81	49	0.6	210	2
D-62631	1.45	0.40		45	33	0.7	190	2
D-62636	2.61	0.44		82	37	0.5	88	2
Høvik	**S (%)**	**TIC (%)**	**TOC (%)**	**AP (kg $CaCO_3$ eq/t)**	**NP (kg $CaCO_3$ eq/t)**	**NP:AP**	**U (mg/kg)**	**Horizon**
KB1 60,05 m	0.16	1.07	0.14	4.9	89	18	2.8	4
KB1 74,84 m	0.09	0.92	0.14	2.9	76	26	2.7	4
KB1 78,15 m	0.03	1.03	0.40	0.8	86	108	7.1	4
KB1 84,73 m	0.55	1.6	<0.21	17.0	133	7.8	2.5	4
KB1 90,36 m	0.38	1.12	0.24	12.0	93	7.8	2.5	4
KB1 95,15 m	0.23	1.07	0.22	7.2	89	12	2.7	4
KB2 37,72 m	0.15	0.54	<0.11	4.8	45	9.5	2.5	4
KB2 45,00 m	0.69	1.62	<0.28	21.6	135	6.3	2.6	4
KB2 50,32 m	1.10	1.46	<0.21	34.4	122	3.5	2.6	4
KB2 55,10 m	0.26	2.23	<0.35	8.1	186	23	2.6	4
KB2 60,54 m	0.59	1.13	0.12	18.5	94	5.1	2.3	4
KB2 65,31 m	0.35	2.09	<0.28	11.1	174	16	3.6	4
KH1 24,75 m	0.47	1.08	<0.14	14.8	90	6.1	3.3	4
KH1 30,60 m	0.61	4.02	<0.57	19.0	335	18	2.7	4

Høvik	**S (%)**	**TIC (%)**	**TOC (%)**	**AP (kg $CaCO_3$ eq/t)**	**NP (kg $CaCO_3$ eq/t)**	**NP:AP**	**U (mg/kg)**	**Horizon**
KH1 34,70 m	0.13	8.25	<1.13	4.2	687	165	1.5	4
KH1 39,75 m	0.14	8.18	<1.13	4.4	682	154	1.5	4
KH1 44,8 m	0.21	0.57	0.11	6.6	47	7.2	3.3	4
KH1 50,85 m	0.30	2.71	<0.42	9.3	226	24	1.7	4
KH1 53,50 m	0.06	2.43	<0.35	1.8	202	114	2.0	4
KB1-2 47,03 m	0.70	1.19	0.20	22	99	4.5	2.3	4
KB1-2 51,34 m	0.56	1.42	0.21	17	118	6.8	2.4	4
Taraldrud	**S (%)**	**TIC (%)**	**TOC (%)**	**AP (kg $CaCO_3$ eq/t)**	**NP (kg $CaCO_3$ eq/t)**	**NP:AP**	**U (mg/kg)**	**Horizon**
Hull 1	0.35	1.91	0.3	11	159	15	6.4	4a
Hull 2b	5.38	0.46	7.31	168	39	0.2	145	2 and 3a
Hull 5	1.91	0.72	5.98	60	60	1.0	52	3bα and 3bβ
Hull 7	5.33	0.04	6.88	167	3.3	0.02	145	2 and 3a
Hull 8	5.05	0.02	7.28	158	2.0	0.01	113	2 and 3a
Hull 11	4.79	0.03	7.61	150	2.2	0.01	130	2 and 3a
Hull 15	1.98	4.54	2.0	62	378	6.1	92	3bα and 3bβ
Hull 16	1.68	0.05	9.0	53	3.7	0.1	44	2 and 3a
Vilberg	**S (%)**	**TIC (%)**	**TOC (%)**	**AP (kg $CaCO_3$ eq/t)**	**NP (kg $CaCO_3$ eq/t)**	**NP:AP**	**U (mg/kg)**	**Horizon**
B1, 8-10m	3.02	1.19	2.3	94	99	1.1	26	3a, 3b
B2, 1-9m	2.41	0.47	3.9	75	39	0.5	29	3a, 3b
B3, 5-6m	2.22	0.90	2.5	69	75	1.1	22	3a, 3b
B3, 9-11m	2.34	1.34	2.8	73	112	1.5	21	3a, 3b
B4, 7-8m	3.16	0.53	4.2	99	44	0.4	26	3a, 3b

Vilberg	S (%)	TIC (%)	TOC (%)	AP (kg $CaCO_3$ eq/t)	NP (kg $CaCO_3$ eq/t)	NP:AP	U (mg/kg)	Horizon
B5, 18-19m	2.98	0.56	3.7	93	47	0.5	47	2
B7, 13,5-14m	2.17	1.65	2.9	68	137	2.0	18	3a, 3b
B9, 8-9m	1.89	0.55	2.8	59	46	0.8	18	3a, 3b
B4, 8-9m	2.49	0.72	3.4	78	60	0.8	22	3a, 3b

* Value is calculated based on half of the LOQ for S and/or TIC
** TIC value calculated based on Ca content

🟩 **NP:AP >3** 🟨 **NP:AP >1 and <3** 🟥 **NP:AP <1** ⬜ **Values over 1 % S or 85 mg U/kg**

Appendix D

PRINCIPAL COMPONENT ANALYSIS OF ROCK SAMPLES

Contents

D1 Further statistical analyses: Principal component analysis (PCA)

Principal component analyses (PCA) were performed with the chemical composition of the shale. The goal of a PCA is to summarize and to visualize the information in a data set containing observations described by multiple inter-correlated quantitative variables, while also finding a small number of linear combinations of the variables which capture most of the variation in the data as a whole. In the PCA plot, information from the variables are extracted and represented as a set of new uncorrelated orthogonal variables called principal components (PC). The variables are unit variance scaled, so that their contribution to the final model is equal, independent of their absolute values. In addition, the variables are mean-centered to increase interpretability. Significant PCs have eigenvalues > 1 and for this report the four PCs with the highest eigenvalues, thus explaining the most variation, was extracted to make PCA plots. When interpreting PCA plots, the general idea is that parameters that clusters together in the loading plot (right in figures below) are positively correlated with each other, while they are negatively correlated with parameters that are on the opposite side of the plot. Parameters that are 90° apart are not correlated. Furthermore, parameters that position themselves close to the origin are not explained very well by the presented PCs information in the dataset, while parameters far from origo are better explained by the presented PCs, and thus the majority of the dataset. The score plot and the loading plot can be overlain to see which samples correlate to the different parameters, thus representing higher or lower concentrations of the analysed chemical components.

When choosing input parameters for a PCA, one should avoid including parameters that are directly depending on each other, such as Fe and Fe:S or AP, NP and AP:NP. Thus, PCA's were performed with a variation in input parameters, and results from two different PCA's are presented below. Because analysis of TOC, TIC, Sr and Th were not performed for the shale samples from NOAH, PCA's were performed with and without these samples.

Samples from Uthus-Kåterud were excluded from the analysis (most of these samples are soil and are thus different from the rest of the samples), as well as samples from Gran containers AT1-AT2 as they did not have analysis of TOC and TIC.

D1.1 PCA with Fe, AP and NP, excluding NOAH samples

In Figure 1, score plots and loading plots are presented from a PCA performed excluding the NOAH samples. The score plots show how the individual samples from the different sampling locations and horizons distribute, while the loading plots show the distribution of the variables in relation to each other. The parameters included in the PCA analyses displayed in Figure 1 are AP, NP, TOC, As, Al, Ba, Cd, Co, Cr, Cu, Fe, Mn, Mo, Ni, Si, Sr, Th, U, V, Y, and Zn, as shown in the loading plot. The score plots to the left show the samples coloured according to sampling location, and the score plots in the middle show the horizon they belong to. Not all samples were successfully categorized to one horizon, and the legend reflects this uncertainty. As shown in the scree plot in the next chapters, Si, Sr, Mn, NP, Cu, Al, Cd, U, Th and Mo contribute to the majority of the variation explained by PC1 and PC2. Si and Al are typically high in most rocks, while Cu, Cd, Mo and U are heavy metals typically enriched in black shales (Falk et al., 2006; Owen et al., 1990; Pabst et al., 2017). U concentrations are expected to be higher in alum shales than in Galgeberg shales, and even lower in other horizons (see triangular plots of reference data in appendix B). The neutralizing potential (NP) is expected to vary between the different horizons in the Cambro-Ordovician successions, and be higher in e.g. horizon 4a that is rich in chalk. See also chapter 2 for more general information on the different horizons.

The values on the axis of the plots show the percent variation in the data that is explained by the two extracted PCs. Thus, in Figure 1 a total of 52.8 % (34.6 % + 18.2 %) of the variation in the chemical parameters of the shale samples is explained by PC1 and PC2, and 19.3 % (12.3 % + 7 %) by PC3 and PC4.

The loading plot for PC1 and PC2 (right in the figure) shows three clusters of parameters that are associated with each other. Down on the left we find a cluster of TOC, AP and a range of "heavy metals". Iron (Fe) also seems to be associated with this group. These parameters are expected to co-vary, as they depend on to the conditions that prevailed during sedimentation of the masses becoming the rock. When the acid-producing black shales were formed, high levels of organic matter lead to reducing conditions, causing reduction of sulphur to sulphide and scavenging of metals from the water column (Alloway, 2013; Swanson 1961). AP and Fe are close to origo, thus little of their variation is explained by PC1 and PC2 in Figure 1. For the plot for PC3-PC4 Fe is the most important parameter, while AP still is not well explained.

Down on the right side in the loading plot for PC1 and PC2, we find a group of NP, Sr and Mn. The NP in the shale samples is estimated from carbonates in the rock, which often occurs as calcite, and Sr and Mn can be substitutes/impurities in calcite (Appelo and Postma, 2010; https://www.mindat.org/min-859.html). Up on the left side in the loading plot we find Si, Al and Th, which seem to be strongly negatively correlated to the NP-group. One possible explanation is that rock masses with a lot of silicates and clays (containing Si and Al) has less carbonates. This is supported by spearman rank correlations confirming negative correlations between Ca and Si ($\rho = -0.60$, p = = 5.2e-12) and between Ca and Al ($\rho = -0.64$, p = 5.2e-14). There is also a strong correlation between Si and Al (spearman rank correlation gives $\rho = 0{,}77$, p = 2.2e-16). These two smaller groups in Figure 1 are ~ 90 ° away from AP and TOC, meaning that they are not correlated. Ba seems to not correlate with any other of the chosen parameters, and little of the variation in Ba is explained by the either of the presented plots.

Samples in horizon 2 and 3a lie on the left side of the plot for PC1 and PC2, more correlated to AP and heavy metals, while samples in horizon 4 are on the right side of the plot and correlated to NP. This fits the expected properties of the horizons well with higher ARD potential in horizons 2 and 3a (see also ch. 2.1 in the main report and e.g. Owen, 1990 and Pabst, 2017). The samples from horizon 3bβ are spread on both sides of the plot, thus there is a wider range in the concentrations of the chemical components in shale from this horizon.

There is a tendency that samples from the same geographical position are clustered together, but these are in many cases also from the same geological horizon. The samples from Taraldrud spreads out quite evenly, and are represented within horizons 2 & 3a, 3bα & 3bβ, as well as 4a. The samples from Kleggerud are spread out on the left side and seem to be the ones with the highest metal concentrations. They are classified as horizons 2 and 3a, which are expected to have high AP, TOC and metal concentrations, except two samples that are classified as horizon 4a and position themselves further away from the AP and metal cluster.

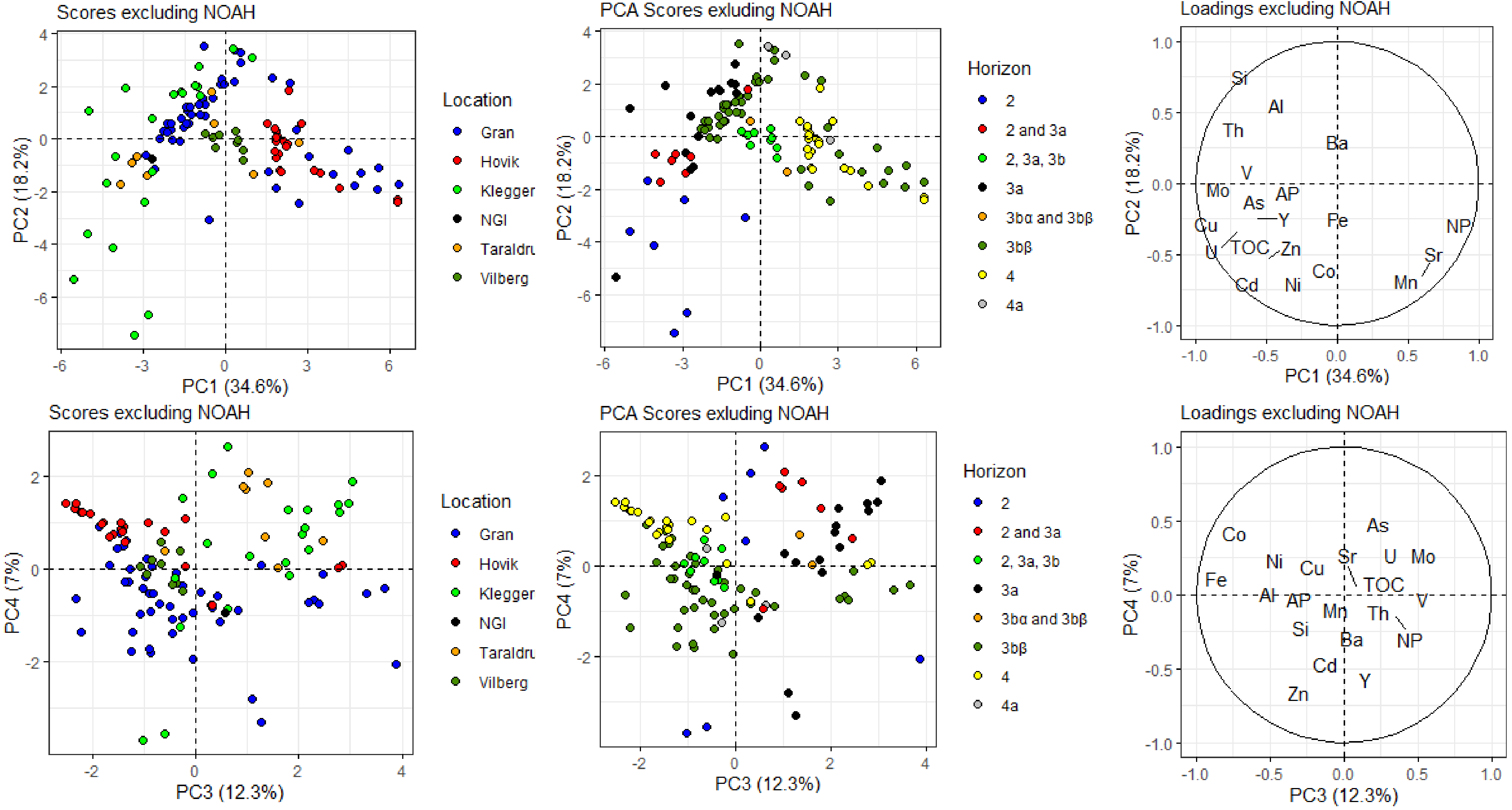

Figure 1 PCA plot excluding samples from NOAH. The upper three plots show PC1 and PC2, while the lower three plots show PC3 and PC4. Score plot to the left show samples grouped according to sampling location, and middle score plots according to horizon. The loadings plots are shown to the left. AP is the acidifying potential and NP is the neutralizing potential.

D1.2 PCA with NP:AP, Fe:S, including NOAH samples

The PCA presented in Figure 2 includes the NOAH samples but fewer parameters compared to the PCA in Figure 1. Fe was exchanged by Fe:S and NP:AP was included instead of NP and AP to investigate how that would affect the PCA. TOC, As, Ba, Cd, Co, Mn, Sr and Th were taken out, partly because of lacking measurements and partly to investigate the correlations in the dataset when fewer of the expectedly less important parameters are included. TIC, TOC, Sr and Th were not analysed for the NOAH samples, and Ca was used to estimate NP for the NOAH samples as these samples lack measurement of TIC.

The overall trends are similar in this PCA as in Figure 1 where NOAH samples are excluded, showing that Si, Al, U, NP:AP, Cu and Mo contribute to the majority of the variation explained by PC1 and PC2 (see scree plot in the next chapters). In the loadings plot in Figure 2, NP:AP opposes Si and Al, in the same way as displayed with NP and Si / Al in Figure 1, for PC1 and PC2. The reason that NP:AP positions itself more as NP than AP in the PCA is likely that the variation in NP (2-917 kg $CaCO_3$ eq/t, see figure 4 in the main report or Appendix C) is greater than in AP (0.8-203 kg $CaCO_3$ eq/t) and thus variation in NP determines more of the variation in NP:AP than AP. In Figure 2 we also see that most of the metals cluster together as shown in Figure 1. As opposed to Fe, Fe:S seems completely unrelated to any of the other parameters in this PCA, and this was also seen in other PCA's including Fe:S.

When looking at the loading plot for PC3 and PC4, Fe:S becomes important, like Fe is in Figure 1, but not strongly correlated to anything.

Looking at the distribution of the samples in the score plot, the spread in the samples is smaller. Overall, a somewhat larger part of the variation in the sample parameters is explained in this PCA: 57.2 % for PC1+PC2 and 20.6 % for PC3+PC4, compared to respectively 52.8 % and 19.23 % in Figure 1.

The samples from NOAH are all from horizon 2 and position themselves closely together in the area were other samples from horizon 2 (and 3a) are gathered. The metal concentrations in these samples seems to be lower than the Kleggerud samples with the highest concentrations.

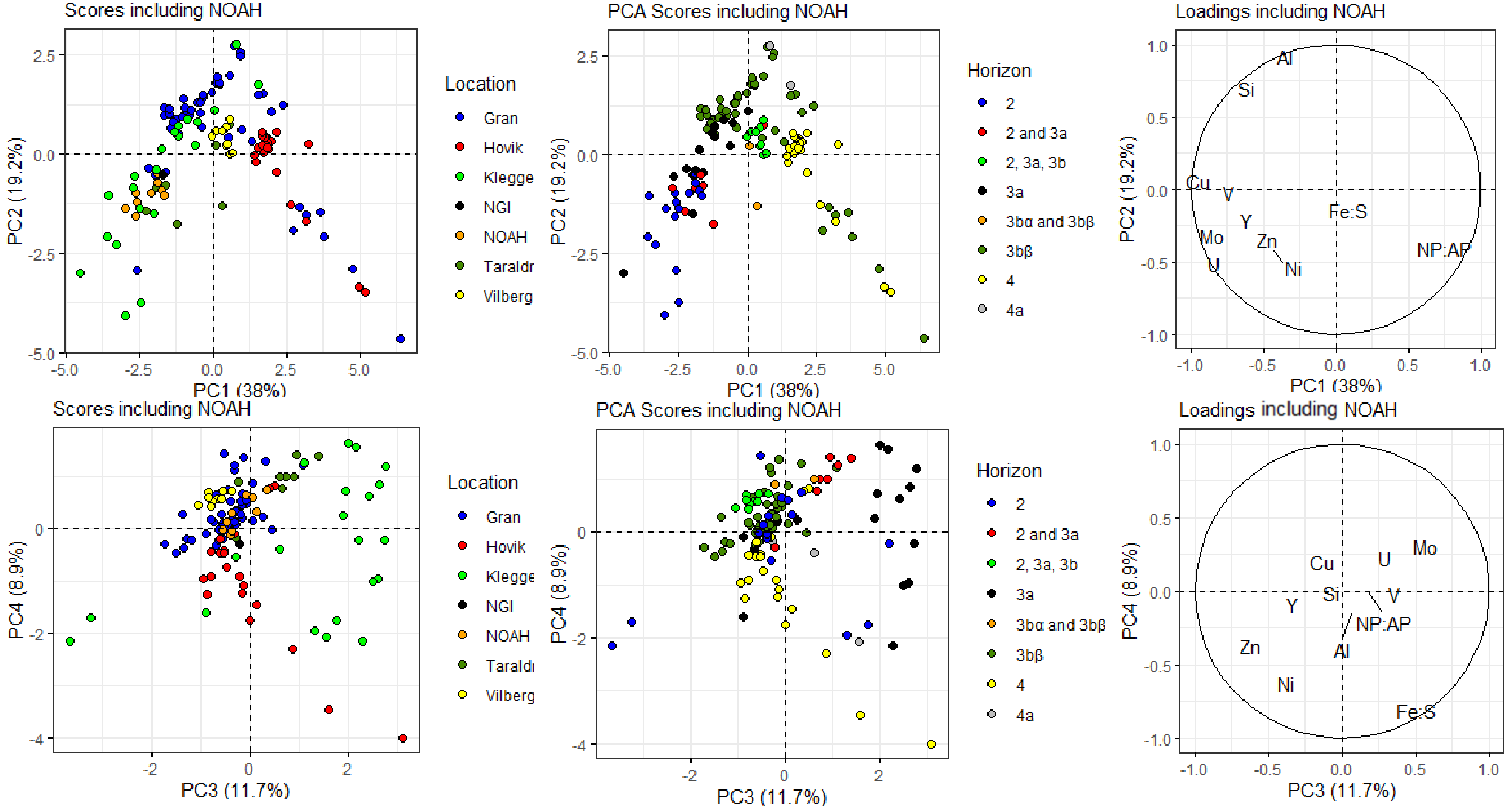

Figure 2 PCA plot including all the shale samples. The upper three plots show PC1 and PC2, while the lower three plots show PC3 and PC4. Score plot to the left show samples grouped according to sampling location, and middle score plots according to horizon. The loadings plots are shown to the left. AP is the acidifying potential and NP is the neutralizing potential.

D2 Supporting information to Mod 3: PCA with Fe, AP and NP, excluding NOAH samples

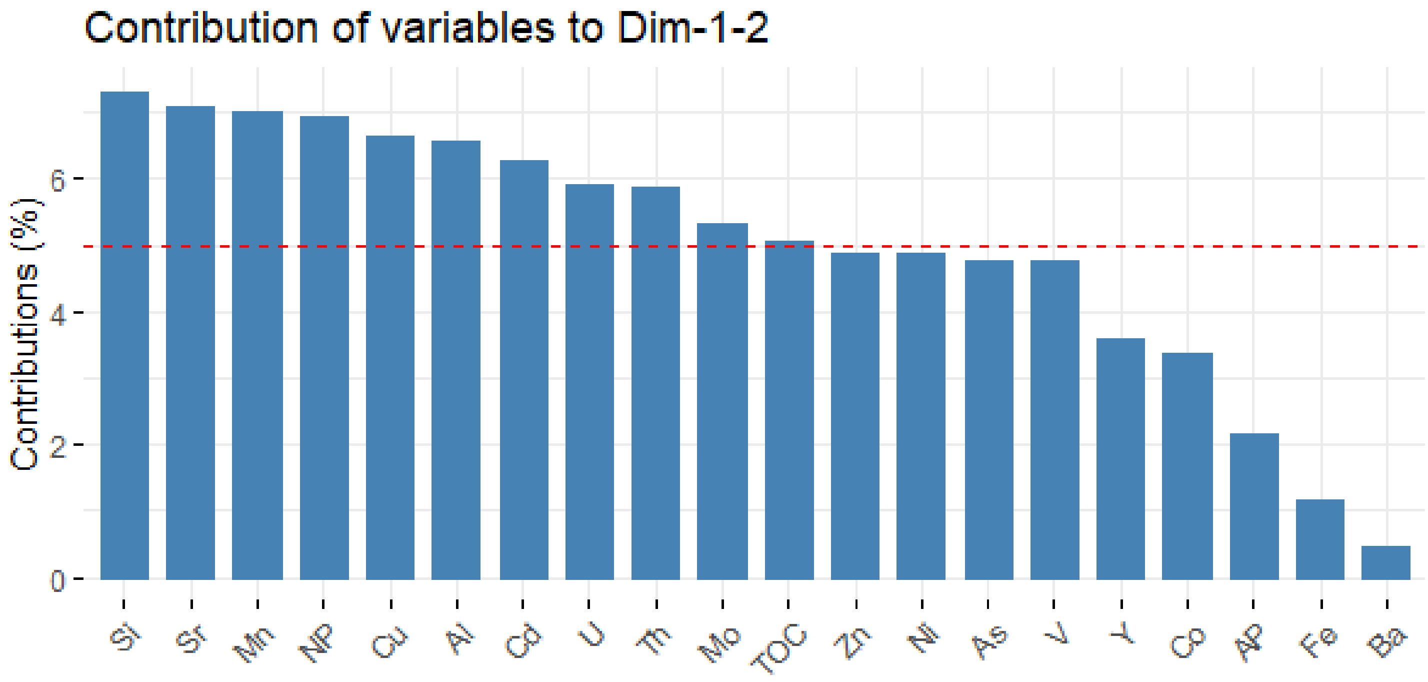

Figure 3 Scree plot for PC1 and PC2 Mod 3: PCA with Fe, AP and NP, excluding NOAH samples.

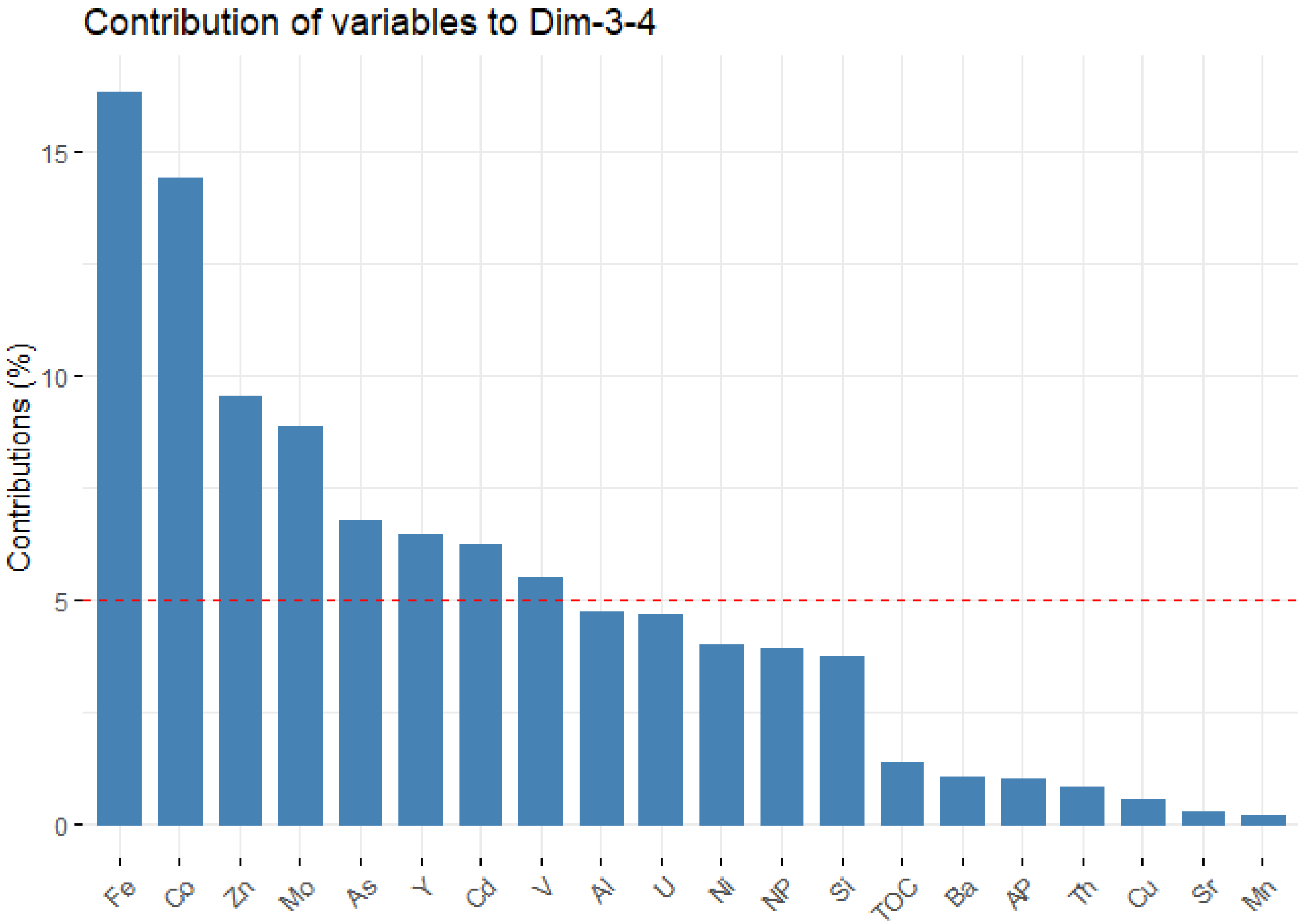

Figure 4 Scree plot for PC3 and PC4 Mod 3: PCA with Fe, AP and NP, excluding NOAH samples.

Table 1: Importance of components

	PC1	PC2	PC3	PC4	PC5	PC6	PC7	PC8	PC9	PC10	PC11	PC12	PC13	PC14	PC15	PC16	PC17	PC18	PC19	PC20
Eigenvalue	6.925	3.63	2.45	1.393	1.273	1.002	0.887	0.579	0.422	0.293	0.233	0.226	0.156	0.136	0.102	0.082	0.063	0.057	0.05	0.039
Standard deviation	2.632	1.905	1.565	1.18	1.13	1	0.94	0.76	0.649	0.542	0.483	0.475	0.395	0.369	0.32	0.287	0.252	0.24	0.224	0.197
Proportion of Variance	0.346	0.182	0.123	0.069	0.064	0.05	0.044	0.029	0.021	0.015	0.012	0.011	0.008	0.007	0.005	0.004	0.003	0.003	0.003	0.002
Cumulative Proportion	0.346	0.528	0.65	0.72	0.784	0.834	0.878	0.907	0.928	0.943	0.954	0.966	0.973	0.98	0.985	0.99	0.993	0.996	0.998	1

Table 2 Loadings from PCA mod 3 with Fe, AP and NP, excluding NOAH samples.

	PC1	PC2	PC3	PC4	PC5	PC6	PC7	PC8	PC9	PC10	PC11	PC12	PC13	PC14	PC15	PC16	PC17	PC18	PC19	PC20
TOC	-0.2527	-0.1597	0.1443	-0.0167	0.358	-0.35	0.0829	-0.1375	0.1994	-0.1117	0.5167	-0.1442	0.145	-0.2202	0.2354	-0.1674	0.0622	-0.0532	0.2456	0.2303
NP	0.2902	-0.2031	0.226	-0.1302	0.0775	0.1133	0.1234	-0.0575	0.184	-0.1377	-0.2299	-0.016	-0.3121	-0.1582	-0.2331	0.1601	0.2126	0.4137	0.3998	0.2909
AP	-0.1699	-0.0871	-0.1206	0.0422	0.6797	-0.0645	0.2653	0.0636	-0.1766	0.2533	-0.174	0.0257	-0.2887	0.4031	-0.1499	-0.0856	-0.0337	-0.0188	-0.0526	0.0211
Al	-0.2	0.3387	-0.271	-0.035	-0.0902	0.1135	0.0989	0.0126	-0.1584	0.0886	0.0094	-0.0148	-0.4722	-0.1503	0.5642	0.2427	0.187	-0.0382	0.1851	0.1134
Si	-0.2222	0.3435	-0.2276	-0.1058	-0.072	-0.0061	0.0062	0.0596	-0.0867	0.1356	0.258	0.1336	0.2881	0.1906	-0.2177	0.1348	-0.252	0.5609	0.2358	0.1784
Mo	-0.2804	-0.0707	0.2917	0.3071	-0.0188	-0.0016	0.013	-0.0625	-0.1408	-0.0271	0.1605	-0.4103	-0.1703	-0.0849	-0.2264	0.5618	-0.1831	0.0358	-0.0337	-0.2808
V	-0.2693	0.0015	0.2904	0.0486	-0.219	-0.1011	-0.1317	-0.3199	-0.2603	0.4269	-0.018	0.3792	-0.1869	-0.2281	-0.2707	-0.2432	0.0498	-0.1374	0.1501	0.0746
Ni	-0.1397	-0.3223	-0.2337	0.1192	-0.166	-0.328	-0.3193	0.2461	0.2405	0.0916	-0.0864	-0.0266	-0.347	-0.1103	0.0472	-0.0607	-0.3192	0.2203	-0.2762	0.2654
Zn	-0.184	-0.278	-0.1422	-0.4769	-0.0982	-0.1119	0.0145	-0.2723	-0.1484	0.0213	-0.1279	-0.0738	0.2197	0.0995	-0.0654	0.4156	0.2005	-0.1753	-0.2561	0.3586
Fe	-0.0331	-0.1784	-0.4877	0.1767	-0.0224	0.3692	0.1083	-0.2686	-0.1001	0.0088	0.2311	-0.2514	-0.041	-0.2561	-0.2365	-0.2902	0.2557	0.1907	-0.2014	-0.0284
U	-0.2694	-0.1819	0.2477	0.1449	0.0131	0.1637	0.058	0.4201	0.0603	0.077	0.1181	0.3615	0.1339	-0.0045	0.1157	0.1237	0.5047	0.2526	-0.2891	-0.0481
Y	-0.214	-0.1318	0.0459	-0.4169	-0.0719	0.3979	0.2006	0.4991	-0.0081	-0.0026	0.1221	-0.0789	-0.0744	-0.206	-0.1852	-0.1262	-0.2864	-0.2961	0.12	0.0676
Ba	-0.0344	0.1074	0.0308	-0.1631	0.4123	0.3084	-0.8188	0.0015	-0.0603	-0.0519	0.0534	-0.0295	-0.0296	-0.0566	-0.031	0.0543	0.074	-0.0145	0.0101	0.0194
Co	-0.0851	-0.2898	-0.4269	0.2775	-0.0732	-0.0281	-0.1363	0.1024	0.1734	-0.0808	0.0261	0.2474	0.0581	0.1508	-0.181	0.2208	0.1493	-0.3323	0.5095	-0.1258
Sr	0.2831	-0.2297	0.0492	0.0473	-0.0274	0.164	-0.0579	0.0465	0.0944	0.768	0.0515	-0.2946	0.2111	0.0592	0.2391	0.081	-0.0199	0.0093	0.1681	0.0218
Cu	-0.3102	-0.099	-0.0651	0.0841	0.2146	0.2313	0.1012	-0.2386	0.1875	-0.006	-0.4906	0.1738	0.3064	-0.3646	0.2193	0.0677	-0.3146	0.1136	0.0421	-0.1291
Mn	0.2461	-0.2973	0.0482	-0.0137	0.0242	0.2908	0.0614	-0.2908	-0.0527	-0.0917	0.4167	0.4501	-0.1962	0.1737	0.2029	0.1644	-0.3646	0.0102	-0.1296	0.0303
Th	-0.2387	0.249	0.0726	-0.1144	-0.0944	0.1849	0.0287	-0.257	0.7524	0.1262	0.0646	-0.0477	-0.1863	0.2842	-0.1209	-0.017	0.0752	-0.095	-0.1295	-0.0482
Cd	-0.2041	-0.3202	0.011	-0.414	-0.1586	-0.0975	-0.0993	-0.0912	-0.0986	-0.0636	-0.0312	-0.0988	-0.1126	0.2365	0.2019	-0.2128	0.0607	0.2991	0.1998	-0.565
As	-0.2564	-0.116	0.2123	0.3266	-0.2058	0.3021	-0.0753	-0.0523	-0.158	-0.2298	-0.1593	-0.2193	0.0764	0.4318	0.1782	-0.2445	-0.0411	-0.0099	0.1409	0.4127

D3 Supporting information to Mod 5: PCA with NP:AP, Fe:S and all samples

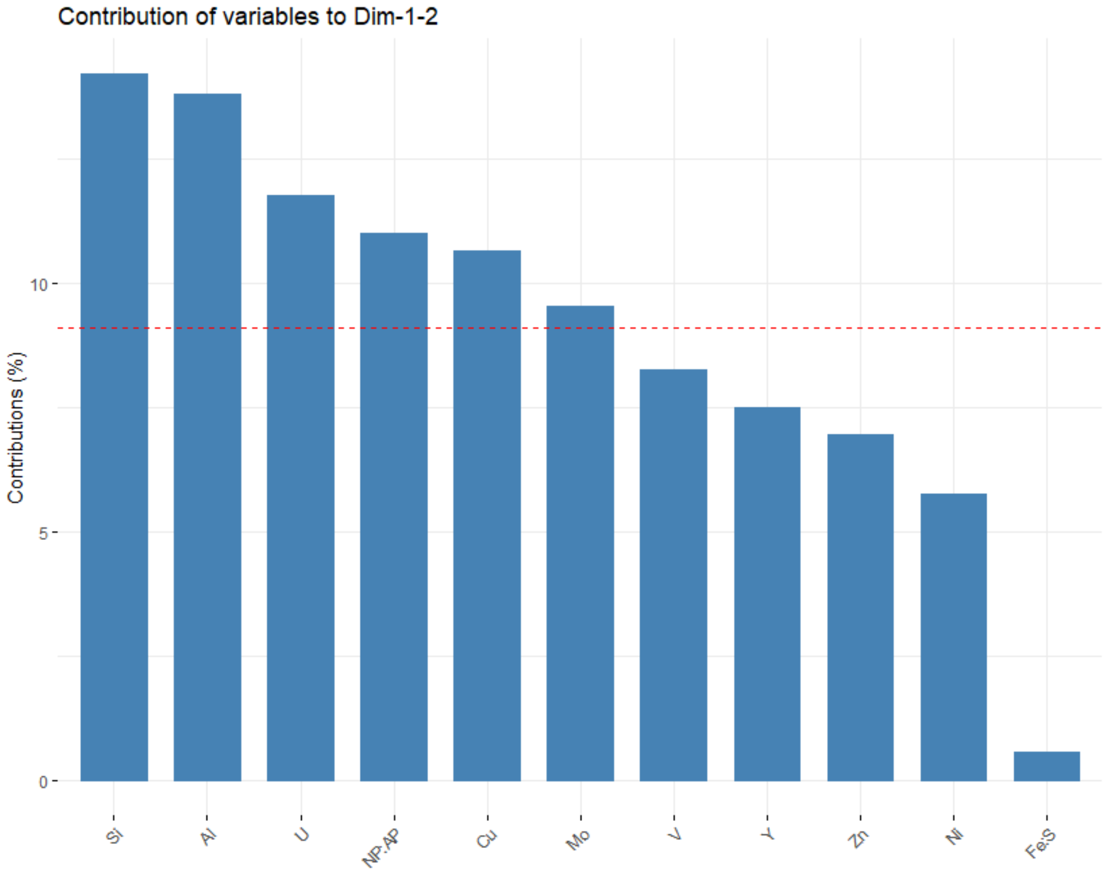

Figure 5 Scree plot for PC1 and PC2 mod 5: PCA with NP:AP, Fe:S and all samples.

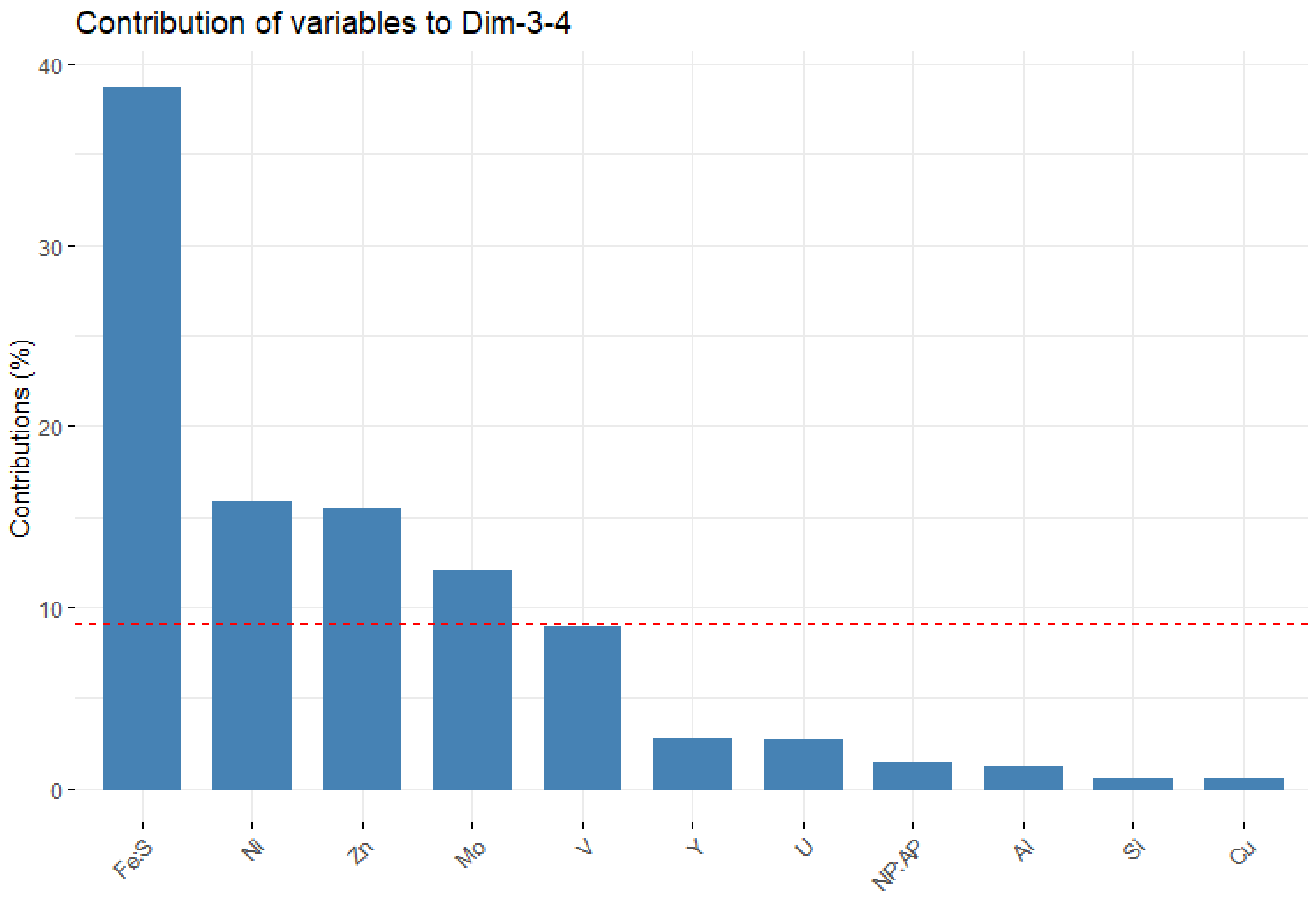

Figure 6 Scree plot for PC3 and PC4 mod 5: PCA with NP:AP, Fe:S and all samples.

Table 3 Importance of components Mod 5: PCA with NP:AP, Fe:S and all samples

	PC1	PC2	PC3	PC4	PC5	PC6	PC7	PC8	PC9	PC10	PC11
Eigenvalue	4.179058	2.115315	1.290088	0.981717	0.766253	0.528007	0.426344	0.267261	0.188127	0.154389	0.103442
Standard deviation	2.0443	1.4544	1.1358	0.99082	0.87536	0.7266	0.65295	0.517	0.4337	0.39292	0.3216
Proportion of Variance	0.3799	0.1923	0.1173	0.08925	0.06966	0.048	0.03876	0.0243	0.0171	0.01404	0.0094
Cumulative Proportion	0.3799	0.5722	0.6895	0.77874	0.8484	0.8964	0.93516	0.9595	0.9766	0.9906	1

Table 4 Loading from Mod 5: PCA with NP:AP, Fe:S and all samples

	PC1	PC2	PC3	PC4	PC5	PC6	PC7	PC8	PC9	PC10	PC11
NP:AP	0.324706	-0.34548	0.155659	-0.0026	0.268325	-0.21556	0.433679	-0.6526	0.00083	0.018082	0.134952
Al	-0.21619	0.563879	0.052624	-0.15537	0.063346	0.006106	0.19365	-0.3559	-0.21311	0.221586	-0.58793
Si	-0.25362	0.543564	0.024417	-0.10838	0.023619	-0.0717	-0.04227	-0.29177	0.239625	-0.37116	0.583164
Mo	-0.35409	-0.18946	0.4227	0.210651	-0.16657	0.030404	0.029175	-0.04559	-0.6256	-0.43883	0.011615
V	-0.34716	-0.08827	0.392845	0.060365	-0.09234	-0.62793	-0.22637	0.017082	0.158318	0.476835	0.083168
Ni	-0.21043	-0.28951	-0.2469	-0.53433	-0.51991	0.215495	-0.11118	-0.32891	-0.12399	0.220406	0.155531
Zn	-0.28707	-0.21032	-0.46193	-0.27528	0.151164	-0.53407	0.115414	0.109283	0.046481	-0.42585	-0.2595
Fe:S	0.091215	-0.03042	0.532479	-0.72349	0.252967	0.106628	0.071258	0.302981	0.0564	-0.0909	-0.01014
Y	-0.32776	-0.10316	-0.22113	-0.01249	0.712149	0.194099	-0.20961	-0.0134	-0.32048	0.283997	0.246114
Cu	-0.39944	-0.0407	-0.03235	0.104926	-0.08179	0.173276	0.781616	0.285402	0.15682	0.205531	0.175515
U	-0.36826	-0.28681	0.177727	0.142124	0.12713	0.377348	-0.18687	-0.25766	0.576807	-0.17829	-0.32555

Kontroll- og referanseside/
Review and reference page

Dokumentinformasjon/*Document information*		
Dokumenttittel/*Document title* WP1 - Temporary storage of black shales – a compilation of case studies, experiences and overall conclusions		**Dokumentnr./*Document no.*** 20200436-03-R
Dokumenttype/*Type of document* Rapport / Report	**Oppdragsgiver/*Client*** NFR	**Dato/*Date*** 2023-01-09
Rettigheter til dokumentet iht kontrakt/ *Proprietary rights to the document according to contract* NGI		**Rev.nr.&dato/*Rev.no.&date*** 0 /
Distribusjon/*Distribution* FRI: Kan distribueres av Dokumentsenteret ved henvendelser / FREE: Can be distributed by the Document Centre on request		
Emneord/*Keywords* Black shale, storage		

Stedfesting/*Geographical information*	
Land, fylke/*Country* Norway	**Havområde/*Offshore area***
Kommune/*Municipality*	**Feltnavn/*Field name***
Sted/*Location*	**Sted/*Location***
Kartblad/*Map*	**Felt, blokknr./*Field, Block No.***
UTM-koordinater/*UTM-coordinates* **Zone: East: North:**	**Koordinater/*Coordinates*** **Projection, datum: East: North:**

Dokumentkontroll/*Document control*

Kvalitetssikring i henhold til/*Quality assurance according to NS-EN ISO9001*

Rev/ *Rev.*	**Revisjonsgrunnlag/*Reason for revision***	**Egenkontroll av/ *Self review by:***	**Sidemanns-kontroll av/ *Colleague review by:***	**Uavhengig kontroll av/ *Independent review by:***	**Tverrfaglig kontroll av/ *Interdisciplinary review by:***
0	Original document	2023-01-09 Frøydis Meen Wærsted	2022-12-23 Gunvor Baardvik 2021-12-20 Mari Engvig Løseth (only PCA part)		

Dokument godkjent for utsendelse/ *Document approved for release*	**Dato/*Date*** 9 January 2023	**Prosjektleder/*Project Manager*** Jenny Langford

NGI (Norwegian Geotechnical Institute) is a leading international centre for research and consulting within the geosciences. NGI develops optimum solutions for society and offers expertise on the behaviour of soil, rock and snow and their interaction with the natural and built environment.

NGI works within the following sectors: Offshore energy – Building, Construction and Transportation – Natural Hazards – Environmental Engineering.

NGI is a private foundation with office and laboratories in Oslo, a branch office in Trondheim and daughter companies in Houston, Texas, USA and in Perth, Western Australia

www.ngi.no

NGI (Norges Geotekniske Institutt) er et internasjonalt ledende senter for forskning og rådgivning innen ingeniørrelaterte geofag. Vi tilbyr ekspertise om jord, berg og snø og deres påvirkning på miljøet, konstruksjoner og anlegg, og hvordan jord og berg kan benyttes som byggegrunn og byggemateriale.

Vi arbeider i følgende markeder: Offshore energi – Bygg, anlegg og samferdsel – Naturfare – Miljøteknologi.

NGI er en privat næringsdrivende stiftelse med kontor og laboratorier i Oslo, avdelingskontor i Trondheim og datterselskaper i Houston, Texas, USA og i Perth, Western Australia.

www.ngi.no

OSLO
TRONDHEIM
HOUSTON
PERTH

NORWEGIAN GEOTECHNICAL INSTITUTE
NGI.NO

Main office
PO Box 3930 Ullevaal St.
NO-0806 Oslo
Norway

Trondheim office
PO Box 5687 Torgarden
NO-7485 Trondheim
Norway

T (+47)22 02 30 00
F (+47)22 23 04 48
NGI@ngi.no

BIC NO. DNBANOKK
IBAN NO26 5096 0501 281
ORGANISATION NO.
958 254 318MVA

ISO 9001/14001
CERTIFIED BY BSI
FS 32989/EMS 612006